FOG

Freiberg Online Geoscience

FOG is an electronic journal registered under **ISSN 1434-7512**

2017, VOL 50

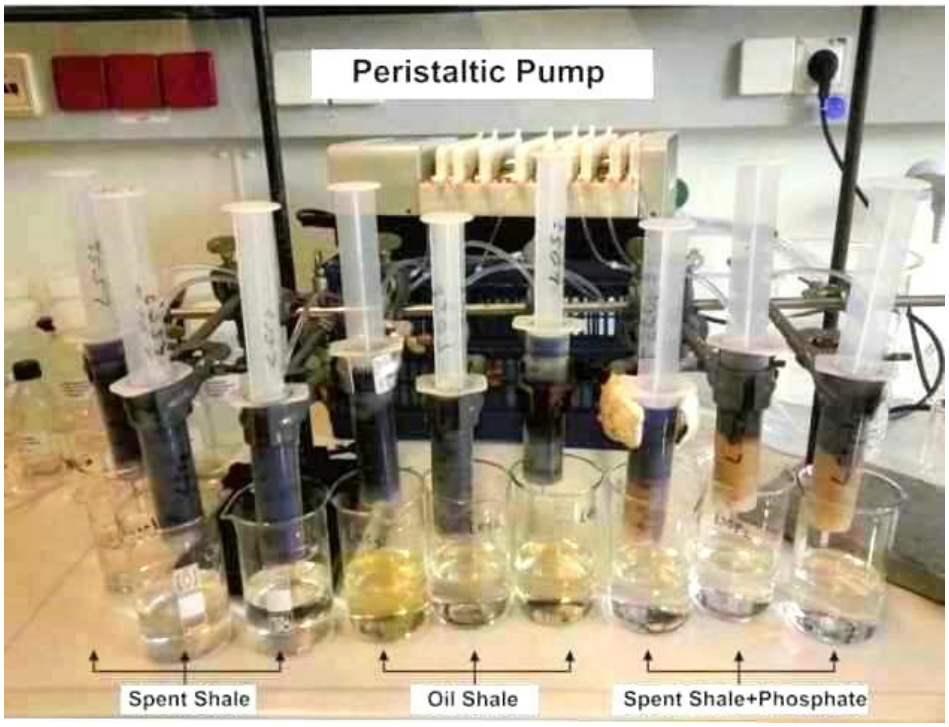

Ahmed Abdalla Gharaibeh

Environmental Impact Assessment on Oil Shale Extraction in Central Jordan

157 pages, 35 figures, 19 tables, 173 references

Acknowledgment

I would like to express my deepest thanks and gratitude to my supervisor; Prof. Dr. habil Broder Merkel (Vice-Rector for Strategy Development TU Bergakademie Freiberg), and, to the co-supervisor Dr. Ayoup Ghrair (Senior Research Scientist at the Royal Scientific Society/Jordan) for their kindness, invaluable guidance, support, fruitful suggestions and their independence oriented supervision, and they taught me not only the scientific research but also the ethics of being a professional scientist.

Special thanks are due to Prof. Dr.-Ing. Moh'd M. Amro director of Institute of Drilling and Fluid mining, Prof. Dr. Olaf Elicki Head of department of palaeontology, TU Bergakademie Freiberg, Dr.-Ing. Ahmad Al-Zoubi, and Dr. Ibrahim Al Taj, for their kindness and faithful assistance. Many thanks are due to Dr. Nicolai-Alexeji Kummer for assistance with practical and theoretical advice in the laboratory and for the analysis.

Special thanks go to friends and colleagues from Ministry of Energy and Mineral Resources (Amman) for their constructive discussions and support during the office and field work, and for their help in drafting some of the figures used in this work: Geol. Khaled Ali Momani, Eng. Jamal Abu qubu, Dr. Mohammad Abdelghafour, Dr. Ali Sawareh, Geol. Ahmad Masri, Eng. Khalid Falah, Dr. Omar M. Radaideh, Geol. Jamal Khataibeh, Geol. Jamal shawagfeh, Geol. Laith Abu Affar. I would like to thank my colleagues: Eng. Khalid Falah, Mr. Hassan Lafi, Eng. Yaha abu Ajamieh, Eng. Eman Fahmawi, Eng. Fatheih Elgamari, Eng. Sadeq alshboul, Mr.Ahmed Zoubi, Mrs. Hanan Akroush for their help in sample preparations and lab work. Great Thanks for Dr. Ibrahim Hamdan from BGR's research office, Amman, for his great effort on GIS work,

Special thanks are due to Dr. Sameh Al-Muqdadi, Mr. Majdi Khasawneh, Mr. Abdulmalik almomani, Eng. Muntasar mujahed, for their kindness and assistance.

I am grateful to the staff, colleagues and friends from the Ministry of Water and Irrigation in Jordan, for providing some of the data, and for their useful discussions, special thanks due to Eng. Refat Bani Khalaf.

The author expresses his gratitude to the university administration office especially Mrs. Dagmer Heim, Mrs Isabel Ruppert, Dr.Corina Dunger -GraFA program, and Mrs. Manuela Junghan from the International University Center (IUZ).

A word of appreciation and love goes to my family: mother, my wife Safa' brothers, and sisters, for their support, words of encouragement and patience. Without this support it would have been impossible to complete my dissertation.

Dedication

This project is dedicated to my late father, who left a great void inside me, to my mother, sisters, and brothers for their love and continuous support.

To my lovely wife; Safa' for her efforts, moral support and unlimited encouragement.

To my children; Lamar, Seedra, Jwa, and Faris, for their understanding during my absence.

with my love to them all.

ABSTRACT

This study focuses on the environmental impact assessment of trace elements concentrations in spent shale, which is the main residual besides gas and steam from the utilization of oil shale.

The study area El-Lajjun covers 28 km^2, located in the centre of Jordan approximately 110 km south of Amman. It belongs mainly to the Wadi Mujib catchment and is considered to be one of the most important catchments in Jordan.

The Wadi El-Lajjun catchment area (370 km^2) consists of two main aquifer systems: The intermediate aquifer (Amman Wadi As Sir Aquifer or B2/A7) and the deep sandstone aquifer (Kurnub/Ram Group Aquifer). The B2/A7 aquifer (Upper Cretaceous) is considered as the main source of fresh water in Jordan.

El-Lajjun oil shale was deposited in a sedimentary basin and comprises massive beds of brown-black, kerogen-rich, bituminous chalky marl. The oil shale was deposited in shallow marine environment. It is by definition a sedimentary rock containing organic material in the rock matrix. The shale oil extraction is an industrial process to decompose oil shale and to convert the kerogen into shale oil by hydrogenation, pyrolysis or by a thermal dissolution.

Several classifications of extraction technologies are known; the classification with respect to the location where the extraction takes place distinguishes between off-site, on-site, and in situ. The oil shale utilization may have serious repercussions on the surrounding environment if these issues are not investigated and evaluated carefully.

Ten representative oil shale rock samples with a total weight about 20 kg were collected from different localities of oil shale exposures in the study area. A standardized laboratory Fischer Assay test was performed with the samples to determine oil shale characteristics and to obtain spent shale, which was used in this study for further investigations. Sequential extraction was used to evaluate the changes in the mobility and distribution of the trace elements: Ti, V Cr, Co, Zn, As Zr, Cd, Pb and U. Column leaching experiments were performed to simulate the leaching behavior of the above elements from oil shale and spent shale to evaluate the possible influence on the groundwater in the study area. The concentrations in the leachate were below the

maximum contaminant levels of the Environmental Protection Agency (EPA) for drinking water and the Jordanian standards for drinking water.

An immobilization method by using Kaolin was applied to reduce the mobilization and bioavailability of the trace elements fraction that are contained in the spent shale. Immobilization was evaluated as a function of liquid-solid ratio (solid-liquid partitioning) and as a function of pH. A comparison between the results obtained from column leaching experiments and the results that were obtained from immobilization for the oil shale and spent shale samples indicated that the immobilization reduced the mobility of the trace element except for Ti, V, and Cr. However, even the concentrations of these elements were lower than the maximum acceptable limits of the Jordanian Standard Specifications for waste water.

The catchment of the study area (Wadi El-Lajjun catchment) is ungauged. Therefore, the soil conservation service (SCS) runoff curve number method was used for predicting direct runoff from rainfall. The results obtained showed that the infiltration of water is very small (approximately 0.6 cm/year) and rarely can´t reach the groundwater through the oil shale beds. Thus, a contamination of groundwater is unlikely under normal conditions.

DRASTIC was used to assess groundwater vulnerability for the B2/A7 aquifer with respect to pollution by oil shale utilization. The aquifer vulnerability map shows that the area is divided into three zones: low (risk index 10-100; intermediate (risk index 101–140) and high groundwater vulnerability (risk index 141-200). The high risk areas are small and mainly located in the northeastern corner of the El-Lajjun graben, where the hydraulic conductivity is relatively high and rocks are highly fractured and faulted.

The water table of the deep sandstone aquifer (Kurnub/Ram group) in the El-Lajjun area is relatively deep. At least two geological formations above the Kurnub aquifer are aquitards and protect the deep aquifer. However, the area is highly fractured and thus there is a certain possibility for contact with surface pollutants.

Finally, further research with respect to trace elements including REE elements and isotopes in the intermediate and deep sandstone aquifers are highly recommended.

Isotopic signatures will be very helpful to investigate to which extend hydraulic connections between the aquifers exist.

Further and in particular mineralogical studies on the spent shale and the possibilities for industrial utilization are recommended because huge quantities of spent shale are expected. Because most oil shale extraction technologies especially the power generation require considerable amounts of water detailed studies on water supply for the oil shale treatment have to be performed.

Table of Content

List of Figures

List of Tables

Chapter 1 INTRODUCTION

1.1 Statement of problem and objectives

Many research studies have focused on the oil-shale in Jordan, related to origin, geology, geochemistry, mineralogy, and chemistry. Some of these studies concerned with the spent shale and trace elements related to environmental impact.

Many questions related to environmental impact assessment on the extraction and utilization of oil shale are still open. Such questions include the environmental impact assessment of trace elements concentrations in spent shale, detailed leaching studies related to spent shale, and the interaction with underlying rocks. A high concern in general is the possible influence on the groundwater in the study area.

The objectives of this research were to investigate the environmental impact of oil shale mining with special emphasis on:

- Trace elements including rare earth elements (REE) within the oil shale and spent shale.
- Interaction with the underlying phosphate unit.
- Potential impacts on groundwater in the study area.

The following methods and procedures have been used in this study:

1. Field survey of the mining data, related to boreholes, and geological survey of the study area.
2. Investigating rock samples from different stratigraphical units using XRD, sequential extraction and analysis, and ICP-MS for toxic elements (Ti, V, Cr, Co, Zn, As, Cd, Pb, and U). Collecting spent shale according to proposed oil recovery techniques and investigating the leaching behaviour of this material and its impact on underlying phosphate unit using batch experiments.
3. Appling technical methods for immobilization of trace elements in spent shale.
4. Using DRASTIC method geographical information system (GIS) techniques to assess the groundwater vulnerability to pollution by oil shale utilization.

1.2: Location and Access

The study area is located in central Jordan (Fig. 1.1) and belongs mainly to the Wadi Mujib catchment. It is considered to be one of the most important catchments in Jordan. El-Lajjun area is located approximately 110 km south of Amman, the capital city, and about 12 km to the east of Al-Karak city, in the mid-way along the main road between Karak and Qatrana. The study area covers 28 km^2 (3.5 × 8 km) and is defined by the following coordinates 230500 to 234000 (E) and 1064000 to 1072000 (N) of the Palestine Belt Grid (PBG).

The study area is located inside the Karak District and is part of the western highlands topographic province that extends from Um Qais city in northwest Jordan to Ras An Naqab mountains in the south. Many small villages are situated around the study area with few nomadic bedouins living there in some seasons. Many tracks and roads in the area make the majority of the study area accessible by four-wheel vehicles.

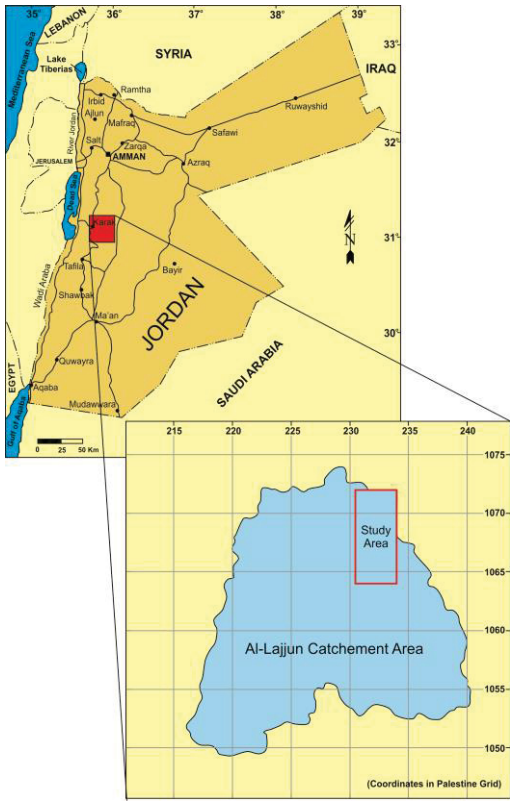

Figure 1.1 Location map of the study area

Chapter 2 OIL SHALE TECHNOLOGIES

2.1 Oil shale

2.1.1 The origin of oil shale

Oil shale is generally defined as sedimentary rocks that contain organic material in its inorganic matrix. The inorganic material is mainly composed of dolomite and limestone (Gary L. Amy, 1978). Generally, oil shale is considered as unconventional and untapped resource of hydrocarbon because the oil cannot be yielded directly by pumping, but is extracted from the shale by using thermal techniques in general (Baughman, 1978, Speight, 2007).

The oil shale is made up of two parts; inorganic material and organic matter. The organic material consists of Kerogen and Bitumen (Fig. 2.1).

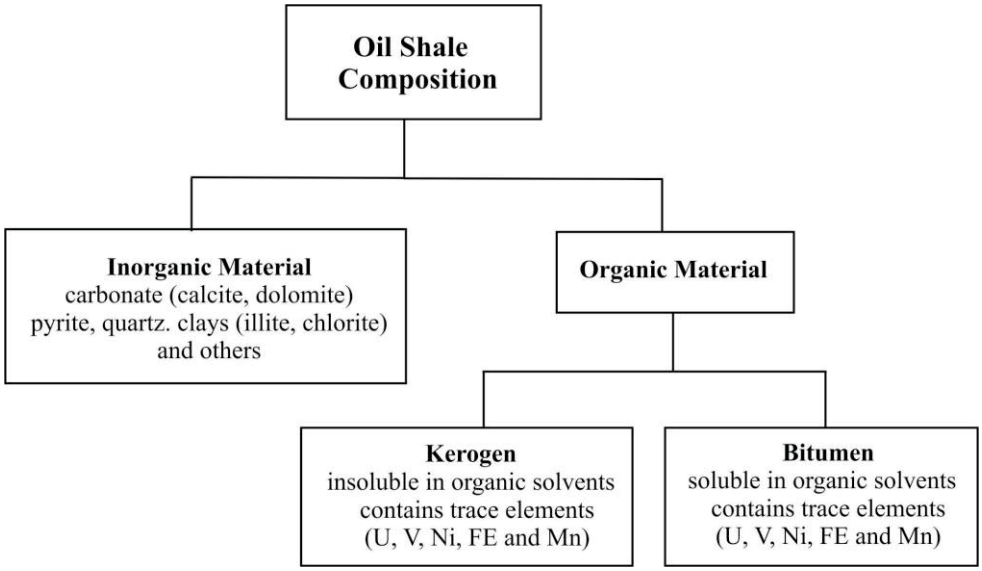

Figure 2.1: Oil shale general components (modified after Yen and Chilingarian, 1976).

The inorganic materials are the major component of the oil shale and the depositional conditions of the host rock determine the general compositions of them. Often they consist of feldspar, quartz, clay minerals (Chlorite, Illite), carbonate (calcite, dolomite), pyrite, and other minerals (Altun et al., 2006).

The organic matter mainly consists of carbon, hydrogen, oxygen, sulfur, and nitrogen (WEC, 2007) and is usually divided into Kerogen and Bitumen:

- **Kerogen:** kerogen is a term used to describe organic matter in sedimentary rocks, which are insoluble in common organic and inorganic solvents. Kerogen is naturally occurring in the source rocks as solid phase and able to yield oil when it is heated. Typical organic constituents of kerogen are woody plant material and algae. In comparison with tar sand and bitumen, Kerogen has a high molecular mass (Speight, 2007, 2009).
- **Bitumen:** it is an extractable organic matter (EOM) and is considered as the soluble part of organic matter that can be dissolved by organic solvents (Speight, 2007, 2009).

Oil shale may be deposited in different environmental varieties. It can be found in freshwater or saline likes and ponds, in marine basins of Cretaceous time, and in shallow ponds as well as in subtidal marine shelves.

Oil shale was deposited during geological times in mid-Cambrian, early Ordovician, late Devonian, and late Jurassic. However, the depositional environments during these times must be anoxic, tectonically stable with very limit activities. The organic matter of the oil shale originated from different type of algae, which were deposited in environments varying from marine to lacustrine, the minority of the organic matter originated from debris formed from land plants driven on both sediment sources and depositional environment (Hutton, 1987, 1991).

2.1.2 Oil shale deposits in Jordan

The first location where Oil shale rocks (OS) were recognized in Jordan was in the Yarmouk region, near Al-Maqqarin Village north of Jordan. This was, during the early time of twentieth century when the oil shale in that area was used by the German Army to produce oil to operate the Hijazi Railway during the First World War (Clapp, 1936, Blake 1939, Quennell, 1951, Burdon, 1959, Bender, 1968).In 1960's the German Geological survey discovered the El-Lajjun deposit and many exploration works took place (Bender, 1974).During the 1980's an intensive exploration activities on oil shale deposits in the central part of Jordan were carried out as a part of the technical cooperation between Natural Resources Authority (NRA) and the German government represented by BGR (Fig. 2.2). As a result of this cooperation other deposits such as Sultani, Hasa, and Jurf Ed Darawish were discovered. Later, many other deposits were discovered in central Jordan

by NRA Attarat Um Ghudran, Wadi Maghar, Siwaqa, Khan El Zabib, and El Thammad with a total reserve of about 4.4 billion tons (Jaber and Probert, 1997; Hamarneh1998).

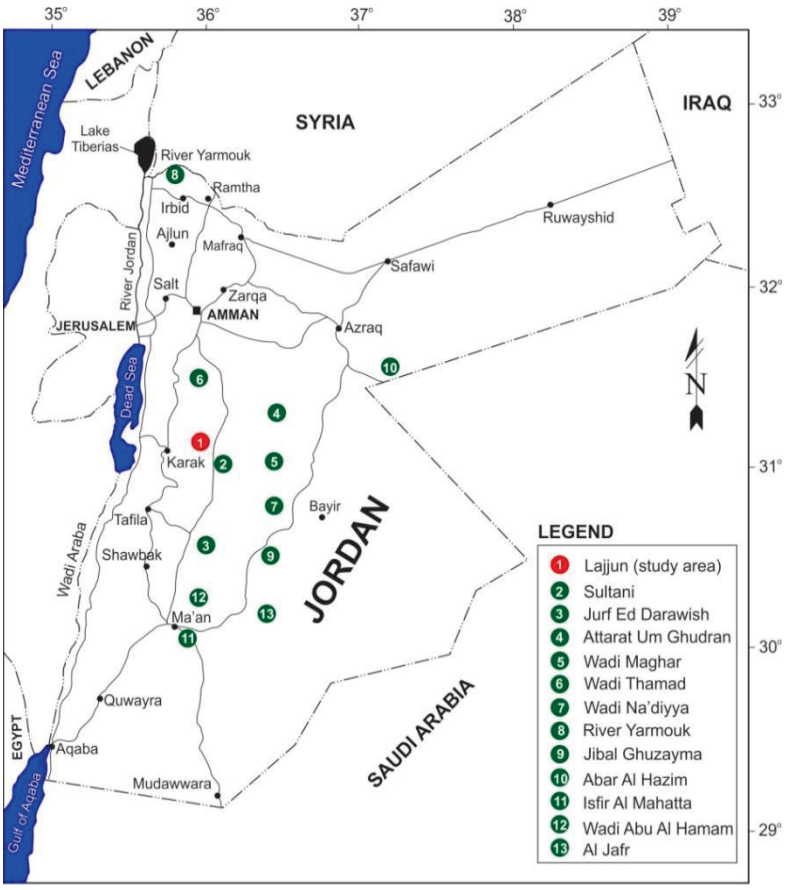

Figure 2.2: Location map of the Jordanian oil shale deposits (source, NRA).

The oil shale of Jordan occurs in the lower part of Upper Cretaceous (Maastrichtian-Palaeocene) Muwaqqar Chalk Marl Formation (MCM). This formation crops out across the central northern and central southern part of Jordan (Hamarneh, 1998). The Jordanian oil shale varies in thickness, overburden, physical and chemical properties, oil content, and the oil shale quantities.

The inorganic matter is mainly made of calcite ($CaCO_3$), which forms the major carbonates, while the minor part is dolomite ($CaMgCO_3$). Besides, there are quartz, phosphate as carbonate fluoroapatite ($Ca_3 (PO_4)_2.Ca_2PO_4 (CO_3, F)$, pyrite ($FeS_2$), clay minerals (illite, kaolinite), and sulfur mineral, beside trace metals, which are associated with the organic matters (e.g. Cr, V, Pb, U, Ni, Mo, Co, Cd, Zn, and Ba). These trace metals present at higher concentrations than normal (Hamarneh1998; Abed et al. 2009).

The organic matter, which creates the dark color of the oil shale, is different in content from one location to another. The deposits in central Jordan are richer in organic matter than those of Yarmouk basin. The organic matter content of Jordanian oil shale varies from few percent up to 37%. El-Lajjun deposit contains almost twice as much compared to the deposits in Yarmouk Basin and in Magarin northern Jordan (Amireh, 1979).

2.1.3 Oil shale deposits in the study area

El-Lajjun deposits are one of the 24 oil shale deposits in sedimentary basins of Central Jordan (Jerry, et al. 2010). During the Cretaceous to Eocene period a major marine transgression occurred over large part of Syria, Lebanon, and Jordan the marine limestone was deposited in the transgression which came from north-northwest during Cenomanian-Turonian times, after that the sea become shallower, However, chalk, chert, and marl (Turonian to Oligocene) were deposited.

Many of these marl deposits were rich in organic matter (Spears, 1969). Micro paleontological studies approved that the depositional age of oil shale deposits in Jordan are transitional between Masstrichian to Paleocene (Jerry et al., 2010). The oil shale deposits of central of Jordan are the shallowest and provide appropriate conditions for open pit mining (Hamarneh, 1998). El-Lajjun oil shale deposits comprise massive beds of brown-black, kerogen-rich, bituminous chalky marl which were deposited in shallow marine environment. The marine sedimentary rocks of late Cretaceous to early Paleocene deposited as syn-tectonic basin infill within El-Lajjun Graben hosted deposits of oil shale. (Speers, 1969).

Approximately 185 boreholes were drilled in El-Lajjun oil shale deposits (Hamarneh, 1998). The following information is obtained from the previous studies, which were done by NRA (Table 2.1).

The major inorganic components in the studied oil shale deposits including El-Lajjun deposit are calcite as the minor component, rarely quartz together with kaolinite, and apatite. Feldspar, muscovite, illite, goethite, and gypsum are available as secondary components. In El-Lajjun deposits dolomite occurs in some carbonate beds (Table 2.2, and Table2.3).

The main elements of oil shale is organic carbon, then silicon and calcium, however, phosphorous, aluminum, sulfur and iron are the minor constituents, the remaining components are at very low concentration. In the bituminous marl in comparison to limestone the following are enriched; chromium, vanadium molybdenum, tungsten and chromium, Zinc, nickel, cobalt and others (Hamarneh, 1998).

Table 2.1: General Information were obtained from El-Lajjun deposit (after Hamarneh,

Area (km^2)	20.4	Average oil content (wt%)	10.5
Average. thickness oil shale (m)	29.6	Total organic mat.(wt%)	22.1
Average. thickness of overburden (m	28.8	Calorific value (kcal/kg)	1590
Stripping ratio (average)	1	$CaCO_3$(wt %)	54.
Geological reserves (Mt)	1196	S (wt %)	3.1
Calculated & indicated reserve (Mt)	1170	Density (g/cm3)	1.81

Table 2.2: The mineralogical composition was determined mainly by X-ray diffraction (after, Hamarneh, 1998).

Constituent	Mineral	%
Main	Calcite	20- 80
	Quartz	10-40
	Kaolinite	5-10
Minor	Apatite	4-14
	Dolomite	2-3.6
	Feldspar	5
Traces	Pyrite	5
	muscovite-illite	5
	Goethite	5
	Gypsum	5
	Opal	Present

Table 2.3: The chemical compositions were determined by wet chemical analysis and X-ray fluorescence. The results are given as oxides in wt % (Hamarneh, 1998).

SiO_2	4.65-41.63	**Na_2O**	0.00- 0.32
TiO_2	0.03- 0.38	**K_2O**	0.02- 0.56
Al_2O_3	0.97- 9.26	**P_2O_5**	0.47- 14.67
Fe_2O_3	0.41- 3.57	**SO_3**	0.07- 6.73
MnO	0.01	**CaO**	15.32- 45.67
MgO	0.17-8.17	**L.O.I**	27.9- 45.9

2.2 Oil shale extraction techniques

In the early of the 10th century, Mesue the Younger (Masawaih Al-Mardini) an Arabian physician extracted oil from some kind of bituminous shale (Forbes, 1970). In 1684, British Crown granted the first shale oil extraction patent done by three persons, who invented a simple extraction technique to make considerable quantities of tar, pitch and oil out from some kind of stones (Moody, 2007; Cane, 1976; Runnels et al., 1952). In France 1838, Alexander Selligue invented an applicable extraction process to produce shale oil as first modern industrial extraction techniques (Runnels et al., 1952).

The first oil shale plants were built in Brazil, Canada, Australia, and Unites States during the late 19th century and early 20th century. Countries like (China, Estonia, New Zealand, and Sweden, began to extract oil from the oil shale. The oil shale industries flourished in the mid-20th century and continued until the oil prices fell down sharply in 1990's. In 2003, the US oil shale program was restarted again after it was stopped in 1991 (Dyni, 2010).

Estonia, Brazil, and China restarted working in the oil shale industries in 2008. Canada, USA and Australia were planning commercial enforcement, after they have tested shale oil extraction techniques by means of demonstration projects. According to this, Jordan and Morocco have announced their intent to do the same (Brendow, 2009).

The largest known reservoir of crude bitumen in the world is in Canada. However, Athabasca oil sands is the largest of three major oil shale deposits in Alberta, oil sand consists of a mixture of crude bitumen (a semi-solid rock-like form of crude oil), clay minerals, silica sand and water (Burrowes et al., 2007).

2.2.1 Processing principles

The shale oil extraction is a technical industrial process to decompose the oil shale and to convert its kerogen into shale oil by hydrogenation, pyrolysis process or by a thermal dissolution (Koel, 1999). To examine and evaluate the efficiencies of extraction processes, their yield should be compared with the results of the Fischer Assay performed on a representative oil shale sample (Speight, 2008).

Destructive distillation (Retorting process) is an old and the most common extraction method of pyrolysis (Speight, 2010). In this chemical process, oil shale is heated to a high temperature in the absence of oxygen or other reagents or catalysts until the kerogen content decomposes into non-condensable combustible oil shale gas and condensable shale oil vapors. Both oil shale gas and oil vapors are collected and cooled down. One of the main by-products is the spent shale which is a solid residual material consisting of inorganic compounds and char. The char itself is a solid material formed as a residual of the process as well. Oil shale ash, one of the products of the process, is formed by burning the char of the spent shale at higher temperatures (Lunge, 1887, Speight, 2010).

Depending on the different compositions of the oil shale, there are other by-products with commercial value. These materials include sulfur, pitch, asphalt, ammonia, and waxes (Johnson et al., 2004).

2.2.2 Classification of extraction technologies

Several classifications are of the extraction technologies are widely used. They are based on:

- process principles,
- heating methods,
- heat carrier,
- retorting orientation,
- raw oil shale particle size,
- complexity of the technology, and
- location of extraction.

The classification with respect to location distinguishes between off-site, on-site, and in situ (Johnson et al., 2004).

2.2.2.1 In-situ technologies

In-situ technology is below-ground heating process for oil shale by thermal injection of a hot fluid through the ground into the bed rock that contains oil shale, or by using planar or linear heating to distribute the heat through the oil shale bed rock. A thermal convection and conduction is used following the source of heat. Vertical wells are drilled into the rock formation to recover the shale oil that has been extracted by this process (USOTA, 1980). By using this type of technology, the wells can reach greater depths through the target area, thus, the capability of extracting more shale oil is increasing (Kök et al., 2008).

This extraction process was implemented in Germany during the World War-II without any significant success. Between the years 1940 and 1966, in Kvarntorp in Sweden, an underground gasification was applied using Ljungström Method, which was the earliest successful in situ process (USOTA, 1980).

During the year 1972, United States was the first to modify in-situ oil shale experiment, and many variations of this technique were explored there (Johnson et al., 2004).

The Shell Oil Company has modified in-situ conversion process (Shell ICP), and successfully carried out small-scale field tests, by using electrical slow heating (Fig. 2.3) The method is based on underground heating via thermal conduction of oil shale layer up to 370 °C over a period of time which reaches about 4 years. However, after a successful small-scale test, a large-scale implementation is required to establish and confirm the technical viability.

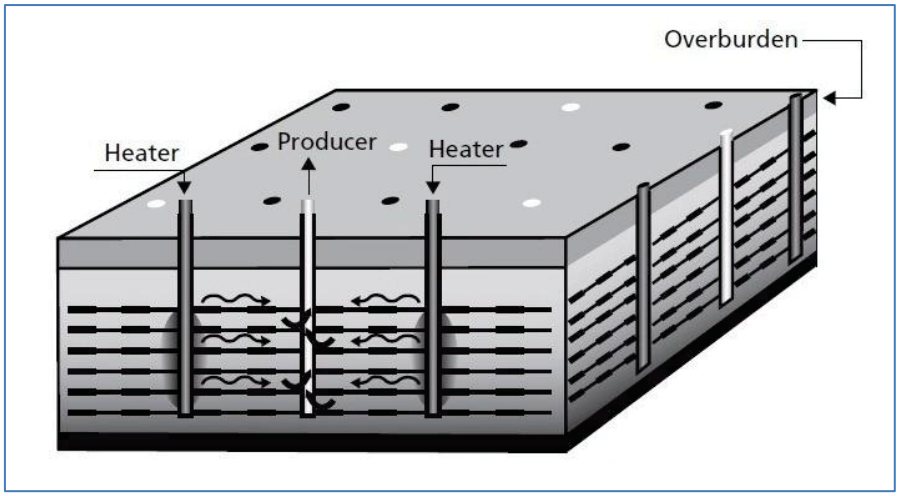

Figure 2.3: The Shell In-Situ Conversion Process (Source: Shell Company, 2016).

In order to isolate the target processed area from surrounding (specially the groundwater aquifers) frozen walls are inserted (Fig. 2.4). These barrier walls consist of wells filled with a circulating super-refrigerant fluid. For economic reasons the target area should be with a thick oil shale ore beds and more than 40 m of overburden for environmental reasons (Bartiset al., 2005).

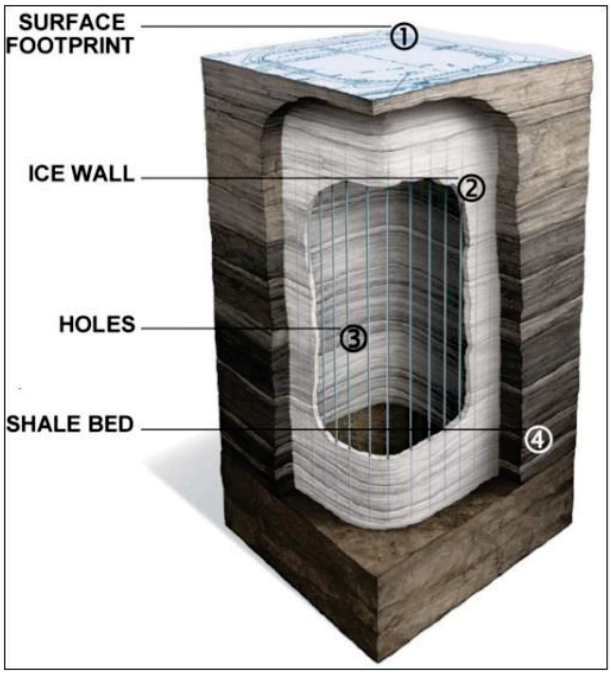

Figure 2.4: Shell's freeze wall, for in-situ shale oil production, separates the process from its surroundings. (Source: Shell Company, 2016).

2.2.2.2 Ex-situ Technologies

Surface retorting, also known as over-ground retorting requires that the raw materials is mined and transported to the processing facilities. Generally, the method depends on internal combustion technologies in a vertical or horizontal reactor for the decomposition at high temperatures (pyrolysis) (Burnham and McConaghy, 2006).

The raw oil shale material is in a first step milled to a suitable grain size (12 to 75 mm) and fed into the vertical or horizontal reactor and heated by hot gases (about 500°C). The hot gases pass through the oil shale and produce kerogen by pyrolysis (decomposition of oil shale). The substances produced by this primary process (evolved gases, cooled combustion gases, and shale oil mist) are removed to a separation unit and condensed shale oil is collected. The non-condensable gas is recycled to heat up the reactor. In the second stage, the air is injected from the lower part of the retort to heat up the spent shale and gases up to 900 °C, whereas the shale ash is cooled by the recycled cold gas (USOTA, 1980).

Several oil shale ex-situ thermal processes, which utilizes mixing of oil shale with hot solid heat carrier (inert material, oil shale ash) to provide heat for oil shale thermal decomposition, have been developed and patented worldwide. Examples of commercial processes include Galoter, Fushun, Alberta Taciuk, Kiviter and Pertosix Lurgi-Ruhrgas or TOSCO II (Elenurm et al., 2008;Qian and Wang, 2006).

1. Galoter

The Galoter process (also known as UTT, TSK) is based on heating fine-grained oil shale in a horizontal rotary kiln-type retort in contact with hot oil shale ash obtained from solid retorting residue combustion (Elenurm et al., 2008).

The process of oil shale pyrolysis was invented in 1944 as a first research on the solid heat carrier process at a laboratory scale in the USSR Academy of Science. The Galoter process was improved from 1945 to 1946, then further developed in 1950´s and used commercially for shale oil production in Estonia. It started with UTT-500 retorting (approximately 500 ton per day of oil shale). The successful studies of commercial experiments reached UTT-3000 (production of 30,000 barrels per day) at Estonian Power Station in the 1980's, which is six-time higher unit throughput rate in comparison with the UTT-500 (Volkov and Stelmakh, 1999; Liive, 2007).

Galoter Retorting (UTT-3000) is a complex retorting technology. This type of retorting is a kind of horizontal, slightly declined cylindrical rotating retort (Fig. 2.5). The oil shale material is milled to grain size up to 25 mm, the product shale ash is used as solid heat carrier in this technology. The shale ash is mixed with dried oil shale in a horizontal cylindrical retort and heated to 500 °C. After 20 minutes, it is pyrolyzed to form shale coke. Both shale ash and shale coke is then moved from the retort into the chamber of vertical fluidized combustion. Shale coke is converted into shale ash by adding up flowing air in the chamber with a temperature of 700-800 °C. The shale ash with the shale coke is re-circulated; in this stage the flue gas which leaves from the cyclone is inserted to a hot waste boiler to dry the oil shale feed. The shale oil vapor which is produced from the retort is cooled. Finally, light oil, heavy oil, high calorific gas, naphtha fractions are obtained by this process (Senchugov, and Kaidalov 1997).

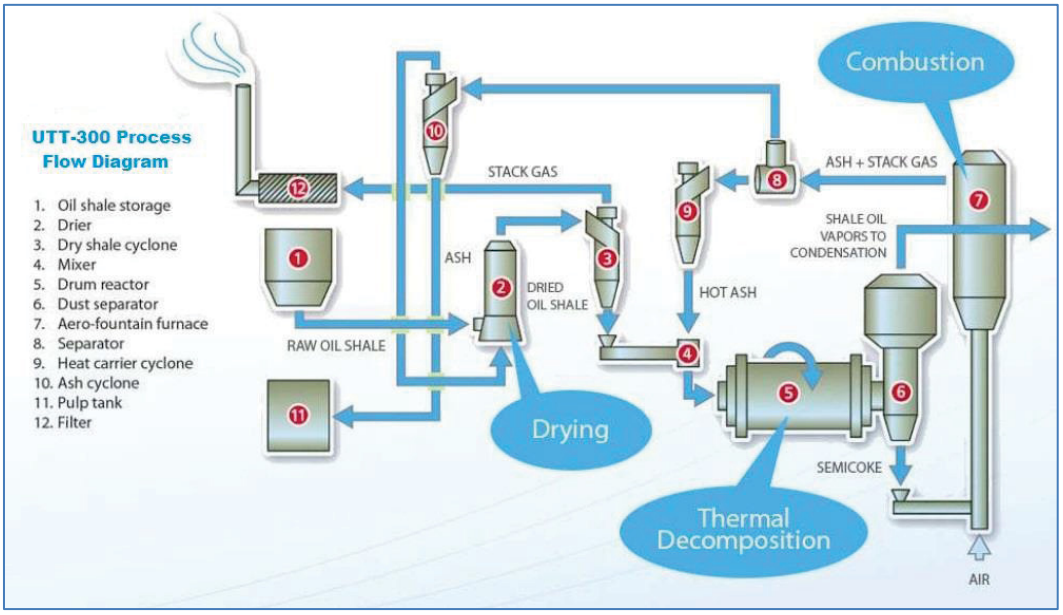

Figure 2.5: UTT 3000 flow diagram (after Öpik, I, 2001).

2. Fushun

The Fushun retort process was utilized in Fushun China during the 1920´s. Fushun retort process was developed for extraction of shale oil in 1992. Fushun Mining Group in China established the Fushun oil shale retorting plant in 2005, since this time China became the largest shale oil producer in the world (Qian and Wang, 2006).

According to Qian and Wang in 2006, the Fushun Technology process uses a shaft retort with the vertical cylindrical type. The raw oil shale material is fed from the top of the retort cylinder with a size of 10-75 mm. The oil shale is dried in the upper section by ascending hot gases. When these gases pass upward through the oil shale, the rock is consequently decomposed. The pyrolysis take place at about 500°C and the gases, which are produced by this process, exit directly from the top of the retort cylinder. The oil shale is decomposed to shale coke during the pyrolysis.

The gasses are heated by the produced shale coke and the ascending air-steam is necessary for pyrolysis. These gases leaving the retorting are recirculated and cooled in a condensation unit. The shale oil is condensed as well, then re-heated to about 500 °C in the heating furnace and then recirculated into the retort. The shale ash exits from the bottom of the retort after cooling. The oil yield of this retort accounts to approximately 65% of the Fischer Assay process (Qian and Wang, 2006).

The Fushun Technology process has many advantages which includes a small investment, stable operating conditions and a high thermal efficiency. On the other hand, the disadvantages of this process are reduced shale oil yield, high water consumption (one barrel of shale oil needs 6 to 7 barrels of water), and production of great quantities of waste shale. Hence, the Fushun Process is not suitable for oil shales with oil content less than 5% (Purga, 2004). The oil yield of this retort accounts approximately 65% of the Fischer Assay process.

3. Alberta Taciuk process (ATP)

Alberta Taciuk process (ATP) is one of the important off-site or on-site retorting technologies for oil shale extraction and is known also as AOSTRA Taciuk process. The research and development of the ATP technology was originally performed for pyrolysis of oil sand in the early 1970´s. William Taciuk, the inventor of this technology formed UMATAC Industrial Processes in 1975. UMATAC Industrial Processes, located in Calgary, Alberta, is the supplier of the Alberta Taciuk Processes (ATP) for extraction, recovery, and primary upgrading of hydrocarbons from oil shale, oil sand, and hydrocarbon waste materials.

The first pilot plant was constructed in 1977, and the first commercial application of this technology was applied in 1989 for the environmental remediation of contaminated soils. The ATP technology was used for shale oil extraction in Australia from 1999 to 2004 (Qian

and Wang, 2006. Odut et. al., 2008). In 2002, an Estonian company tested this technology (BNN, 2002).

The ATP is classified as a hot recycled solids technology; the technology that deliver heat to the oil shale by recycling hot solid particles (typically oil shale ash), most of the processes occurs within a single rotating multi-chamber horizontal retort including drying and pyrolysis of the oil shale, combusting, recycling and cooling of residues and spent shale (Fig. 2.6). Oil shale is fed as very fine particles (less than 25 mm). The fed is dried and preheated in preheat tubes of the retort at about 250 °C. These tubes are indirectly heated by hot flue gas and hot shale ash (Qian and Wang, 2006; Õpik, 1999).

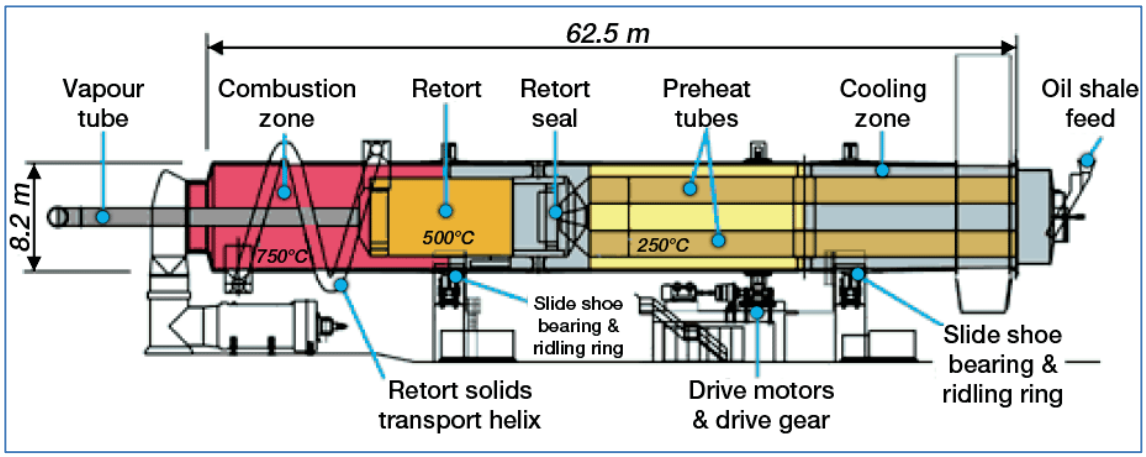

Figure 2.6: Alberta Taciuk Processor (ATP) retorts (Johnson, 2004).

The fine oil shale particles are mixed with hot shale ash in the pyrolysis zone at a temperatures between (500 to 550 °C). The shale oil vapor that results in this stage is recovered by condensation after it is withdrawn through the vapor tube from the retort chamber. The residuals of char and ash are moved to the combustion zone and burnt at approximately 800 °C. By this the shale ash is formed. However, part of the forming ash is transferred to the pyrolysis chamber and recycled as a hot solid carrier. The other part of the ash is delivered to the cooling zone where it is cooled by the combustion gases. In this process the hot ash is used to heat up the new fed of oil shale.

The ATP technology has many advantages for shale oil extraction; it is a simple technology with a simple and robust design, energy self-sufficient, requires low amount of water, and produce high oil yields of about 85-90 % of the Fisher Assay. The spent shale, as one of the residues, is less than 30%. The most disadvantage of ATP is that the

retorting operation process reaches a high temperature in process of decomposition of the shale and that increases the greenhouse gas emissions (Qian and Wang, 2006 and Brandt, 2007).

4. Petrosix

Petrosix is the largest surface oil shale retort in the world. The retort is about 11 meter diameter vertical shaft. Petrobras, the Brazilian energy company started research and development of oil shale extraction technology in 1953 and founded Petrosix Technology as a company. In 1980, Petrobras started limited commercial operations. In 1982, the current Petrosix process was started with a 0.2m internal diameter retort pilot plant; a 2 m retort demonstration plant was applied in1984 (Fig. 2.7). In 1992, the current commercial production started with a 11 m internal diameter retort plant. Meanwhile, the company operates two vertical shaft retorts (Qian and Wang, 2006; Johnson, et al., 2004). The Petrosix Technology uses the externally generated hot gas for the oil shale pyrolysis (Burnham and McConaghy, 2006).

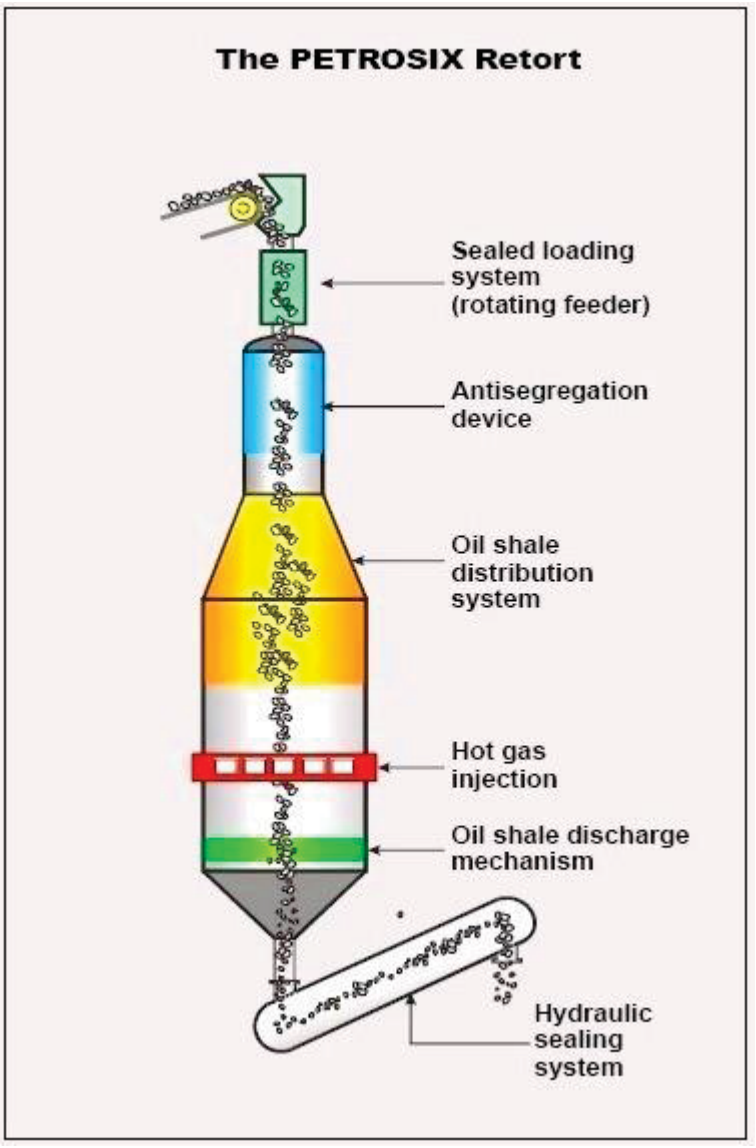

Figure 2.7: Petrosix Retort (Casimiro 2016).

The oil shale particles with approximately 12 mm size are transported on a belt to a vertical cylindrical vessel. The shale is heated for pyrolysis to temperatures up to 500 °C. Here the oil shale is fed from the top of the retort and the hot gases are injected from the middle. The oil shale is moving down and heated by the injected gases. By this process, the kerogen in the oil shale decomposes and oil vapor and other gases are produced. From the bottom of the retort a cold gas is injected to cool and recover heat from the residue spent shale, which is discharged through a water seal with a drag conveyor below the retort (Fig. 2.8) (Qian and Wang, 2006). The cooled gases and oil mist are driven through the top of the retort and pass in a wet electrostatic precipitator, where the oil

droplets are collected. In the last process the gas is compressed and split into three parts (Jaber, 2008).

- One part of the gas is heated to 600°C and re-injected to the retort from the milled to heat and the oil shale.
- The second part is used to cool the spent shale in the bottom of the retort and so it recovers some heat to the pyrolysis section.
- The third part gains an extra cooling to the light oil and water removal and is sent to the gas treatment units to produce the liquid petroleum gas and fuel gas. Sulfur is recovered in this unit.

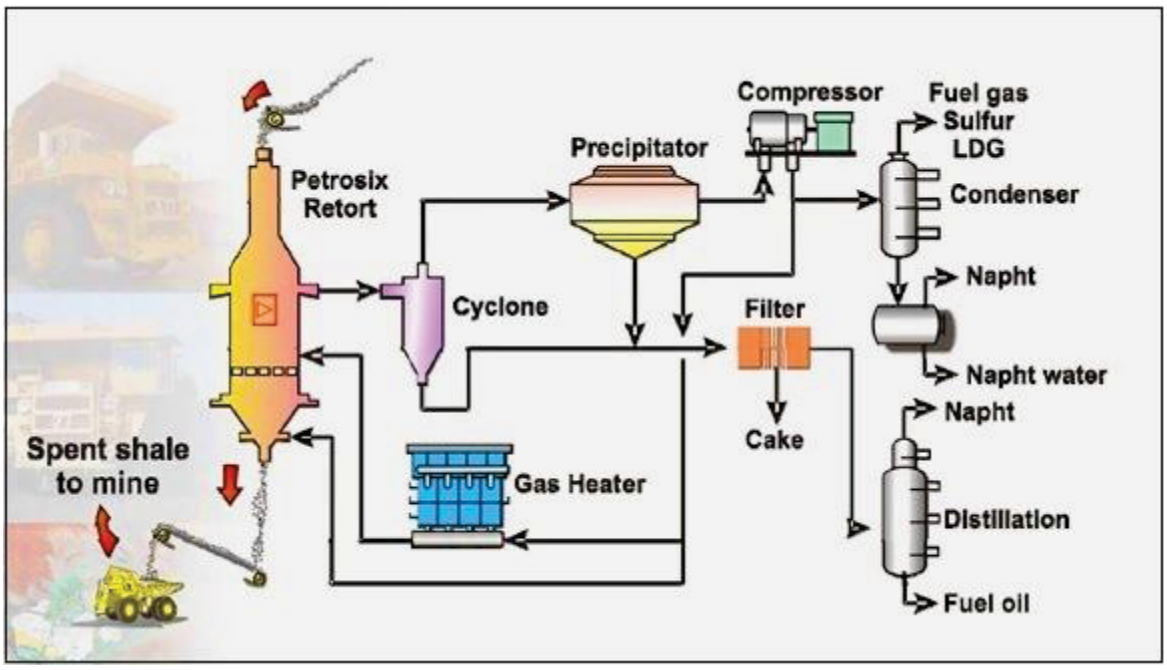

Figure 2.8: Petrosix Process (Casimiro2016).

5. Red Leaf (In-Capsule Process)

Red Leaf Resources Incorporation is a Canadian company founded in 2006, based in Salt Lake City, Utah, USA. The company developed a technology, of oil shale extraction (EcoShale In-Capsule Process), which is focused on the production of high-quality oil extracted from shale resources (Patten, 2007). EcoShale in-capsule process is similar to the in situ processes by using a lower-temperature heating method, and by operating

within a confined geological environment. Hot gas is circulated in a parallel pipes rising up the temperature of oil shale rubble.

The EcoShale In-Capsule Process can be summarized as follows: the oil shale is mined in a normal mining process, and then placed in an excavation that is isolated by an impermeable clay liner. The heating pipes are placed in a horizontal order throughout the excavation (capsule). The hydrocarbon vapor is collected by a liquid drain system included in the bottom of the capsule and perforated pipes at the top. The natural gas (which is burned to heat up the capsule at the first stage) burners produce hot exhaust gas that is distributed by circulation through the capsule.

2.3 Characteristics of spent shale and risk assessment

Jordan has very large reserves of oil shale. More than 50 billion tons of geological reserve located in more than 24 known deposits (surface, near surface and deep deposits of oil shale). The occurrences have been retorted in most of the Jordanian districts.

El-Lajjun and other four best known of Jordanian oil shale deposits are located 100 to 120 km south of Amman. These localities contain more than 22 billion tons of raw oil shale (NRA, 2007). Jordan has signed many (MOUs) with international oil shale companies to assess the commercial potential oil shale deposits and to mine and process oil shale in their areas of interest (Hamarneh, 1998).

The proposed extraction techniques for utilization of the oil shale rocks are mainly by retorting process, or by direct combustion as source of energy for electricity generation. However, a high percentage of ash as solid waste (50-60 %) is generated. The organic matter is up to 25% in average. Besides, a considerable percent of toxic trace metals are associated with it. Production of shale oil makes the future of utilization of oil shale as a source of liquid fuel uncertain due to the huge quantities of ash which represents one of the main environmental obstacles (Jaber et al., 1999). One of these concerns is mainly the leaching propensity of trace elements of the spent oil shale into both surface water and groundwater aquifers.

The technical analysis which were performed by NRA and BGR (started in 1968), and farther analysis among this study included the Fischer Assay Analysis, the amount of oil shale, gas and residue (spent shale) were recorded. Besides, other more representative samples were analyzed to determine organic matters, sulfur, moisture, trace elements and

other inorganic constituents. The results of different analysis are presented below (Table 2.4).

Table 2.4: The results of different analyses for the main products by using the Fischer Assay analysis (modified after Hamarneh, 1998).

Fischer Assay	**High**	**Lean**	**Average**
Oil %	16.7	8	13.4
Water %	2.1	3.3	2.6
Spent shale %	83.	76.5	80.3
Gas and loss %	5.7	3.7	4.6
Specific gravity of oil 60 ° F/ 60 ° F	0.977	0.964	0.966
Spent Shale %	**High**	**Lean**	**Average**
Total carbon	15.2	9.9	15.8
Mineral carbon	6.86	3.3	5.87
Organic carbon	9.3	6.6	8.0
Type of hydrocarbon	**High grade**	**Lean**	**Average**
Saturated hydrocarbons	9.63	8.01	9.06
Aromatic hydrocarbons	75.77	78.	76.32
Asphaltic compounds	15.67	12.96	14.61

During the retorting and the combustion stages, the chemical nature of mineral in the spent shale can be change which affects both chemical and physical stability of the spent shale. Hence, it is very important to consider that on the disposal strategies for the solid waste (Bell et al., 1986). According to the European Academies Science Advisory Council, it needs additional land use for the disposal of mining wastes (Francu et al., 2007). However, these waste material occupies a greater volume than the ore material that has been extracted (generally, one ton of spent shale per barrel of shale oil), and therefore cannot be wholly disposed underground. The primary threat to water quality is considered to be the leachate from spent shale. (EASAC, 2007).

Many studies were performed for the migration behavior of trace elements in the oil shale retorting. For example, tests were performed in laboratory with oil shale of the Huadian deposit of China; one of the results indicated that the trace elements in the oil shale and spent shale were richer than that in the earth crust.(Bai et al., 2008).
Many biogeochemical processes (oxidation reduction reactions, biological transformations, scavenging or sorption, radioactive decay, transport of water, precipitation, weathering of rocks, and atmospheric deposition) influence the quantity and its distribution in the environment (Hamarneh, 1998).

2.4 Oil Shale Extraction Techniques Proposed in Jordan

The Oil shale deposits of Jordan have been investigated since the 1960's. The investigations focused on economic and environmental methods for utilizing oil shale resources for power generation and/or retorting

In 2006, the Government of Jordan launched the strategy for utilizing oil shale in Jordan. The Natural Resources Authority (NRA) invited pioneer companies in oil shale field to submit their proposal to utilize and develop the oil shale of Jordan using different extraction technologies. The objective was to establish a private oil shale project to produce oil (off-site and deep in situ treatment) and to generate electricity based on a build, own and operate (BOO) scheme.

Many international oil shale companies with proven oil shale and oil sand extraction experience have signed MOU's with the government of Jordan to assess the commercial potential oil shale deposits. Four concession agreements were signed with the government. The agreements give the right to the companies to mine and process oil shale in their claims. These companies are namely: Jordan Oil Shale Company (JOSCO), Enefit Company, Karak International Oil (KIO), and Saudi Arabian Oil Shale Corporation (SACOS).

1) Jordan Oil Shale Company (JOSCO)

JOSCO Company is a subsidiary of Royal Dutch Shell plc. In 2009, the company signed an Oil Shale Concession Agreement (OSCA) with the government of Jordan to assess and develop the commercial potential of deep oil shale deposits in Jordan.

JOSCO will use a novel technology based on in-situ (retorting) process (ICP). The ICP technology of oil shale is based on in-situ heating without excavation or mining. The oil shale is heated in place and the organic matter of the oil shale is treated by pyrolyse and converted to oil and gas.

The ICP technology can be applied to deep and thick oil shale with a rich content of oil. JOSCO will apply ICP in Jordan at depth of up to 1000 m. The light crude oil that is produced through this technology requires less refining process to have high quality fuels in comparison with the surface retorting. ICP technology can produce a large volume of oil and gas from a relatively small surface area and the pyrolysed shale remains underground in its place.

JOSCO has constructed the Jordan Field Experiment (JFE) in September 2015. JFE is a small scale field located in the central part of eastern Jordan. The test has applied at an underground oil shale block with approximately 350 m^3. The JEF is aiming to test how the Jordanian oil shale deposits reacts to the ICP technology to demonstrate if this technology can be applied in a commercial scale on Jordan Oil Shale (MEMR open file).http://www.josco.jo (2016,October).

2) Enefit company

The Estonian EestiEnergia Company (Enefit), has developed a modern technology that converts oil shale into oil and gas and generates electricity as a by-product. In 2008 the company has signed a concession agreement with National Electricity Power Company (NEPCO) to start the proposed oil shale fired power plant project with 550 megawatts in central Jordan. The investment will be in Wadi Attarat Um-AL-Ghudran area, with an area about 70 km^2.

In 2010, the company has signed an Oil Shale Surface Retort Concession Agreement (SRCA) with the government of Jordan which gives a right to the company to explore and produce about 2.3 billion tons of oil shale in Wadi Attarat Um-AL-Ghudran area.

The Enefit Company will apply the Enefit 280 oil shale extraction technology, which is a technology based on the Galoter (UTT 300) process. In this process 100% of the mined oil shale will be used and all the organic matter is fully utilized.

https://www.enefit.com/en/jordan (2016, October).

3) Karak International Oil (KIO)

KIO, a Jordanian Company, has signed a concession agreement with the government of Jordan in 2011, that gives the right to mine and process oil shale in El-Lajjun Area (35 km^2). KIO will apply the proven oil shale extraction technology of the Alberta Taciuk process (ATP). The plan is to produce from the oil shale 50,000 barrels and 15 megawatts of electrical power per day during the life time of the project which is 40 years (MEMR open file).

4) Saudi Arabian Oil Shale Corporation (SACOS)

SACOS has signed an agreement with the government of Jordan in 2014. The government of Jordan grants SACOS the right to mine, process, and develop the oil shale in Wadi Attarat Um-AL-Ghudran area (11 km^2) which lays about 50 km to the east of the study area. SACOS will use the Galoter process (UTT 3000). The project is expected to produce 30,000 barrels per day in addition to an electrical power of 600 megawatts per day (MEMR open file, 2014).

Eight oil shale investment companies have signed MOU's with the government of Jordan to utilize and develop oil shale in Jordan .The companies investigate their claimed areas in details to submit a feasibility study to the Jordan government in order to sign a concession agreement. These companies are summarized in table 2.5.

Table 2.5: : Companies that signed MOU with Government of Jordan for Oil Shale

Company	**Area**	**Proposed pechnoology**
Al_Qamer_for_Energy_and_Infrastructure	Attarat Um-AL-Ghudran	Galter
_Company_for_Oil_Shale(APCO)	Wadi el Na'dieh	Galter
Fushun Mining Group of China	Wadi el Na'dieh	Fushun
Canadian_Investment_Company (GOSH)	Sphere Al – Mahatta Attarat Um-AL-Ghudran	In Capsule
National company for the production of oil and energy(JOSECO)	Sultani	Galter
El-Lajjun oil shale company	Al-Lajjun	Fushun
Whitehorn Canadian company	Wadi Abu Hamam area	In Capsule
Questerre_Energy_Canadian_company	Al Jafr and Isfir Al Mahatta	In Capsule

Chapter 3 ENVIRONMENTAL BOUNDARY CONDITIONS

3.1 Geology of Jordan

The geology of Jordan has been studied since the middle of the 19th century. Bibliographies of early works can be found in Lartet (1869), Blankenhorn (1914), Ionides and Blake (1939), Picard (1943) and Quennell (1951). Extensive descriptions of the geology of Jordan are found in Burdon (1959), Bender (1974), Abed (1982, 2000), Powell (1989 a, b), Masri et al. (2014), and in the Natural Resources Authority (NRA) with the 1:50 000 National Mapping Project Bulletins (1985-2015).

Jordan is located on the western margin of the Arabian Plate and comprising Precambrian basement rocks, Phanerozoic sedimentary rocks and Neogenevolcanics. Precambrian rocks represent the northern part of the Arabian Nubian Shield. They are disconformably overlain by Palaeozoic rocks in the southern part of Jordan and along the rift margins (Fig. 3.1). The Palaeozoic rocks are unconformably overlain by the Cretaceous, Permian, Triassic and Jurassic rocks. A major transgression took place in early Cenomanian and continued to early Palaeogene resulting in deposition of fully marine carbonate sediments of Ajlun and Belqa groups in Jordan (Powell, 1989b).

3.1.1 Structural geology of Jordan

The Dead Sea Transform Fault (DST) is one of the most conspicuous structural features of Jordan that has a long tectonic history from pre-Cambrian to recent times (Quennell, 1956). It separates the Arabian plate to the east from the Sinai and Palestine Plate to the west. The DST Fault is trending N-S and extends more than 1000 km linking the Red Sea spreading centre in the south to the Taurus-Zagros convergence in the north. The DST Fault has been described in terms of plate tectonic theory as a transform fault with a sinistral movement between the Arabian Plate and the Sinai-Palestine Plate (Mackenzie et al., 1970 and Garfunkel, 1981, Kesten et al 2008, Segev et. al.., 2014).

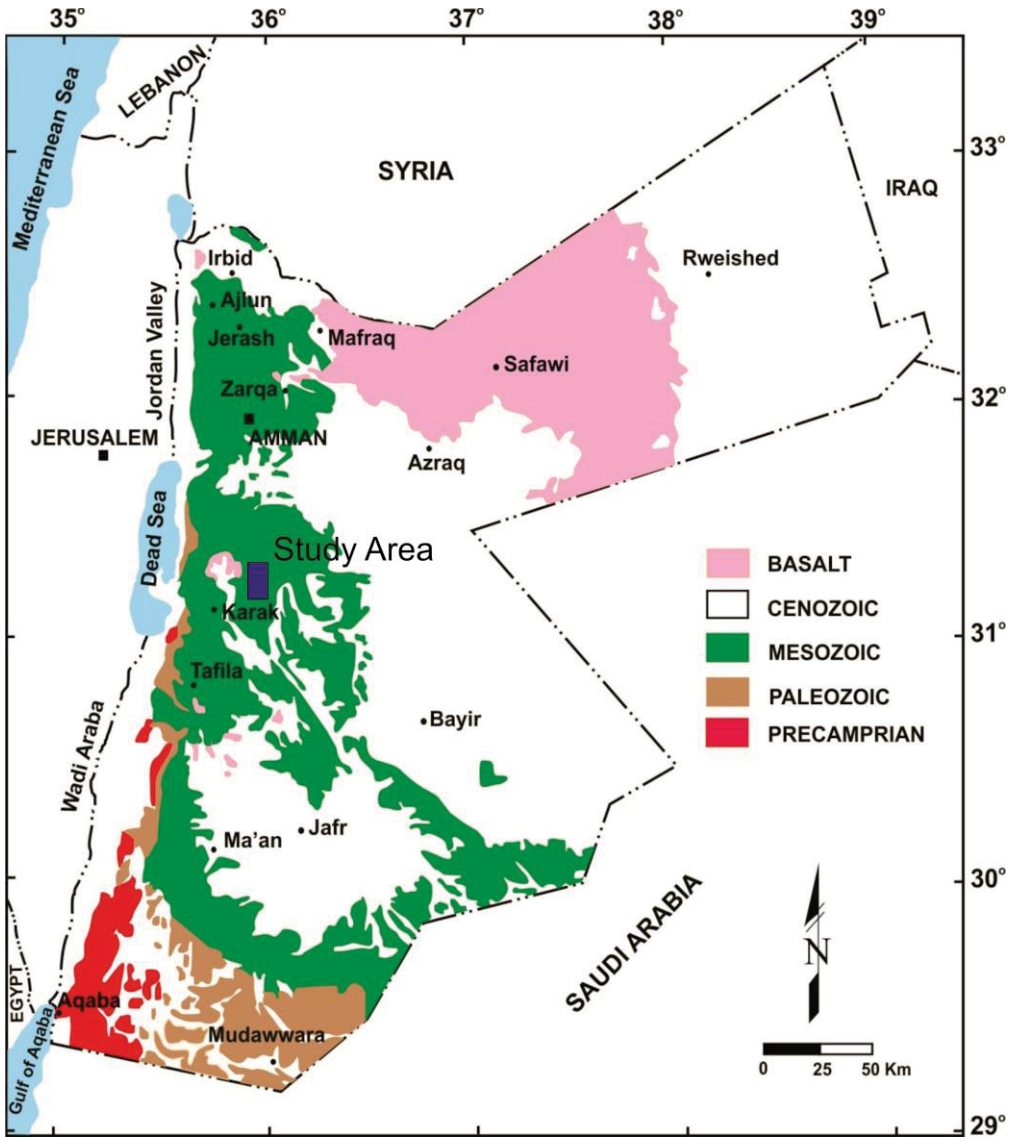

Figure 3.1: Simplified geological map of Jordan (NRA open files, 2013).

The DST consists of two faults: the northern fault, Jordan Valley Fault and the southern fault, Wadi Araba or Risha Fault starts from Gulf of Aqaba to Risha area in the middle of Wadi Araba and to Dead Sea basin along its eastern shore and ends at its northern eastern corner. The Jordan Valley Fault starts in the southern western part of the Dead Sea and continue to the north along its western shore to the east of the Tiberias lake.(Quennell, 1956; Freund et al. 1970; Abed, 1982; Girdler, 1983, Segev etal ,2014).

As a result of major structures (Transverse Fault System and Dead Sea Rift, Syrian Arc) and the continuous northward movement of the Arabian plate, faults of different ages and

trends have developed (Figure 3.2). The main fault trends are E-W dextral strike-slip faults, N-S sinistral strike-slip faults, NE-SW compressional faults and NW-SE tensional faults.

The crossing of the fault systems acted locally as conduits for the Neogene-Pleistocene basaltic flows and intrusions. Many of the E-W faults are traceable for tens of kilometers from the Rift inside the country (Abu Ajameih, 1980, Masri, 2002).

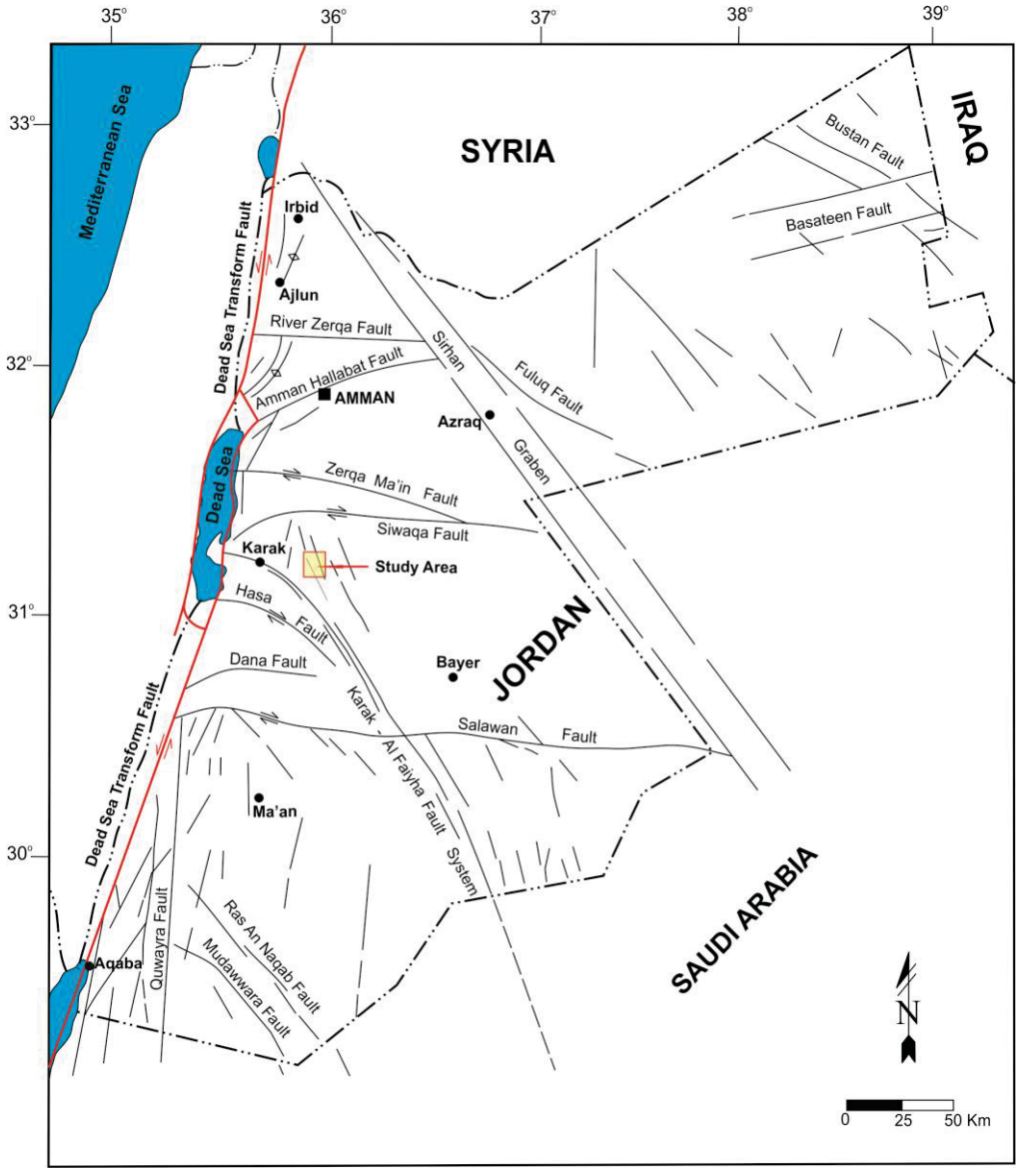

Figure 3.2: The structural map of Jordan (After Diabat and Masri, 2002).

3.2 Geology of the study area

The Cretaceous-Palaeogene succession in Jordan provides an excellent example of the evolution of depositional sequences ranging from alluvial and paralic, through rimmed carbonate-shelf to pelagic ramp settings on a passive continental margin (Powell and Khalil, 2011).

The upper Cretaceous sedimentary rocks are the most dominant formations in the study area; Figure (3.3) shows the geological map of the study area. The upper Cretaceous rocks are composed mainly of marl, chalky marl, oil shale, limestone, chert, phosphorite, silicified limestone, and massive limestone (Powell, 1989b), in addition to alluvial gravels of Pleistocene age.

The Cretaceous-Palaeogene rocks in Jordan are divided into four lithostratigraphical groups (Powell, 1989b); Kurnub, Ajlun, Belqa and Batn Al Ghul. The Kurnub sandstone group consists mainly of continental silicic calstics. The Ajlun Group comprises predominantly marine carbonate platform sediments and six formations. These are represented in upward sequence as in Table 3.1; Naur (A1-2), Fuhays (A3), Hummar (A4), Shuayb (A5/6), Wadi As Sir Formation (A7), and Khuraij Formation.

Neither The Kurnub Group nor The Ajlun Group are exposed in the study area, but they are recorded in some of the deep boreholes within the catchment area. Meanwhile, the study area is mainly covered by sedimentary rocks of the Belqa Group (Campanian-Maastrichtian), Neogenevolcanics and Quaternary sediments (Table 3.1, Fig. 3.3).

Table 3.1 :Lithostratigaphic rock units in Jordan; blue shaded rock units are exposed in El-Lajjun area. Aquifers are yellow shaded (NRA, 2011, open files).

Period	Age	Group	Formation			Aquifers
Neogene	Holocene		Superficial sediments			
	Pleistocene		Lake sediments, garvels, soil			
	Pliocene		Volcanics			
	Miocene					
Paleogene	Oligocene		Dana Conglomerate			
	Eocene	Belqa	WadiShallala			B5
			Umm Rijam			B4
	Paleocene		Muwaqqar			B3
Cretaceous	Maastrichtian		Al Hisa			B2b
	Campanian		Amman			B2a
			Wadi Umm Ghudran		Batn Al Ghul Group (SE Jordan)	B1
	Santonian	Ajlun	Khuraij			
	Coniacian		Wadi As Sir			A7
	Turonian		Shua'yb	F/H/S (Undifferentiated)		A5-6
	Cenomanian		Hummar			A4
			Fuhays			A3
			Na'ur			A1-2
	Aptian-Albian	**Kurnub Group**				K1, K2
Jurassic		**Azab Group**				Aquifer
Triassic		**ZarqaMa'in**				
Permian			Umm Irna Sandstone			
Devonian and Carboniferous (No Records in Jordan)						
Silurian		Khrayim	Khushsha Sandstone			Aquitard
Ordovician			Mudawwara Sandstone			
			Dubaydib Sandstone			
			Hiswah Sandstone			
		Ram	Umm Sahm Sandstone			Deep Sandstone
			Disi Sandstone			
Cambrian			Umm Ishrin Sandstone			
			Burj	Abu Khushayba		
			Salib Sandstone			
Pre-Cambrian		**Aqaba and Araba Complexes** (Metamorphics, Granitoides, Volcanics)				

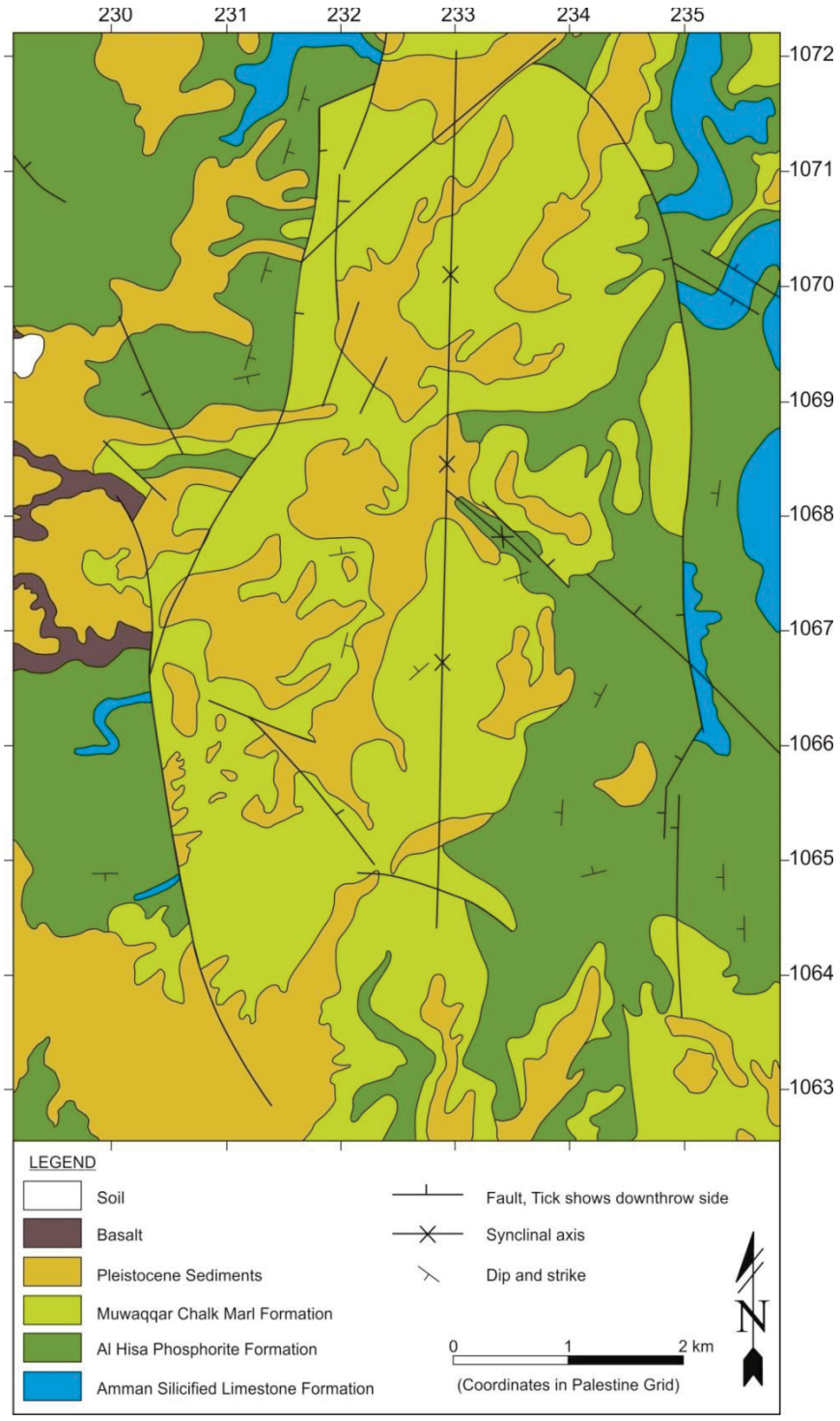

Figure 3.3: Geological map of the study area (After Shawabkeh, 1990).

3.2.1 Ajlun Group

3.2.1.1 Wadi As Sir Formation

Wadi As Sir Formation (Turonian) is not exposed in the study area, but is was recorded in the water wells within El-Lajjun catchment area. Wadi As Sir Formation (A7) is exposed to the north of the study area. This formation consists of medium to thick bedded massive limestone and ranges in thickness from 80 to 100 m. This formation is highly fractured and saturated with water and represents the lower part of Amman-Wadi As Sir (B2-A7) Aquifer System.

3.2.2 Belqa Group

The Belqa Group (Coniacian-Palaeogene) forms the greater part of Jordan Plateau. The sediments of Belqa Group are pelagic chalk, phosphate, marl, chalky limestone, chert, coquina, silicic clastics, and locally bituminous. The Belqa Group comprises six formations (Table 3.1). These are in upward sequence; Wadi Umm Ghudran (B1), Amman Silicified and Al Hisa Phosphorite (B2), Muwaqqar Chalk Marl (B3), Umm Rijam Chert Limestone (B4), and Wadi Shallala Chalk formations (Quennell, 1951, Parker 1970, Powell, 1989b). The exposed rock units in the study area include Amman Silicified, Al Hisa Phosphorite and Muwaqqar Chalk Marl and will be discussed in the following sections:

3.2.2.1 Amman Silicified Limestone

Amman Silicified Limestone Formation (Campanian) is exposed in the north and northeastern part of the study area (Fig. 3.3). The formation consists of massive, hard, dark grey, autobrecciated chert interbedded with dolomitic limestone, chert, chalk, phosphatic chert and phosphaticmarly limestone. The phosphatic facies increase upwards through the formation. The maximum thickness of the formation is 60 m in the Wadi Al Mujib area (Masri, 1996, 2010), and it is up to 55 m thick in the study area (Shawabkeh, 1990). This formation was deposited in a subtidal to shallow shelf environment (Powell, 1988, 1989b, Powell and Khalil, 2011). The formation is locally characterized by small to medium scale syn-sedimentary folds. The massive hard chert beds of this formation producing a distinctive landform with steep slopes.

3.2.2.2 Al Hisa Phosphorite Formation

In Central Jordan, the Al Hisa phosphorite formation (Campanian-Maastrichtian) covers broad areas in southeastern and northwestern part of the study area. The formation was subdivided by Hiyari (1985) into three members, in ascending order, Sultani Phosphorite, Bahiya Coquina and Qatrana Phosphorite (Table 3.1). The high proportion of soft marl, phosphate and phosphatic limestone in Al Hisa phosphate formation make it less resistant to weathering and this is reflected in more gently sloping morphological features than the underlying Amman silicified formation. Bahiya Coquina member is a prominent marker horizon in the Upper Cretaceous of Central Jordan. This is due to its hardness and resistance to weathering, and to the distinctive reef-like appearance with large-scale cross-bedding.

The formation consists of diverse lithologies including phosphate, cherty phosphate, phosphatic limestone, chert, limestone, coquina and marl. Phosphate is economically important and occurs as soft peloids. The formation is up to 70 m thick in Wadi Mujib area (Masri, 1996), and it is up to 60 m thick in the study area. The formation was deposited in subtidal to shallow shelf environment based on the presence of benthic, nektonic fauna and Thalassinoides burrows (Powell, 1989b).

3.2.2.3 Muwaqqar Chalk Marl Formation

The Al Hisa Phosphorite Formation is overlain by the Muwaqqar chalk marl formation (Maastrichtian-Palaeocene). The Muwaqqar chalk marl formation covers broad areas of the area of interest of this study. It is mainly characterized by buff to yellow, soft weathering marl with an absence of stratification (Fig. 3.3). The formation is potentially the most important geological unit from the economic point of view as significant quantities of oil shale occur in the lower part of this formation (Figs 3.4, 3.5). The formation consists of pale yellow, and grey chalky marl, marl and marly limestone. Beds of dark grey bituminous marl “oil shale” up to 86 m thick occur in the lower part of this formation (Shawabkeh, 1991).

The formation shows lateral and vertical variations in thickness in Jordan, The maximum thickness of the Muwaqqar Chalk Marl Formation at outcrop is about 332 m in the northern part of Jordan in the Yarmouk area (Parker, 1970), up 100 m in Wadi Mujib area (Masri, 2010), 100-150 m in central Jordan (Barjous, 1986), and 146 m thick in the study area (Shawabkeh, 1990). This formation was deposited in a moderate to deep marine pelagic environment (Powell, 1989b).

The absences of stratification, morphology, tone and dendritic drainage pattern are prominent features which distinguish the formation from others on aerial photographs and in the field.

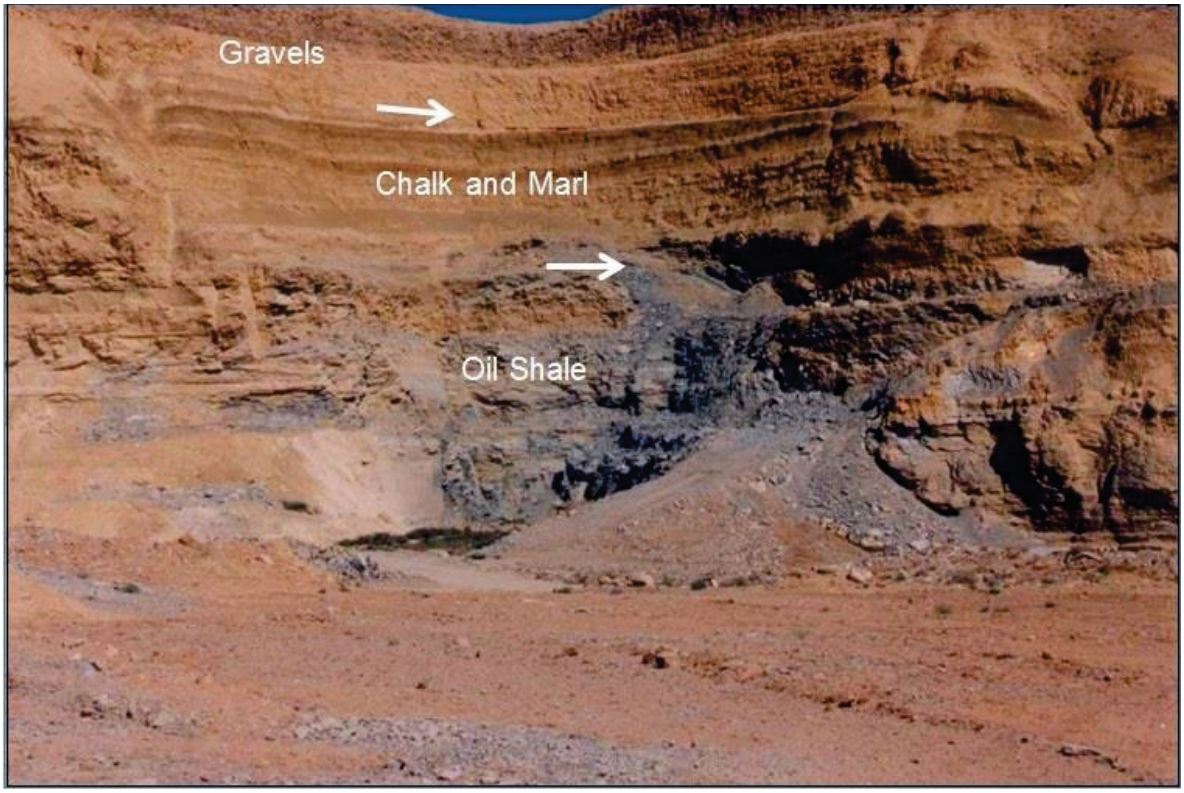

Figure 3.4: Exposure of oil shale in the lower part of Muwaqqar formation in the northern part of the study area (NRA, 2000, open files).

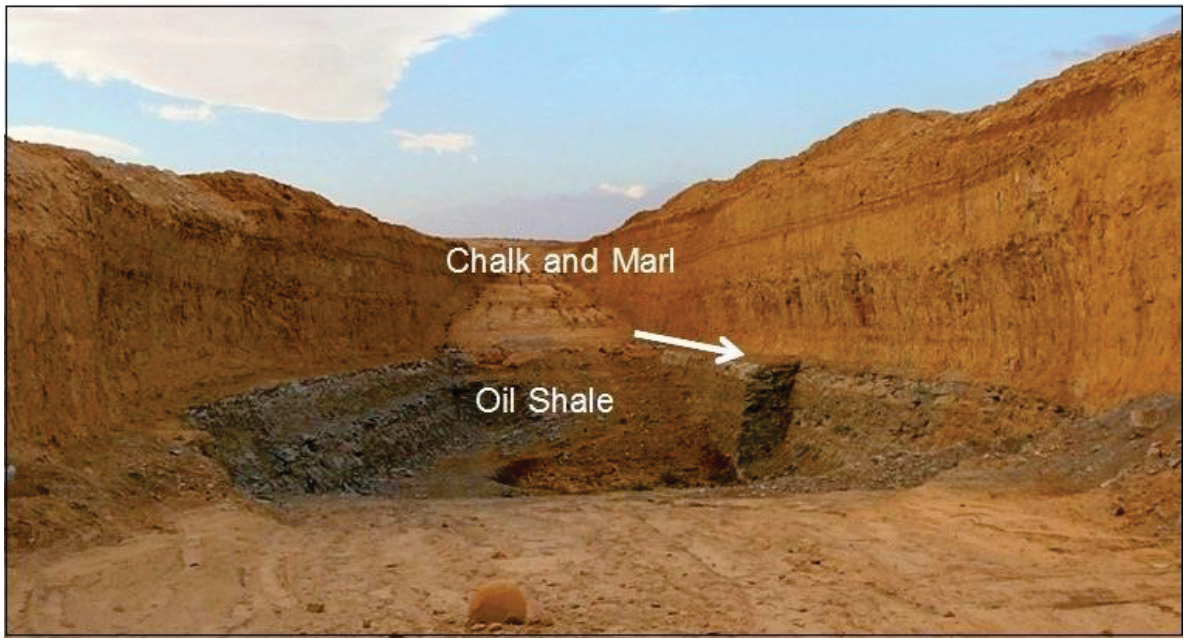

Figure 3.5: Open-pit mine within the Muwaqqar formation in the northern part of the study area. (Photo by the Author, 2014).

The depositional environment was moderate to deep marine (Khalil, 1992). Anoxic reducing bottom-conditions are indicated by the higher bitumen content, probably resulting from a stratified ocean with a dense, anoxic basal water-mass (Powell, 1989b).

3.2.3 Volcanic rocks

Basalts (Neogene-Quaternary) are exposed in the western part of the study area (Fig. 3.3). The basaltic rocks in Jordan are well described by Bender (1968; 1974), Barberi et al. (1979), Ibrahim (1987, 1993, 1996), Ibrahim et al. (1994) and Masri (2010). The basalts in the study area belong to the eastern margins basalts of Jabal Shihan volcano, which is located about 80 km south of Amman and 20-25 km northwest of the study area. The lava poured from the vent some six million years ago (Barberi et al., 1979) covered broad areas including the study area. At present time huge parts of the basalt are covered by soil (Khalil, 1988 and Masri, 1996). The basalt in the study area comprises wadi fill lava, exposed along the present-day wadis. It is composed of blocky, massive, and light grey basalt (Masri, 2010). Chemical analyses indicate that the Shihan basaltic group belongs to the hawaiite and basanite basalt that represent the alkaline series (Masri, 2010).

3.2.4 Superficial sediments

Superficial deposits (Quaternary) in the study area can be differentiated in alluvial gravels, wadi sediments, and Pleistocene gravels. Coarse-grained gravels of different lithologies are present above the present-day drainage levels in the study area. These deposits are poorly sorted and poorly indurated and comprise angular to subangular and subrounded gravels. Alluvial deposits consist of clasts of varying sizes from sand, pebbles and cobbles. Angular to subangular chert and cherty phosphate clasts are the predominant lithology, whereas sub-rounded to rounded clasts are mostly limestone, phosphatic limestone and basalt. This unit is up to 10 m thick and is mostly covered by thin calcareous reddish brown soil (1-2 m) overlain by dark pavement of residual chert and basalt, and rarely limestone. The grain shape and poor sorting suggest a short distance of transport and provenance from the Cretaceous-Neogene rocks.

3.2.5 Structural Geology of the region of interest

Jordan is crossed by different regional fault zones. The Dead Sea Transform Fault (DST), Karak-Al Fayha Fault System and Siwaqa Fault (Fig. 3.2) are the nearest faults zones to the study area: The DST Fault represents the western margin of the Arabian Plate and was formed as suture weakness zone in the late Precambrian (Bender, 1974).

The DST appears to have been left-lateral shearing, first suggested by Dubertret. (1932). The Karak-Al Fayha Fault System, trending NW-SE, and crossing the entire Jordan from the Dead Sea to the Saudi Arabia and extending 300 km in Jordan (Bender, 1974). Siwaqa Fault trending E-W from the Dead Sea to Wadi Sirhan Graben (Fig 3.2). Many accommodation faults in the study area are present between Karak-Al Fayha and Siwaqa faults. These faults are trending NNW-SSE and NW-SE forming graben structures in the study area (Shawabkeh, 1991).

The most important structural elements present in the study area are faults and faulted blocks (Figs 3.2, 3.3). The study area is bounded by two major faults (Fig. 3.6) trending NNW-SSE forming major, elongated graben (i.e. El-Lajjun Graben).

The graben is marked by a broad topographic low consisting of down faulted Muwaqqar Chalk Marl formation overlain by Pleistocene gravels.

It is considered as the most important graben in central Jordan where considerable thicknesses of oil shale deposits are preserved in the lower part of the Muwaqqar chalk marl formation (Abu Ajamieh, 1980, Shawabkeh, 1991). The southern part of El-Lajjun Graben is symmetrical, and tilted to the west-northwest, the deepest part of the graben is near the western boundary fault, where the downthrown is up to 150-200 m (Shawabkeh, 1991).

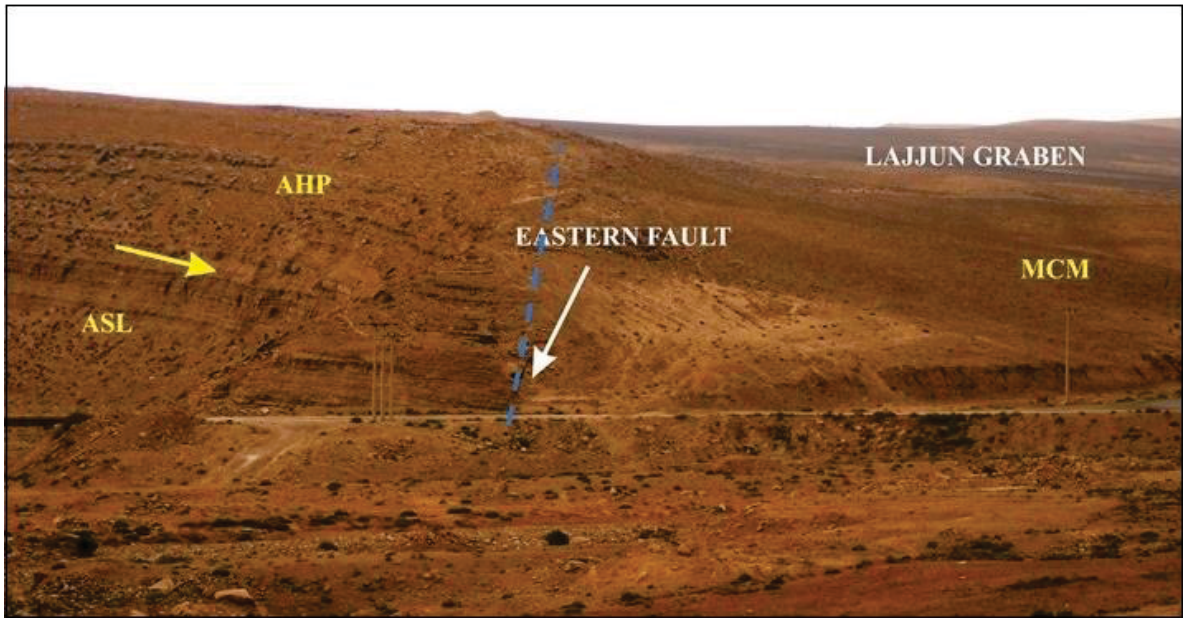

Figure 3.6: Exposure of the eastern fault (white arrow) of El-Lajjun Graben forming a topographic low in this part of the study area. The rocks exposed on both sides of the fault are Amman silicified limestone (ASL), Al Hisa Phosphorite formation (AHP), and the Mu

3.3 Hydrogeology

3.3.1 Hydrogeology of Jordan

3.3.1.1 Climatic Conditions

Jordan represents an area of about 89.600 km^2, located in the northwestern corner of Arabian Peninsula. The dominant climate is the Mediterranean type (Kottek et. Al. 2006), where the average rainfall is less than 300 mm/y. Summer starts around mid of May and winter starts around mid of November, with two short transitional periods in between (autumn and spring). The prevailing wind direction is northwest, west and southwest. Precipitation in Jordan falls normally in rainfall form, snowfall occurs normally twice or three times a year. The average rainfall differs between the northern highlands (650 mm/y) and the desert area, which has an average less than 30 mm/y. Most of Jordan areas receive less than 100 mm as an annual average rainfall, which represents 7200 10^6 m^3/year. This information is presented in (Fig. 3.7) (Jordan Climatological Hand Book 2000).

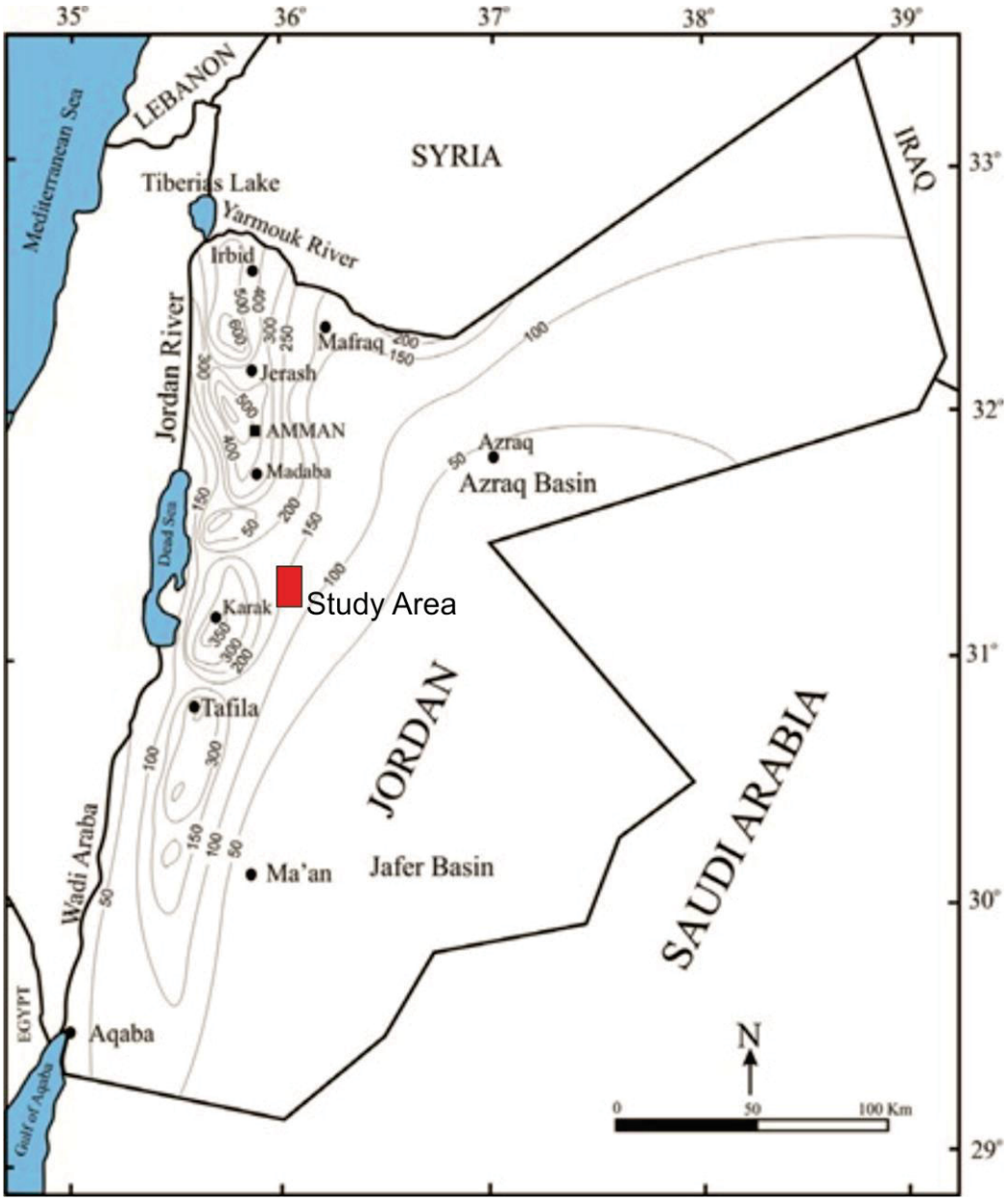

Figure 3.7: Rainfall long-term (1938-2010) average distribution (after WAJ open files).

3.3.1.2 Water Resources

Surface water and groundwater are considered as the main water resources in Jordan. Surface water is represented by the direct uses of the runoff and dammed water on many down streams, which is used mostly in agricultural aspects. On the other hand, the groundwater resources are the main water supply for drinking purposes. (Salameh and Banayan, 1993).

3.3.1.2.1 Surface water

There is a limited amount of surface water in Jordan and adjacent areas due to low rainfall and high evapotranspiration. The stream flow characteristics follow the precipitation pattern and increase from east to west where it is getting closer to the Mediterranean moisture. Also it decreases from north to south of the country due to increase of both temperature and evaporation (Exact 2000).

There are fifteen surface water basins distributed in Jordan as permanent and flood flows The Yarmouk River Basin drains both base and flood flows of Syrian and Jordanian territories .It is the major contributor of about 40% of the total surface water in Jordan (NWMP, 2003). Other major basins include side wadis of Jordan River, Dead Sea Zarka, Mujib, Hasa, and Wadi Araba. Table-3.2 shows the total flow and the areas of the main surface water basins.

The study area is located within Wadi Mujib catchment (including Hidan).The catchment of Wadi Mujib is located in central Jordan and consists of two major sub-catchments; Wadi Waleh/Heidan and Wadi Mujib, with a total catchment area of about 6.596 km². The catchment area ranges in elevation from about 700 -900 m above sea level (a.s.l) to about 1100m (a.s.l) near Karak and Mazar. Precipitation over the catchment area fall in a form of normal rain, and it is very rare to have a snow expect some times over Mazar city. The rainfall ranges from 350 mm/y over the high mountains and about 100 mm/y at the shoreline of the Dear Sea. The potential evaporation is very high at the Dead Sea shores (estimated about 2450 mm/y), while it is about 3500 mm/y in the eastern part of the catchment area. Wadi Mujib major catchment discharges about 83 10^6 m^3/y directly to the Dead Sea. This was before the construction of two Dams at the main wadis on the catchment (Mujib Dam, and Wala Dam). The catchment of the Mujib dam has a total length of about 765 m, a maximum high about 62 m, and a reservoir length 5 km. The storage capacity of the dam reservoir is about 32 10^6

Table 3.2: The area and total flow of main basins in Jordan (NWMP.,2003).

Basin	**Area (km^2)**	**Total flow (10^6 m^3/yr)**
Yarmouk	6790	360
Jordan Valley	18194	400
North Jordan river Side wadis	267 (W. Al-Arab) 106 (WadiZiglab)	28 10
South Jordan river Side wadis	180 (WadiShueib) 189 (WadiKafrain)	5.71 6.4
Zarka river	4025	64.88
Dead Sea	272 (W. ZarqaMa'in) 190 (WadiKarak) 972 (in between Wadis)	30 18 30
Mujib	6596	83
Hasa	2520	34
North WadiAraba	2938	26
South WadiAraba	1278	1
Southern desert	4400 (W. El-Yutum)	1.5
Azraq	11600	27
Sirhan	15155	-
Hammad	19270	10
Jafer	12200	15

The study area is located in the southern part of Wadi Mujib catchment and the drainage surface water system is directed to the North- North West to Mujib Dam (Salameh and Banayan, 1993).

Jordan has built ten dams on the main streams and rivers, the actual water storage volume dependent on rainfall. Figure 3.8 shows the location of these dams and their potential annual water storage volume.

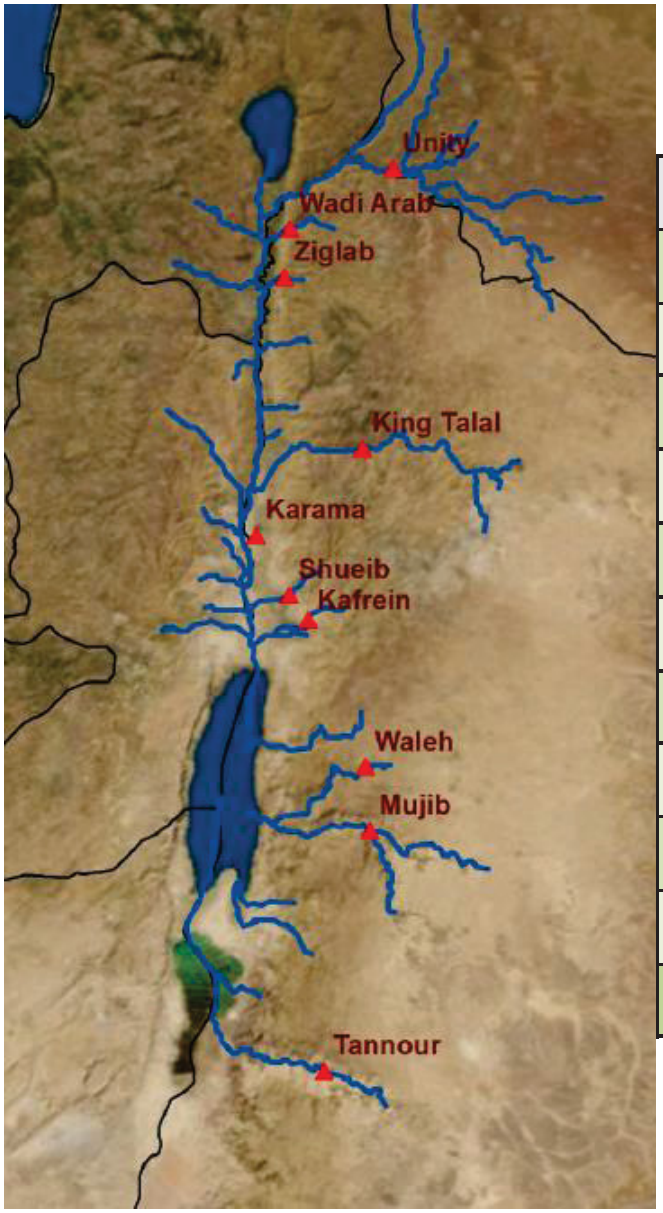

Dam	Storage 10^6 m^3/YR)
Unity Dam	110.0
WadiAraba	17.0
Ziglab	3.8
King Talal	75.0
Karama	55.0
Shueib	1.4
Kafrein	8.4
Waleh	9.3
Mujib	35.0
Tannour	16.0
Total	331.7

Figure 3.8: Dams along rivers and side valleys in Jordan, along with their annual storage capacity in 106 m3 per year.(modified after Altz-Stamm, 2012).

3.3.1.2.2 Groundwater

The Groundwater aquifer systems in Jordan are divided into three main systems, namely, the deep Sandstone Aquifer, the intermediate aquifer system, and the Shallow Aquifer system.

1. Deep Sandstone Aquifer System

This aquifer system consists of two main aquifers: The Ram Group (Disi Sandstone) and the Kurnub/Zarqa aquifers. The Disi Sandstone Aquifer is the deepest and the oldest water bearing sediments in Jordan of Paleozoic age. This aquifer underlies most of the country area and it crops out only in the southern parts of Jordan in Muddawara and Qa' Disi, Wadi Yutum, and southern part of Dead Sea region forming the fresh water. Large parts of this aquifer probably contain mineralized groundwater (Bender 1974).

The Kurnub/Zarka Aquifer (Jurassic-Lower Cretaceous) is overlying the Disi aquifer and extends excessively in Jordan. This aquifer also consists of sandstone, crops out along the Dead Sea escarpment and along Zarka River basin. Due to the small outcrop area the aquifer has limited direct recharge. Nevertheless, this aquifer has fairly good yields, the sandstone aquifer system is considered hydraulically as one unit (Bender 1974).

2. Intermediate Aquifer System

This aquifer system of upper Cretaceous age is considered as the most important aquifer system in Jordan, it's mainly composed of limestone and carbonates rocks and hydraulically separated from the underlying sandstone aquifers by marly limestone and marl of rock formation (Cenomanian age). This aquifer has a highest groundwater recharge rates in western highland of the country where it's cropping out. While it is confined by the thick layers of marl rocks of Upper Cretaceous and Lower Tertiary age to the east, the groundwater flows partly to the western of Dead Sea escarpment.

The groundwater flows after infiltration partly toward the western escarpment, and mainly towards the east of the Dead Sea escarpment forming groundwater divide. This groundwater infiltrates through the aquitard of underlying (Cenomanian age) rocks down to the deep sandstone aquifer complex (Salameh and Udluft, 1985).

3. Shallow Aquifers System

This system consists of two main aquifers:

a) The Basalt aquifer consists of basalts (Neogene -Quaternary age) which extend from southwestern Syria (Jabal Druz) toward Azraq and Wadi Dhuleil region northeastern

Jordan. The precipitation water in the elevated area of Jabal Druz recharge this aquifer and the groundwater flow is in radial form to all directions. (Agrar und Hydrotechnic, 1977).

b) The Sedimentary Rocks and alluvial deposits of Tertiary and Quaternary age. These types of aquifers are distributed all over the country forming local aquifers, overlying partly the complexes mentioned above. They are mainly occurring in Jordan Valley, Yarmouk River area, Wadi Araba and in the eastern desert area. These types of aquifers are recharge directly from the surrounding aquifers or through the underlying basalt aquifer. (Salameh and Bannayan, 1993).

3.3.2 Hydrology of the study area

3.3.2.1 Topography

The study area is located within the Highlands Topographic region, which is one of the three elongated distinctive topographic provinces in Jordan that are trending in general north – south direction (Salameh and Bannayan,1993). The topography of the study is characterized by hilly morphology with gentile to moderate slope terrain. It forms the eastern pediment plan of mountainous physiographic province in Central Jordan. The topographic elevation varies from 620 m (a.s.l) in the lower wadis, and 880 m a.s.l at the top of the existing hills (mountains) (Fig. 3.9). However, there are various hills in the site which penetrated by wadi systems that holds seasonal floods during the wet seasons. These wadis host most of the vegetation in the area while the hills and the small flat platoons have very low vegetation covers respectively is restricted to an annual herbaceous cover.

3.3.2.2 Climate and rainfall

The study area is characterized by the Saharan Mediterranean bio-climatic zone. It extends from south of Jiza until Aqaba at the southern tip of the Jordan Rift valley, Generally the climate is characterized by the relatively short rainfall period during the cool winter season between November and March while the summer season is characterized by an extensive drought. However, rainfall varies considerably in space and time**.** The amount of the rainfall in El-Lajjun area decreases from northwest to southeast to the west

of Karak. The average rainfall reaches 300 mm/yr. in the highland area. With decreasing elevation the average amount of rainfall drops drastically towards east, reaching around 190mm/yr. in Al-Lajjun. In the northwestern corner of the study the rainfall is around 200mm/yr. and in the southeastern corner is around 170 mm/yr.

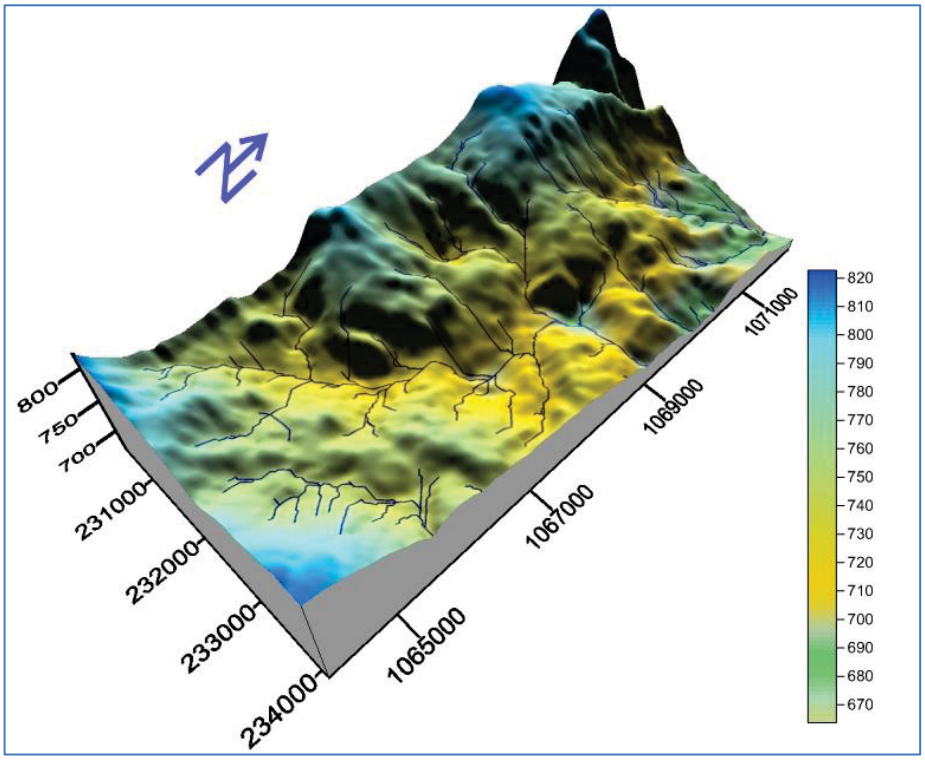

Figure 3.9: 3D topographic map of the study showing; the morphology, distributions of the elevations and the drainage system.

Temperature also varies in an east – west direction across the study area. According to the Rabba' climatologic station which is in the western part of the study area, the average minimum temperature of the coldest month is 1.2 – 7.2 ºC while the maximum temperature of the hottest month is 30.2 – 36.3 °C. (Jordan Climatological Hand Book 2014).

3.3.2.3 Stream discharge

The discharge from the intermediate aquifer system in El-Lajjun catchment area is represented by the only water spring (Ain Al-Lajjun). The spring is located at the northern

part of the study area, and emerges effectively by El-Lajjun Graben. The discharge of this spring is measured since 1947. The measurement were, unfortunately, very rare. There were not more than 4 measurements per year. Hence the discharge is very difficult to evaluate. The long term average measured discharge of this spring is approximately 1039.5 m^3/h (0.3 $*10^6$ m^3/year).

3.3.3 Hydrogeology of the study area

The catchment of the study area (Wadi El-Lajjun) lies between the coordinates 215800 - 240000 E and 1049000 – 1073000 (according to Palestine Belt Grid, and covers an area of about (370 km^2). Wadi El-Lajjun catchment area is part of the Wadi Mujib groundwater catchment located in the southern part of it (Fig 3.10).

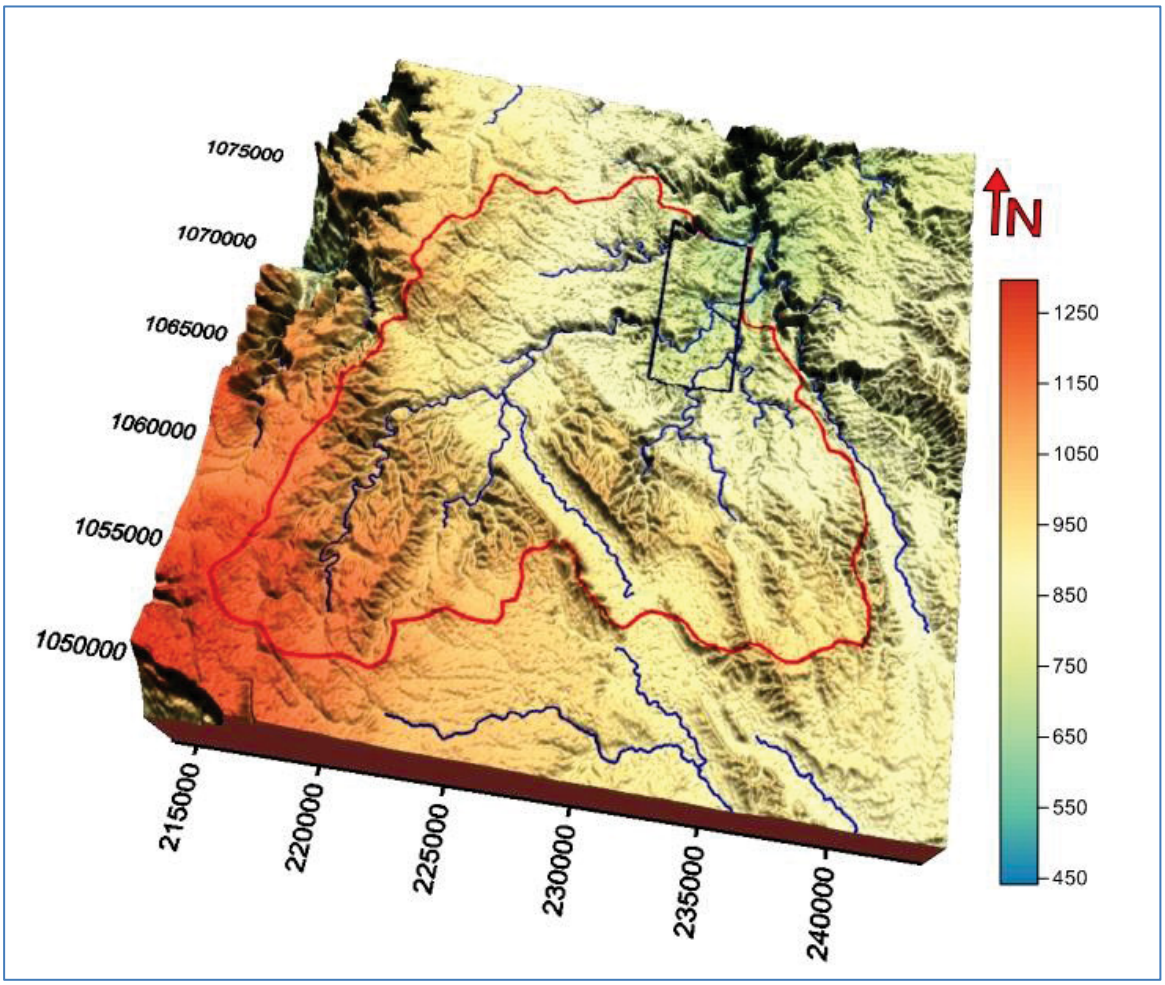

Figure 3.10: Location map of the project area within the drainage system of El-Lajjun catchment area.

3.3.3.1 Aquifers

The hydrogeology of the study area is controlled by the geological setting, which controls the piezometers, occurrence and movement of the groundwater, and the distribution of productive areas in the aquifers (BGR, 1987). The main aquifers in El-Lajjun catchment area consist of two main systems: the intermediate aquifer system (Amman Wadi As Sir Aquifer) (B2/A7) and the deep sandstone aquifer system (Kurnub /Ram Group) Aquifer. The most important aquifer system in the study area is the intermediate aquifers system (Amman- Wadi As Sir Aquifer) the B2/A7. It attains a combined thickness of around 320 m of which, however, only a portion is saturated.

The B2/A7 aquifer is underlain by the (A1\6) sequence, consisting predominantly of marl, marly limestone and limestone. This sequence is regarded as an aquitard. It hydraulically separates the B2/A7 aquifer from the underlying Kurnub/Ram Group aquifer. In this aquifer, hydraulic head is much lower than in the B2/A7 aquifer, confirming the hydraulic function of the A1/6. Muwaqqar Chalk Formation (B3) is also regarded as an aquitard, and overlies the Amman- Wadi As Sir Aquifer B2/A7 (Bender et.al, 1987).

There are many wells in and around the study area, but there are about 34 wells in close distance to the study area (Appendix 1). The depth of these wells range from 158 to 1050 m. A total of 28 wells penetrate the Amman - Wadi As Sir Aquifer systems (B2/A7). The yield of these wells ranges from 17 to 270 m^3/hr. Ten wells penetrate the Kurnub and Ram aquifer with a yield of 40 to 120 m^3/hr. (WAJ open files, 1990).

1. **The Intermediate Aquifer System(B2/A7**)

Amman- Wadi As Sir Aquifer (B2/A7) is the upper most important aquifer in the study area and regionally. It is important for the groundwater development as well. This aquifer system consists of two major formations; Amman (B2) and Wadi As Sir (A7). The two formations are hydraulically interconnected. The formations are separated by Um Ghudran formation (B1) which acts an aquiclude and/or as aquitard (JICA, 1986). The aquifer system mainly consist of silicified limestone, marly limestone, phosphatic rocks, marl and chert,(Bender, 1974). The units of the aquifer system are semi-uniform, and widespread in the study area with a thickness lays between 100 to 300 m (Abu Ajameh, 1980). In the western part of Wadi Muijb catchment, the B2/A7 acts a phreatic aquifer. However, the precipitations penetrates directly through the fractures, faults and joint of the outcrops rocks of Amman and Wadi As Sir formations. In the eastern part of Wadi Mujib catchment,

the overline Muwaqqar formation (B3), acts as confined layer, in the meantime. The Aquifer is underline by Ajloun Group (A1-6) which can be considered as aquitard. However, it forms low-permeable base to the aquifer (B2/A7) (BGR 1987).

There are many water wells drilled in the catchment study area that are penetrating this aquifer system. The depth of these wells ranges between 196 m (CD3499) to more than 378 m (CD3225) (Appendix 1).

According to the drilling files of Water Authority of Jordan (WAJ), the horizontal hydraulic conductivity ranges from 0.5 m/d to approximately 9 m/d. The transmissivity in the Wadi Mujib catchment area ranges from 100 to 400 m^2/d (about 100 m^2/d in El-Lajjun catchment). However, the hydraulic parameters of this aquifer system are quite variable, and that is expected of the limestone aquifer. The system is considered productive when it has fissures and joints (Abu Ajameh, 1980).

The hydraulic parameters in the study area, shows that the general conductivity increases SW direction, while the faulting system is NNW-SSE, which involve the El-Lajjun graben as well. This indicates the fact that the faulting system is controlling the groundwater movement trend NW direction (Fig: 3.11).

These faults structure behave like barriers, which are effecting the groundwater movement of the intermediate aquifer. Some major faults are acceding and extending to influence the groundwater movement of the deep sandstone aquifers of Kurnub/Ram Group aquifer.

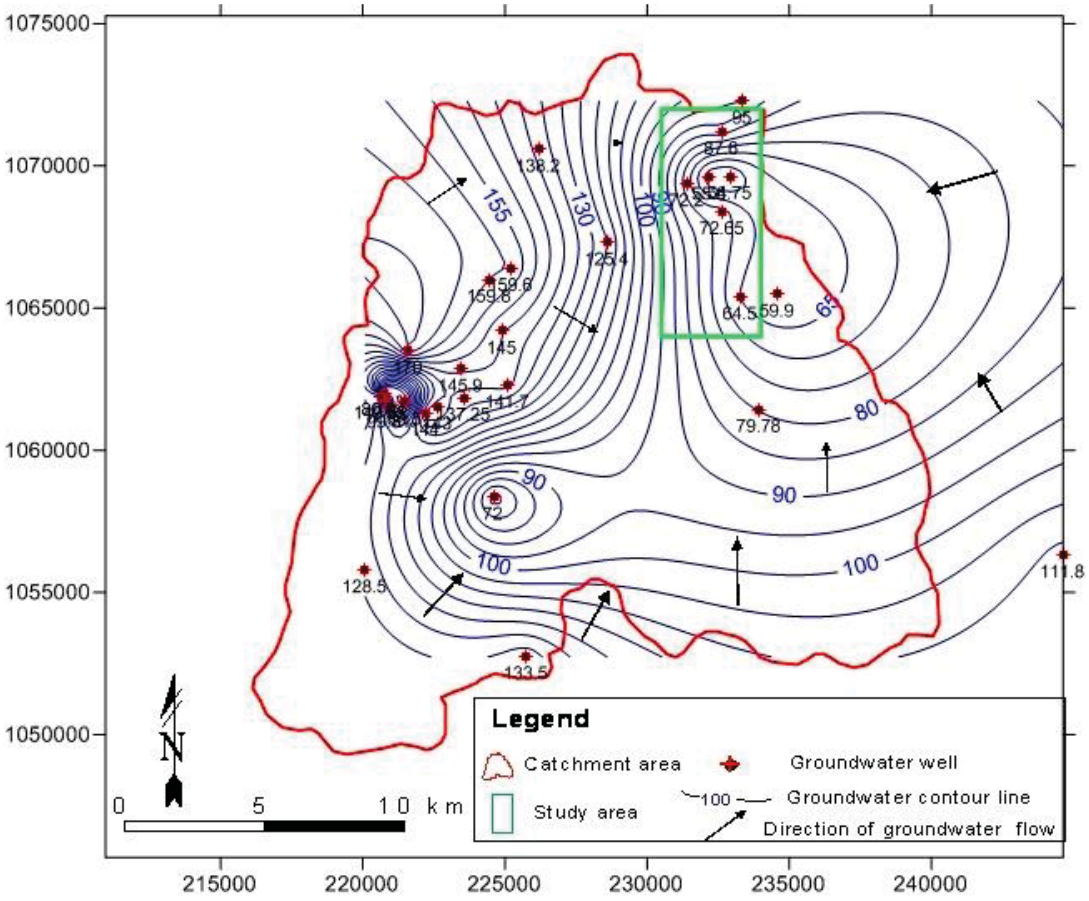

Figure 3.11L Groundwater Movement Map for B2/A7 Aquifer in the catchment area

2. The Lower deep aquifer system

A. The lower Palaeozoic rocks

The lower Paleozoic rocks in Jordan comprises two groups; the Ram Group of Cambro-Ordovician age and the younger Khreim Group of Ordovician-Silurian age. Ram group rests unconformable on the basement rocks of Precambrian Complex (Aqaba-Araba Complexes). Both groups crop out in the southern desert. Ram Group extends southwards into Saudi Arabia and northwards to the east shoreline of the Dead Sea. Ram Group occurs at depth of 1500 m to more than 3000 m in east and northeast Jordan, and it is 500-1000 m in southwest and central Jordan (Powell 1989 b).

Khreim Group overlies the Ram Group in east and south Jordan, but Khreim is absent in west of Jordan and so the Ram is directly overlain by Permo-Teriassic and Jurassic rocks

in the south west and by the Kurnub sandstone of Cretaceous south west Jordan (Charalambous, 2016). In general, the base of the Khreim Group dips from the outcrop areas to the northeast and the increase in thickness follows roughly the same direction. (Andrews, 1991). Khreim comprises alternating cycles of siltstone and micaceous sandstone subordinate mudstone. it is defined of graptolite-bearing at the base formation. (Powell 1989 b).

Groundwater bearing rocks in Khreim is of poor quality and the rocks acts locally as an aquitard and separates Ram sandstone (Disi Aquifer) from the Kurnub/Zarka Aquifer (Jurassic-Lower Cretaceous) and is interconnected through the Khreim Group on the large scale.,These rocks are considered as a single basal Aquifer system and hydraulic complex (Agrar- und Hydrotechnic, 1977).

The Ram Group is divided into five formations. The top two formations are Umm Sahim and Disi sandstone. They have been exploited for groundwater (Appendix 1). Ram has a thickness, in general, of about 500m, and is rapidly increasing towards the east and the north east to reach more than 2500 m in thickness (Abu Saad and Andrews, 1993).

The top formations of the group comprises reddish-brown, hard, and ferruginous sandstone and white-cream friable sandstone in the Disi formation, and consists of uniform medium to coarse-grained quartz sandstone intercalations of minor Kaolin thin layers (Powell, 1989 b).

The Precambrian basement rocks are at the base of Ram Group. The aquifer is unconfined in general where it crops out, and at the top of the group is defined by phreatic surface. Groundwater occurs in Khreim and Ram groups, in Khreim occurs with of poor quality, while The Ram Group constitutes fertile aquifer with a good water quality in general (Agrar- und Hydrotechnic 1977).

The hydraulic parameters from pumping test done for different groundwater wells of the Ram Aquifer indicates that the Transmissivities range from less than 100 $m^{2/}$day to approximately 6000 m^2/day, the permeability ranges from 0.2 to 20 m/day, the storage coefficients ranges from 0.001 to 0.0001, and specific yields from 1.5 to 14% (Charalambous, 2016).

B. The Mesozoic (Kurnub Sandstone Group)

This formation of Lower Cretaceous age consists mainly of varicolored sandstone, massive whitish sandstone, intercalations of clay stone, and siltstone slightly cemented. This aquifer is overlained by about 400 m of A1-A6 quitard. Kurnub sandstone does outcrop neither in the study area nor in the El-Lajjun catchment (Bender et.al, 987). The thickness of this formation ranges from less than 400 m to more than 500 m in the project area. Very few wells have been drilled in the Kurnub aquifer and pumping test date is completely unavailable. Based on the Lithology of this unit, Howard Humphreys LTD., (1986) assumed that permeability ranges between 0.1 m/d to 1 m/d and that transmissivity reaches 20 m^2/d to 80 m^2/d.

Khreim group separates Ram sandstone (Disi Aquifer) from The Kurnub/Zarka Aquifer (Jurassic-Lower Cretaceous). However they are interconnected through the Khreim Group on the large scale, and they are considered as a single basal Aquifer system and hydraulic complex (Agrar- und Hydrotechnic, 1977).

The groundwater movement of the Deep Sandstone Aquifer system (Kurnub/Ram Group Aquifer) in El-Lajjun catchment is generally from SE to NW towards Wadi Mujib. However, it is generally thought that the movement of Ram Group is from the outcrop area south Jordan and North Saudi Arabia towards Central Jordan. Eventually it emerges at or below sea level at the Dead Sea and recharging it (Charalambous, 2016) as presented in (Fig. 3.12). Recently, a new model done by BRM suggested that small amount of the flow reaches Dead Sea from Saudi Arabia, much of flow converges near the Jordan–Saudi border where it leaks upwards into younger strata in the Sirhan–Azraq graben along permeable fault planes (BRGM 2006).

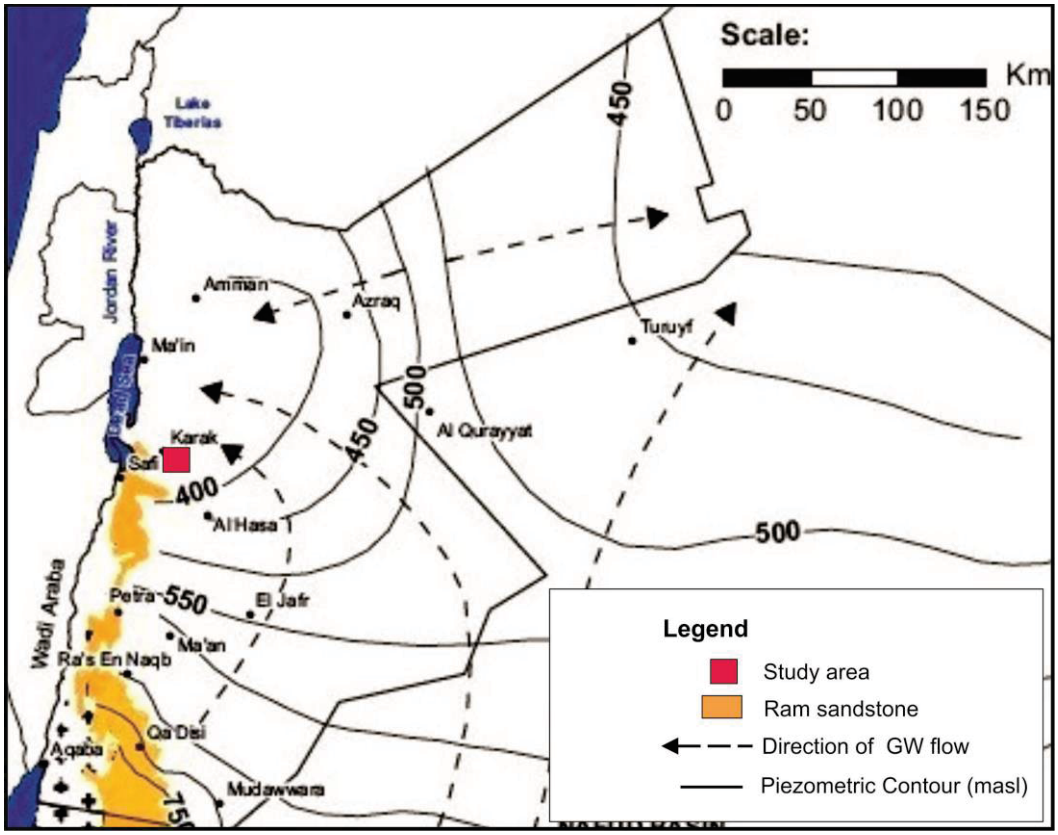

Figure 3.12: Regional groundwater flow of Ram aquifer in Jordan from NW Saudi Arabia (Modified after Charalambous, 2016).

3.3.3.2 Aquitards

The sequence rocks of (A1\6), which are underlining the intermediate aquifer system (B2/A7), are considered as a local aquitard. It separates hydraulically the B2/A7 aquifer from the underlying Kurnub/Ram Group aquifer. The Muwaqqar Chalk Formation (B3), which contains the Oil shale layers is also considered as aquitard, and overlies the Amman- Wadi As Sir Aquifer B2/A7 (Bender et.al., 1987).

The Khreim group of Paleozoic rock often acts as a local aquitard. It separates the Ram sandstone (Disi Aquifer) from the Kurnub/Zarka Aquifer (Jurassic-Lower Cretaceous). However they are interconnected through the Khreim group on the large scale, and it is considered as a single basal aquifer system and hydraulic complex (Agrar, 1977, Salamehand Bannayan, 1993).

Chapter 4 MATERIAL AND METHODS

4.1 Data Management

The data used in this work were collected from previous studies, literature review, field work, laboratory analysis, and experimental results.

All geological maps with different scales, geological bulletins and reports, technical reports, M.Sc. and Ph.D. thesis, unpublished and internal reports related to oil shale, geology, hydrogeology and hydrochemistry, extractions, and investment were gathered and carefully evaluated.

4.2 Field work and sampling

Many field trips have been carried out to El-Lajjun area and the surroundings of central Jordan. Besides, all previous data regarding geology, lithology, chemistry, and mineralogy were collected and reviewed. According to that, ten representative oil shale (OS) rock samples (with a total weight of about 20 kg) were collected from different localities of oil shale exposures and from the open-pit mine within the Muwaqqar formation in the northern part of the study area.

The Cretaceous kaolin samples used in experiments of the immobilization of trace elements were collected from Batn Al Ghul (Jabal Al Harad) in the south of Jordan about 70 km south of Ma'an city. The phosphate sample used in the column leaching experiment was collected from the field as well.

Groundwater samples were collected from different water wells in the study area representing the ground water from the intermediate and the deep sandstone aquifers.

4.3 Laboratory experiments

Representative oil shale samples were collected from various locations. The sampled specimens were air-dried, crushed, milled, homogenized, and passed through 8-mesh sieve (2.36 mm opening). A compost sample (about 2 kg) was treated to obtain the spent shale by extract the shale oil from the samples by using the Fischer Assay method.

4.3.1 Fischer assay method

The Fischer assay is a laboratory standard test used for the determination of shale oil yield (Dyni 2006). The technique was modified in the United States and adapted for analyzing the oil shale of the Green River Formation (Stanfield and Frost, 1949).

The oil shale samples were crushed to an appropriate size (2.36 mm or 8 meshes) and then heated up to 520 °C in a cast aluminum-alloy retorts for 40 minutes. The reaction products (vapors of oil, gas and steam) were cooled in the condenser and then gradually collected in centrifugal tubes (Dyni, John R., 2006) as shown in Figure. 4.1.

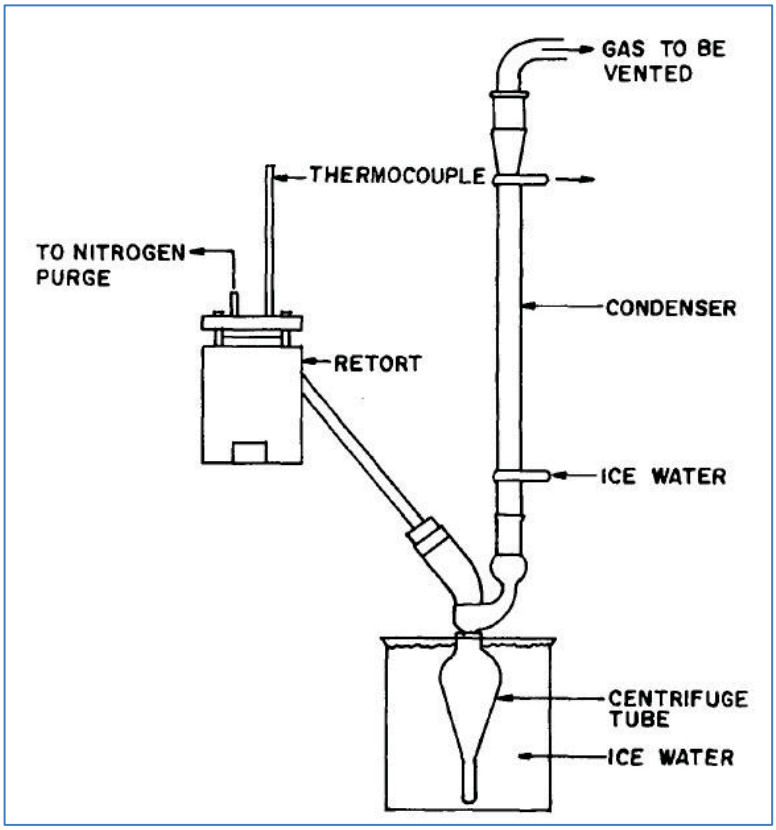

Figure 4.1: Simplified sketch for the Fischer Assay method (after Heistand, 1976).

The spent shale (SS) samples resulting from several runs of the Fischer assay methods were milled, grinded, and passed through 104 μm mesh. These steps were done with the

origin oil shale samples as well. The samples were then considered to be ready for the sequential extraction method and other experiments for this research.

4.3.2 Sequential extraction

Sequential extraction is an analytical process that leaches elements from sediments, soil, and sludge samples in order to distinguish between the different binding forms of elements (Tessier et al.,1979).

The extraction procedure in this study has been used to evaluate the changes in the mobility and distribution of Ti, V, Cr, Co Zn, As, Zr, Cd, Pb, and U. The assessment of elements mobility and environmental influence becomes possible based on these partitioning into specific fractions.

The sequential extraction procedure used in this study was a procedure modified after Zeien and Brümmer (1989) and according to Gonzalez-Alcaraz et al. (2013). This method was used previously by several authors such as Rinkleb and Shaheen (2014), Ghrair (2009, Luo and Christie (1998), and Bell et al. (1991).

Two samples were used: the first one was oil shale (OS) and the second one was spent shale (SS). Both OS and SS samples were crushed into 105 µm.

The trace element fractions defined by extraction solution used and shaking times are given in (table 4.1)

A 2 g of homogenized dried OS and SS sample was added to 50 ml extraction agent and shaken at room temperature for a certain time (table 4.2). After wards samples were centrifuged for 15 minutes at 2500 rpm. Then solutions were filtered with a pore size of 0.2 µm. Blank samples of all extraction fluids (50ml) were taken as well.

The total metal content (F7) was determined by digestion of 0.5 gram of samples dissolved in concentrated acids (HCL, HNO_3 and HF in the ratio of 3:1:2) (e.g. HCL: 15ml, HNO_3: 5 ml and HF: 10ml) respectively using molarity of HCL=11.599 M, HF =22.99M, and HNO_3 = 15.7 M. Acids and samples were kept in platinum dishes for more than 7 h., then removed to Teflon cups and heated on a hot plate for 2 hours. (89 - 95 C˚). Furthermore, 20 ml (± 5ml) of boric acid (0.35M H_3BO_3) were added to each sample.

The residual fraction can be estimated from the subtraction of F7 minus ∑ F1-F6

The mobilization of elements decreases mainly in the order: soluble (mobile) > exchangeable > sorbed and bound to carbonate) > Fe–Mn oxide > bound to organic > residual (Ma and Rao, 1997).

Table 4.1: The trace elements fractions defined by extraction solution used and shaking time (modified after Zeien and Brümmer, 1989, Ghrair 2009).

Symbol	Fraction	Extraction Solution	Shaking Time
F1	Mobile Soluble + Exchangeable fraction	1M NH_4NO_3, Ph 7	24 h
F2	Bound to carbonates (Easily mobilizable fraction)	1M NaO Ac-HO Ac pH 5, adjusted with 50% acetic acid	6 h
F3	Bound to Mn oxides	0.1M NH_2OH-HCl +1M NH4O Ac pH6, adjusted with NH_4OH solution.	30 min.
F4	Bound to organic matter	0.025M NH4-EDTA pH 4.6, adjusted with NH_4OH solution	90 min
F5	Bound to amorphous and poorly crystalline Fe oxides	0.2M NH_4-oxalate pH 3.25, adjusted with NH_4OH solution	4 h
F6	Bound to crystalline Fe oxides	0.1M ascorbic acid in 0.2 M NH_4-oxalate pH 3.25, adjusted with NH_4OH solution	30 min. in water 96 C
F7	Residual fraction	Total metal content minus sum of extracted fractions = (F8 – (ΣF1–F6))	by calculations
F8	Total metal content	Complete digestion by Aqua Regia Conc.($HCl+HNO_3$) + HF andH_3BO_3	

4.3.3 Column leaching experiment

The spent shale, which is one of the residues of oil shale extraction technologies that are proposed in El-Lajjun area, contains at least 75% of the original material (Hamarneh, 1998). This huge amount of ash must be stored in certain places which are environmentally safe. The ash is hot (at the first few days), fine, and may react easily with the rain water.

The main idea behind the column leaching experiment was to simulate the leaching behavior of the trace elements under the actual field conditions. The OS, SS and a representative phosphate rock sample (PR) were used in this experiment. Both (OS) and (SS) samples have been crushed into 104 mm while the phosphate sample had the grain size of sand (about 2 mm). Every experiment was performed as triplicates.

Nine syringes (60 cc and 3 cm diameter) were used for these experiments. For the OS and SS A sample of 45 g were used and of 30 g for phosphate. By means of a peristaltic pump distilled water was pumped with a flow rate of 110 ml/day through the columns from top to bottom. Leachate samples were collected at the outlet of each syringe every 24 hours. The experiment was run for 10 days. At the end, 90 samples of leachate water were investigated by ICP-MS. The experimental setup is shown in Figure 4.2.

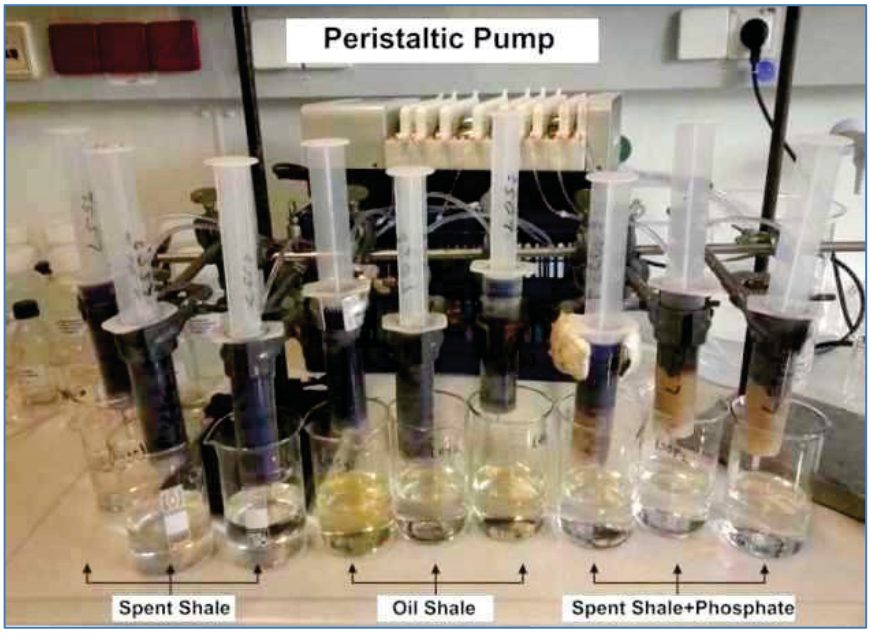

Figure 4.2: Column leaching experiment : The Peristaltic Pump with pumping tubes and hose, was running over ten days, the flow rate was adjusted to about 110ml/day, distilled water were leachate through 9 syringes fixed horizontally and were filled with three different triplicate samples; (3 syringes filled with spent shale, 3 syringes filled with oil shale, and 3 syringes filled with phosphate underneath spent shale), 9 glass beakers underneath the bottom of the syringes to receive the daily leachate water.

4.3.4 Immobilization of trace element in trace spent shale

The Immobilization or so called stabilization of trace elements in the spent shale is a remediation method that is used to reduce the mobilization and bioavailability of the

contaminants by using soil amendments. The main aim of the method is to immobilize the trace elements fraction in soil that can be easily released into soil solution or enter the biological cycle or being leached to groundwater (Kumpiene, 2010).

The immobilization of the trace elements that are contained in the spent shale can be achieved by changing their chemical state using soil amendments that are able to stabilize the trace elements. Kaolin was used in this study.

4.3.4.1 Laboratory samples preparation

A representative Kaolin sample (Cretaceous age) was collected from outcropping lenses in Batn Al Ghul (Jabal Al Harad) in southern Jordan.

The Kaolin sample (K) was crushed, grinded and passed through a 104-µm mesh, eight molds were made; three of them were made by mixing spent shale with Kaolin (SS+K) in different rations, and three molds were made by mixing oil shale with kaolin (OS+K) in different ratios, the other two molds were made from kaolin sample (K)only, The total weight was 10 g for each mold with 5.3 cm diameters (Table 4.2). 2 g of pure cellulose were added to the mold to keep the material cohesive. The disks were put in furnace and the temperature gradually increased up to 1000 ºC, and kept at this temperature for two hours and then cooled down. Samples were crushed, grinded, and passed through a 104 µm mesh. The above processes were repeated many times to have enough material required for the next experiments.

Table 4.2 : Samples preparation and ratios: Spent shale and Kaolin (SSK), Oil shale with Kaolin (OSK), and Kaolin (K).

Sample No.	SS	K	Sample No.	OS	K
SS-A	5%	95%	OS-A	5%	95%
SS-B	15%	85%	OS-B	15%	85%
SS-C	25%	75%	OS-C	25%	75%
K	0	100%	K	0	100%

4.3.4.2 Liquid-solid partitioning as a function of liquid-solid ratio

The liquid-solid partitioning was performed according to M1316 Kossen et al., 2002 and was provided at natural pH which was developed from the method of SR003 (Kossen et

al., 2002), using the methodology which is accepted and reviewed by the Environmental Protection Agency (EPA) (Sanchez et al.,2006, 2008). This method is similar to the batch liquid /solid (L/S) method, which was developed for Comité Européen de Normalisation (CEN) (EN12457, 2001).

This method consists of five parallel extractions of particle-size reduced solid material in reagent water over a range of liquid-solid rations to facilitate the approach to equilibrium with liquid-solid values ranging from 0.5 to 10 ml per g of solid. The liquid-solid ratios used were 1/10, 1/5, 1/2, 1/1, and 1/0.5. The solid material were placed separately with extraction vessels and deionized water was added at (L/S) of 1/10, 1/5, 1/2, 1/1, 1/0.5. The vessels which filled with water and the solid samples were turned upside down (end-over end) for constant time to allow the extraction to reach equilibrium. Measurement of conductivity and pH were recorded. The samples were filtered and the final liquid samples were then investigated by ICP-MS (Appendix 2).

4.3.4.3 Liquid-solid partitioning as a function of pH

Liquid-solid partitioning (LSP) can be performed as a function of pH. This method (M1313) has been derived from procedure SR002 (Kossen et al., 2002) by using the accepted and reviewed methodologies of EPA (Sanchez et al., 2006, 2008). This method is similar to CEN/TS 14429 (2005), which has been developed for the Comité Européen de Normalisation(CEN).

In principle, the procedure consists of nine parallel batch extractions of particle-size reduced material over a broad range of pH. In this research seven parallel patch extractions were applied with a pH range of 4, 5, 6, 7, 8, 10, and 12.

The samples used in this experiment were taken from the; Spent shale and Kaolin (SSK), Oil shale and Kaolin (OSK), and the Kaolin (K) preparation. 3 g of solid material (grain size of < 300μm) were placed in each extraction vessel filled with 30 ml distilled water. The specified final pH values were achieved by adding acid or base (HNO_3 or KOH). The vessels were left for 2 hours in an end-over-end shaker. Conductivity and pH were recorded. The samples were passed through 0.2 μm filters. The final liquid samples were analyzed by means of ICP-MS (Appendix 3).

4.4 Chemical analysis

4.4.1 Hydrochemical data analysis

There are many water wells in El-Lajjun area drilled by the Ministry of Water and Irrigations (MWI) and by private persons. Many of these wells are penetrating the intermediate aquifer (B2/A7), while others tap the deep sandstone aquifer (Kurnub/Ram Group) at 1000 m depth. The later wells were drilled in El-Lajjun water field to supply Amman with domestic water.

A total of 22 chemical analyses were used in this study (some are taken from the MWI open file report), with17 water samples from El-Lajjun water well field, 7 samples from the intermediate aquifer (B2/A7), and 10 water samples from the deep sandstone aquifer (Kurnub/Ram Group Aquifer). 30 trace elements and metals were determined by using ICP-MS in the laboratories of the hydrogeology department at the TU Bergakademie Freiberg. These analyses were done for 5 water samples from 5 different water wells.
Other samples were analyzed in the Water Authority Labs, Amman for the major cations and anions, and some others records were obtained from the open file of the (MWI). Other field measurements were obtained like pH and the electric conductivity (EC). EC is directly related to the total dissolved ions in the water, and it measures the ability of water to conduct an electric current. The EC is independent on temperature; however, it increases by increasing the temperature. EC is reported in µS/cm. Besides, the amount of total dissolved salts (TDS) or the total amount of dissolved ions in the water was calculated.

4.5 Rainfall – Runoff Calculations

The study area is characterized by arid climate with an average annual rainfall of less than 200 mm (UNEP, 1992). The rainfall records of the last 15 years are shown in Table 3.5 with an average of 190 mm. The Isohyetal lines are shown in Fig. 4.3..

Table 4.3 :Rainfall station average annual rainfall (mm).

Hydrological year	MUHAI St	MAZAR	HEMUD	Rabba	Karak	QATRANA EVA	Average mm
1999 /2000	41.7	178.6	138.3	142.2	264	26	131.8
2000/2001	131.7	221.5	203.6	204.9	293	66.9	187.0
2001/2002	149.3	266.5	228	274.3	441	111.3	245.1
2002/2003	150.8	461.6	323.3	444.8	202	133.5	286.0
2003/2004	23.4	163	178.4	219.6	448	101.5	188.9
2004/2005	182.7	449.2	325	414.1	265	113.6	291.6
2005/2006	151.5	205.1	189	261.1	312	70.8	198.3
2006/2007	162.3	252.3	312.8	324.8	306	116	245.6
2007/2008	197.8	289.3	230.9	289.6	162	89.3	209.7
2008/2009	132.7	198.8	217	220.8	191	81.3	173.5
2009/2010	90.6	172.3	173.6	213.6	322	63.1	172.5
2010/2011	255	341.5	264	351.8	222	104.8	256.5
2011/2012	162	230.5	173.7	196.6	124	51.1	156.3
2012/2013	147.4	206.7	279.4	297.4	297	52.7	213.4
3013/2014	158.3	233.3	232.3	235.8	225	76.8	193.7
Average	142.48	258.01	231.29	272.76	271.43	83.91	

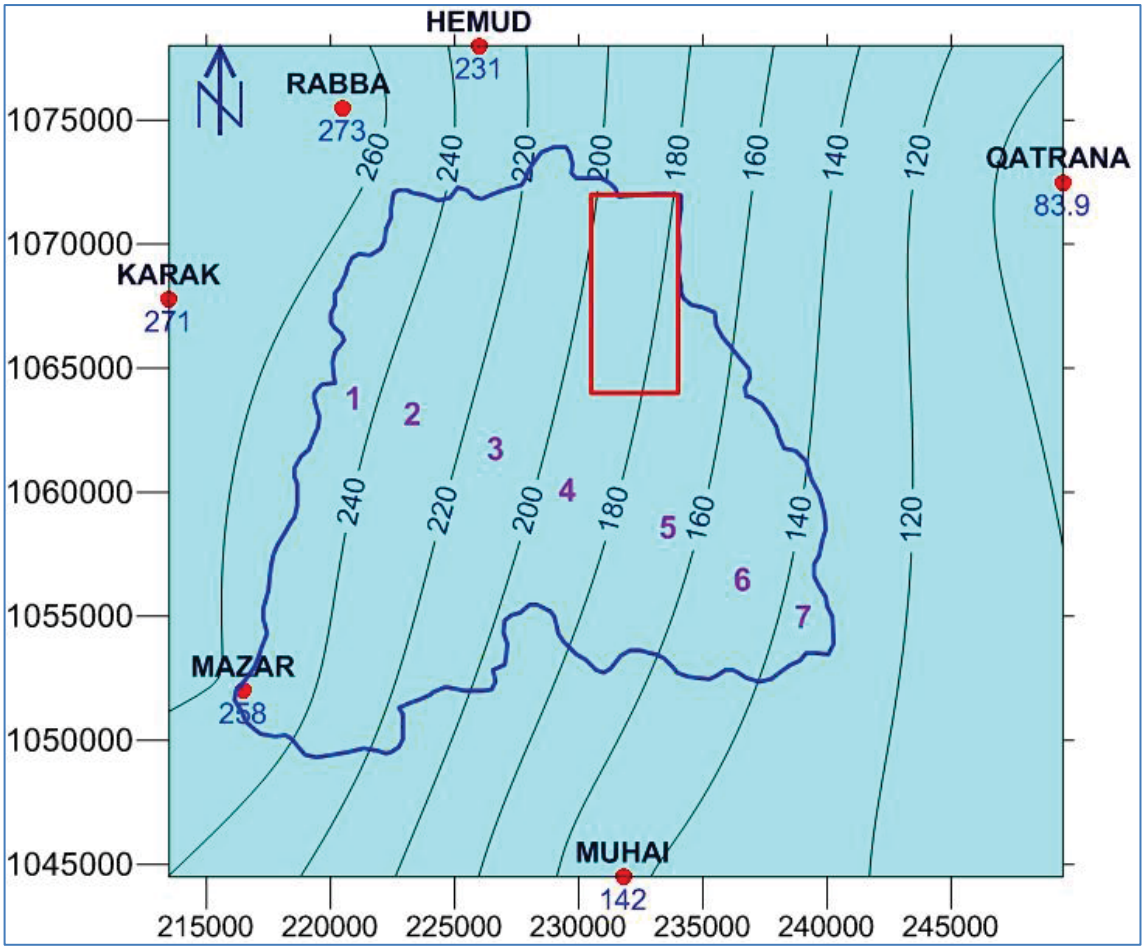

Figure 4.3: Rainfall contour map based on 15 years average. (20 mm increment).

The calculations are based on the strip element method discussed in Abuqubu et al. (2016) where the region of interest is divided into seven elements fall between the successive isohyetal lines. Then, the obtained area for each part is multiplied by the average value of the bounded isohyetal lines value. So, the total rainfall amount is calculated by adding all values for the whole parts (Table 3.5). The results give the total amount of 75 $x10^9$ m^3 of rainfall water.

Table 4.4 : The calculated rainfall amounts.

Elements	Area (Km^2)	Average Rainfall (mm)	Rainfall Amount 10^6 m^3
1	53.3	250	13325
2	81	230	18630
3	72.8	210	15288
4	59.2	190	11248
5	51.6	170	8772
6	42.2	150	6330
7	10.48	130	1362.4
Sum	370.58	190	74955

- **SCS Runoff Curve Number (CN) Method**

The catchment of the study area (Wadi El-Lajjun catchment) is ungagged; therefore, the SCS runoff curve number method is used for predicting direct runoff from rainfall excess, and then the amount of infiltration water could be estimated. This infiltration rainwater may leach trace elements from oil shale layers to the groundwater aquifers.

Estimating the runoff in this study was based on the Natural Resources Conservation Service (NRCS) runoff equation method, this relationship was early described version, investigations and applications by Mockus 1949, Sherman 1942, and Andrews 1954), However, this method was developed to estimate total storm runoff from storm rainfall (USDA-NRCS, 2004)

The following equation was used to estimate the direct runoff (Q):

$Q = (P - Ia)^2 / (P - Ia + S)$……(1)

$P > Ia$

$P \leq Ia$ then Q = 0,

where:

Q = depth of runoff, in inches,

P = depth of rainfall, in inches,

I_a = initial abstraction, in inches, and

S = maximum potential retention, in inches.

The SCS method takes in consideration the initial abstraction of rainfall in inches, the antecedent moisture condition, and the land use

Many investigations and studies have been carried out on different water- watershed in the United States. S was determined from these different studies. I_a and S are related to the soil cover conditions (REF)

If (I_a)= 0, then equation (1) is reduced to,

Q = P2 / P- S

QP – QS = P2

QP – P2 = QS

P (Q- P) = QS, Using F = Q-P, then one gets:

PF = QS, then F\S = Q\P …….. (2)

I_a = 0.2 S…… (3)

Applying equations (2) in (1) one gets:

Q = (P – 0.2)2 / (P – 0.8 +S)…… (4)

Kent (1966) established the relation between the Curve Number (CN) and S in the following relation:

S = (1000 / CN) – 10 …… (5)

4.6 Risk assessment of groundwater vulnerability with DRASTIC

Jordan has limited water resources and may not be able to meet its fresh water demands by the coming years (Seckler et al., 1999). Therefore, the quality and quantity of fresh water is becoming more and more important. Many oil shale industrial activities will take place in El-Lajjun area and surroundings in the near future. Oil shale utilization processes; mining, products and byproducts, could have serious repercussions on the surrounding environment if these issues are not investigated and treated accordingly.

Generally, groundwater is safer in comparison to surface water and considered asa reliable source of clean water. However, once the groundwater is polluted it is not easy to remediate. The mining activities including the deposition of spent shale during the utilization of oil shale in the study area will endanger the groundwater quality.

The changing in topography and relief, changing in land use, and land cover pattern, besides the residuals of oil shale extractions, all together, form a very serious risk on groundwater resources in the study area.

A main issue which is facing Jordan is the urgent need to protect the water resources; surface and groundwater in quantity and quality. Vulnerability studies represent the most important protection actions to sustain the water resources for present and the future.

Groundwater vulnerability is a measure of how likely it is for pollutants spread at the soil surface that they may reach the groundwater.

The vulnerability can be assessed by many methods which can be classified into three main procedures: statistical methods, process-based computer simulations, and overlay index methods (Tesoriero et al., 1998).

Overlay index methods are based on assembling information on the most relevant factors affecting aquifer vulnerability (geologic formation type, soil type, recharge, etc.). They are interpreted by scoring of parameters to produce an index ranking or a class of vulnerability. These ranking and integration methods are based on expert opinion rather than processes and are inherently subjective to some degree.

Statistical methods use response variables such as the occurrence of contaminate and its frequency, and concentration or its probability. However the concept of uncertainty is the base of these methods (NRC, 1993). The main possible goal of applying such methods is to identify variables that can be used to define the probability of groundwater contamination (Burkart et al., 1999a).

Process-based computer simulations are assessment methods in this category and usually are more elaborated than simple overlay or index methods. However, it affords a great amount of realistic complexity and detail to be built into the vulnerability assessment. This model can account for complex chemical and physical processes and at a very detailed scale and include different degrees of complexity from process-based indices to complex 3- D simulation models. Geologic and hydrogeological variations with depth can, therefore, be reproduced to evaluate their effect on vulnerability (BAM; Jury and Ghodrati, 1989, Rao et al., 1985).

Several index vulnerability assessment techniques have been developed. The most often used method is DRASTIC (Aller et al., 1987) beside GOD (Foster 1987), KAVI (Beynenp.e. ET AL, 2012), SINTACS (Civita1994), and PI (Goldscheider et al., 2000).

DRASTIC, GOD, SINTACS and other conventional methods can distinguish degrees of vulnerability on a regional scale involving different lithology (Vias et al., 2005).

DRASTIC has been developed in cooperation between the United States Environmental Protection Agency (EPA) and the National Water Well Association on the USA. The procedure provides a systematic evaluation and assessment of groundwater pollution potential in any hydrogeological setting. Therefore it has been used in many countries around the world, (Aller et al., 1987).DRASTIC has been used in several regions (Melloul and Collin 1998 Cameron and Peloso 2001, Al-Adamat et al., 2003; Jamrah et al., 2007, Sener.et al 2009; Massone et al., 2010; Arzu and Fatma, 2013).

In this study, geographical information system (GIS) based DRASTIC model have been used to assess groundwater vulnerability to pollution by oil shale utilization. GIS techniques, combined with hydrogeological data layers such as depth of water, net recharge, aquifer media, soil media, topography (slope), impact of vadose zone, and hydraulic conductivity were applied;.

The seven physical parameters used by DRASTIC are:

- **D: Depth to groundwater:** Depth from the ground surface to the water table in unconfined aquifer and to the bottom of the aquiclude in confined aquifer. The unsaturated zone may filtrate, sorb and thus will hold contaminants. The thicker this zone is the better the well hold rate.
- **R: Net recharge:** More net recharge may transport more pollutants to the groundwater.

- **A: Aquifer media**: Properties of the aquifer materials control the withhold rate in particular by filtration and sorption.
- **S: Soil media:** Soils as the uppermost part of the unsaturated zone may have a distinct capability to withhold contaminants due to several physical, chemical and biochemical processes.
- **T: Topography**, Surface slope controls the runoff, and more runoff causes less infiltration, and thus less vulnerability for the respective cell. However, DRASTIC does not consider that neighboring cells receive a higher contamination load.
- **I: Vadose zone:** In addition to the depth to groundwater the media of the unsaturated zone controls as well the withhold rate for contaminants. Finer sediments provide more sorption capacity and lower infiltration rates which is defined as the unsaturated zone above the water table. The texture and compaction of the vadose zone determines the travel time of the contaminations through it to the aquifer.
- **C: Hydraulic conductivity of the aquifer:** Permeable aquifers transport contaminations more readily than less permeable aquifers

DRASTIC is based on an empirical ranking system consisting of three parts: ranges and associated ratings plus weights. This system is used to assess and evaluate the groundwater pollution potential for each hydrogeological spot (e.g. pixel in raster based GIS). In this study (Aller et al., 1987):

Range: Each DRASTIC factor is divided into ranges or significant media types.

Rating: The rating of DRASTIC factors runs from 1 to 10 which represent low risk to high risk, respectively.

Weight: Each DRASTIC factor has a relative weight ranges from 1 to 5 to define the relative importance of each factor. (Table 4.5 and Table 4.6).

The groundwater vulnerability map has been prepared by entering the values of various parameters in GIS environment. These values were converted into shape files. The shape files were converted into raster files, and then a respective parameter maps were prepared. Later, these maps were converted into rating maps followed by index map by multiplying weights into the ratings to get DRASTIC parameter index units.

Finally, all the seven parameter index map layers were combined by using Arc GIS with its special combine tool to obtain a final groundwater vulnerability map.

There is no standard algorithm to test or to validate result. Therefore some researchers tried to improve the methods by correlating the DASTIC vulnerability index with pollutants and contamination parameters in the aquifer (Kalinski et al., 1994). Other searchers made a correlation of land use with vulnerability (Worrall and Koplin, 2004).

DRASTIC parameters in the study area (ratings and weights) have been adapted for the specific hydrological conditions in the region of interest. However, the depth to groundwater has wide ranges and thus, it has been modified in this study.

Table 4.5 :DRASTIC rating and weights for each hydrogeological setting (modified after Aller et al., 1987), (**): the modified rating and weights.

Depth to water Table (m)		**Depth to water Table (m) (**)**		**Topography (slope %)**		**Topography (slope %) (**)**	
Range	Rating	Range	Rating	Range	Rating	Range	Rating
0-1.5	10	1-30	10	0-2	10	0-2	10
1.5-4.6	9	30-60	9	2-6	9	2-4	9
4.6-9.1	7	60 -90	7	6-12	5	4-6	7
9.1-15.2	5	90-120	6	12- 18	3	6- 8	5
15.2-22.8	3	120-140	5	>18	1	8- 10	3
22.8-30.4	2	140-150	3			>18	1
> 30.4	1	> 150	1				
Weight = 5		Weight = 5		Weight = 1		Weight = 1	

Recharge (mm)		**Conductivity (m/d)**	
Range	Rating	Range	Rating
0-2	1	0-4.1	1
2 -4	2	4.1-12.3	2
4-6	4	12.3-28.7	4
6-8	6	28.7-41	6
8-10	8	41-82	8
> 10	9	>82	10
Weight = 4		Weight = 3	

Table 4.6 :Rating and weights for each hydrogeological setting (after Aller et al., 1987)

Aquifer Media		**Vadose Zone Material**		**Soil Media**	
	Rating		**Rating**		**Rating**
Massive Shale	2	Confining Layer	1	Gravel	10
				Thin or Absent	
Metamorphic/ Igneous	3	Silt/Clay	3	Sand	9
Weather Metamorphic Igneous	4	Shale	3	Peat	8
Glacial till	5	Limestone	3	Shrinking Clay	7
Bedded sandstone, limestone	6	Sanstone	6	Sandy Loam	6
Massive sandstone	6	Bedded Limestone, Sanstone	6	Loam	5
Massive Limestone	8	Sand and Gravel With Signification Silt	6	Silty Loam	4
Sand and Gravel	8	Sand and Gravel	8	Clay Loam	3
Basalt	9	Basalt	9	Muck	2
Karsts Limestone	10	Karsts Limestone	10	No Shrinking Clay	1
Weight = 3		Weight = 5		Weight = 2	

The higher DRASTIC index value, the greater is the pollution potential. DRASTIC index can be divided into four categories: low, moderate, high, and very high.

Table 4.7 :DRASTIC Index Classification (after Aller et al., 1987).

Value	**Class**
1-100	Low
101-140	Moderate
141-200	High
>200	Extremely high

The final result is a numerical value which is calculated based on the following equation (Aller et al., 1987):

$V = \sum_{i=1}^{7} (Wi \times Ri)$…….. (1)

Where:

V: the Index value

W_i: weighting coefficient for parameter (i) with an associating value of (R_i)

Chapter 5 RESULTS AND DISCUSSION

5.1 Mineralogy of the oil shale

The X-ray diffraction (XRD) results. Indicate that the mineralogical content of the oil shale is Calcite and Quartz as major constituents, while the others like Apatite, Dolomite, Feldspar Pyrite, are either minor or trace constituents (Table 5.1).

Table 5.1: Analysis of the major elements by X-ray diffraction (XRD) for oil shale representative samples.

Constituents	Minerals	%
Main	Calcite	20 – 80
	Quartz	10 – 40
	Kaolinite	5 – 10
Minor	Apatite	4 – 14
	Dolomite	2 – 3.6
	Feldspar	5
Traces	Pyrite	5
	Muscovite	5
	Geothite	5
	Gypsum	5
	Opal	Present

Moreover, The XRD results of several oil shale samples indicate that the mineralogy of El-Lajjun oil shale as a whole is uniform with depth.

5.2 Fischer assay method

Fisher assay results indicate that the oil shale in the study area and generally in Jordan is rich in organic matter. Thus the Jordanian oil shales are within the world average (Table 5.2).

Table 5.2: Comparison of properties of world oil shale deposits (Besieso, 2007), with the Jordanian oil shale, (from El-Lajjun study area*). The analysis results are for representative samples using the Fischer assay method

Contents (%)	Kvarntrop Sweden	Kukersite Estonia	Green River USA	Irate Brazil	Maoming China	Lajjun* Jordan
Moisture Content. Wt.	2.0	Dry	Dry	4.6	5.0	**4.0**
Water	-	1.9	1.4	1.2	3.2	**1.40**
Oil	5.7	22.0	10.4	6.9	7.3	**10.84**
Residue	87.2	70.5	85.7	83.6	80.6	**81.50**
Gas and Losses	5.1	5.6	2.5	3.7	3.7	**2.53**

The table shows that the spent shale content is relatively high (81.5 %) in average, and it will be the main residual products of the extraction techniques. This result is in full agreement with those reported in previous investigations for the same oil shale deposit; Hamarneh (1998), Jaber et al. (1999), and Ibrahim and Jaber (2007).

The severest concern over the spent shale after extraction and retorting process is the leachability tendency of trace toxic elements of spent shale into surface and groundwater water.

5.3 Sequential Extraction

The metal distribution to the different fractions was significantly changed by converting the OS to SS.

The results presented in Figures 5.1, and 5.2. show that the metals move from one fraction to anther fraction as result of heating up the OS. According to Knox et al.2006, Ghrair, 2009, and Zhong et al. 2011, the metals were bounded to seven fractions as the following:

- F1 is the mobile (soluble and exchangeable).
- F2 bound to carbonates (easily mobilized).
- F3 bound to manganese oxides.
- F4 bound to organic matter including sulfides.
- F5 bound to amorphous and poorly crystalline iron oxides.
- F6 bound to crystalline iron oxides.
- F7 is the residual fraction by calculation, which is the total metal content minus summation of extracted fractions: F7= F8 – (ΣF1–F6).
- F8 is total element content by the complete digestion by Aqua Regia.

Usman, et al., 2004 and Ghrair, 2009 have reported that the first fraction (F1) is the readily the mobile fraction. The fractions F2, F3, F4, F5, and F6 bound strength is increasing by increasing the fraction number, where F5 and F6 represent the most strongly bound fractions. The fractions F2 to F4 have the potential to move from the solid phase to the aqueous phase as a response to the changing of environmental conditions, such as pH,

redox potential, temperature, etc. (Knox et al. 2006). Contaminants in the fractions F2 to F4 represent a potential threat to the environment organisms (Ma and Rao 1997, Zhong et al. 2011). The results of OS sequential fraction revealed that V, As, Zr, Cr, Co, and U are mainly bound to carbonates (F2) and to crystalline iron oxides (F6). In addition Zn, Cd and Pb are bound to carbonates (F2) and organic matter (F4). Ti is mainly bound to poorly and crystalline fractions (F5 and F6). The higher concentration elements in OS are V, Zn, and U (Fig 5.1), (Sequential extraction results of oil shale and spent shale samples, the averages, slandered deviation, and the median, are in Appendix 4).

The results of the SS sequential extraction show different distribution pattern of trace elements on six fractions in comparison with OS (Fig. 5.2). Moreover, the concentrations of trace elements increased relatively as a result of retorting of OS.

Ti and As are mainly bound to poorly and crystalline iron oxides (F5 and F6). These two fractions have the least potential for leaching. In order to release trace elements from these fractions, high acidic conditions (pH 3.25) are required to occur in nature environment. Thus, it is not expected to find a high concentration of these elements in the study area.

Elements such as V, Cr, Co, Zn, and U are accumulated and mainly bound to carbonates (F2) and poorly crystalline iron oxides (F5). F2 has high leaching potential; therefore elements in these fractions represent a serious threat in the study area. Furthermore, Zr, Cd, and Pb are mainly bound to carbonates (F2) and organic matter residues (F4). These elements have high affinity toward the carbonate and organic fractions which remains in the spent shale (Usman, et al., 2004; Salminen, et al., 2005; and Gharir,2009). Trace elements in F2 and F4 have a high leaching potential and represent a serious threat for the environment.

The most mobile elements in SS are V and As. These elements are bio- available in the environment and represent serious threat to the environment.

The loss of ignition (LOI) is about 40% during retorting the OS at 520 ºC by Fischer Assay, due to degradation of organic matter, loss of water, and gasses. Consequently, the trace elements were enriched in SS as far as they are not volatized during the heating.

In the case of the SS samples, however the concentration of above mentioned elements increases in the most of the fraction steps, and it is in a high concentration in (F5) than the others, this indicates that the bound of the above elements to amorphous and poorly crystalline Fe oxides become weaken by retorting heating process, and they can be easily fractionated by sequential extraction, the result shows that Zr is with high concentration in

the organic matter, which is not completely driven by retorting heat process. However, the rest of the concentration appeared in the extracted solution in fraction (F4).

On contrary, sequential extraction results of OS show higher concentrations of Cr, Co, Cd, Zn, Pb, and U in fraction (F2) (bound to carbonate). These elements have low concentrations in other fractions except Pb, which shows considerable concentrations in fraction 4 (bound to organic matter).

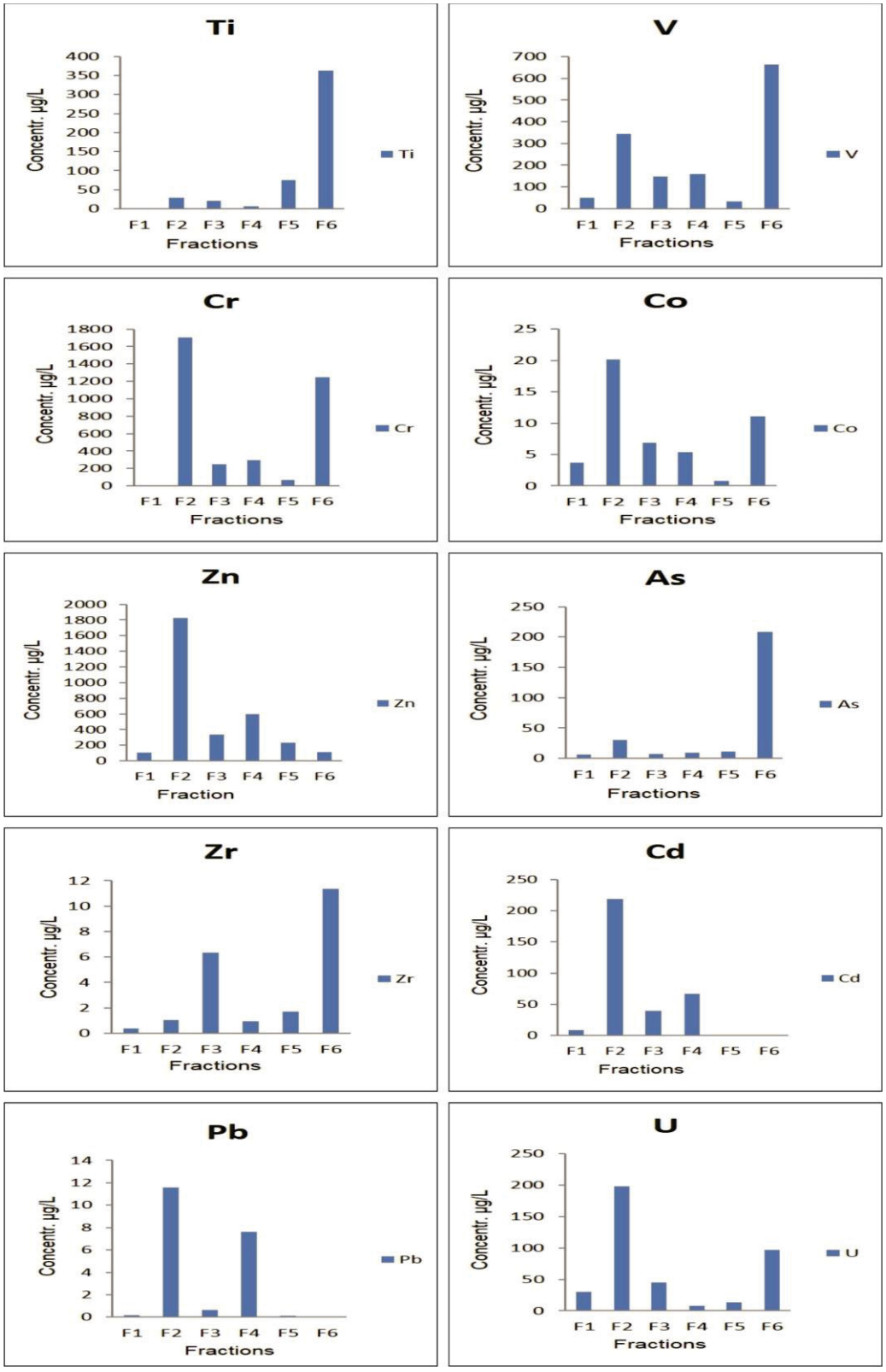

Figure 5.1: Concentrations (µg/L) of some trace elements (Ti, V, Cr, Co, Zn, As, Zr, Cd, Pb, and U) obtained by sequential extraction for oil shale (OS).

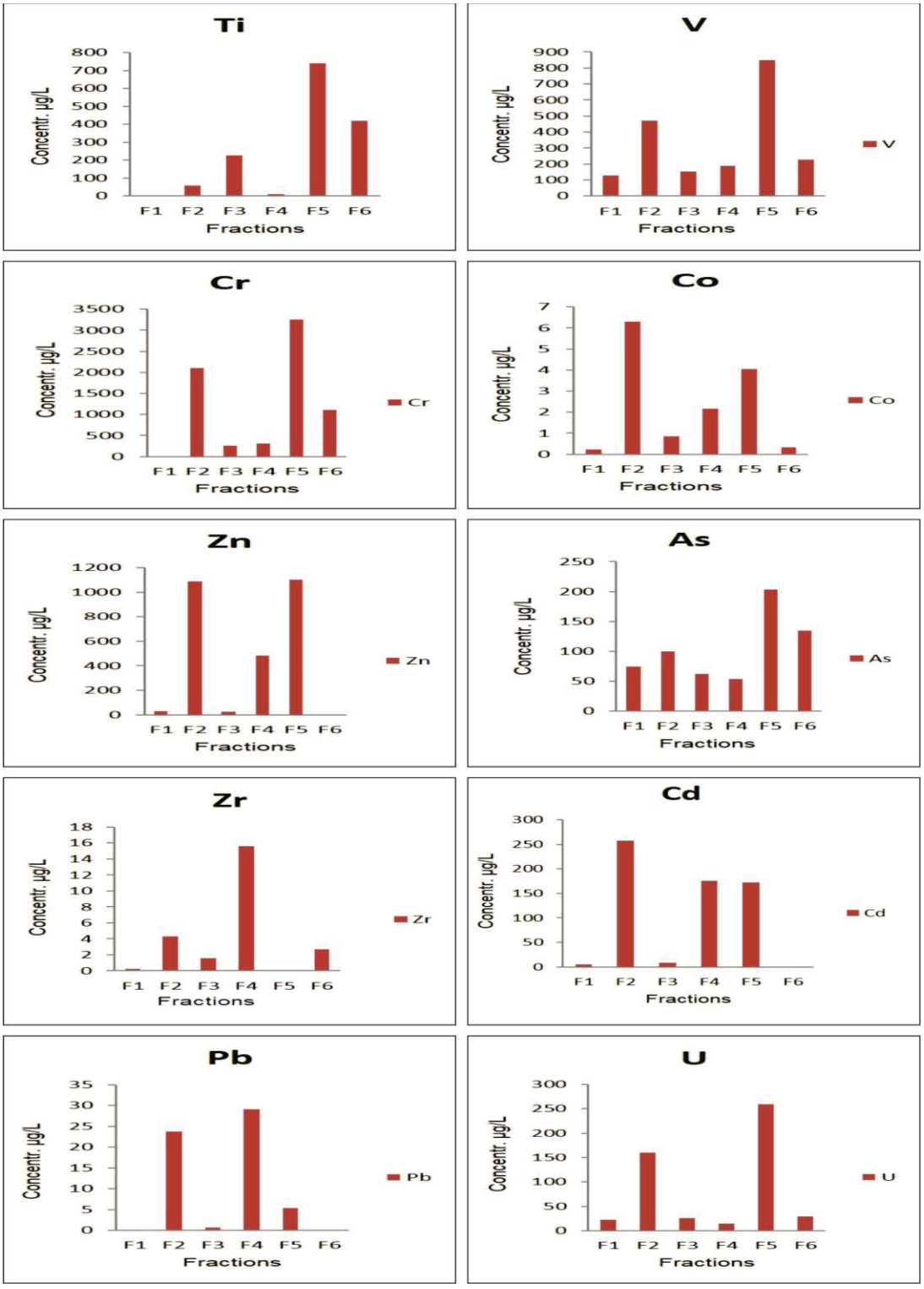

Figure 5.2: Concentrations (µg/L) of some trace elements (Ti, V, Cr, Co, Zn, As, Zr, Cd, Pb, and U) obtained by sequential extraction for spent shale (SS).

The results represent in Figure 5.3 show that the accumulation of each elements concentrations in SS mobile and potential labile fractions are higher than the same elements in OS. The only exception is Zn (it is 15% less in SS in comparison to OS) This is probably due to the fact that Zn has a high affinity to organic matter (Wedepohl, 1978), It seems that the Zn was separated with the oil vapor and shale gas from the solids during the pyrolysis process.

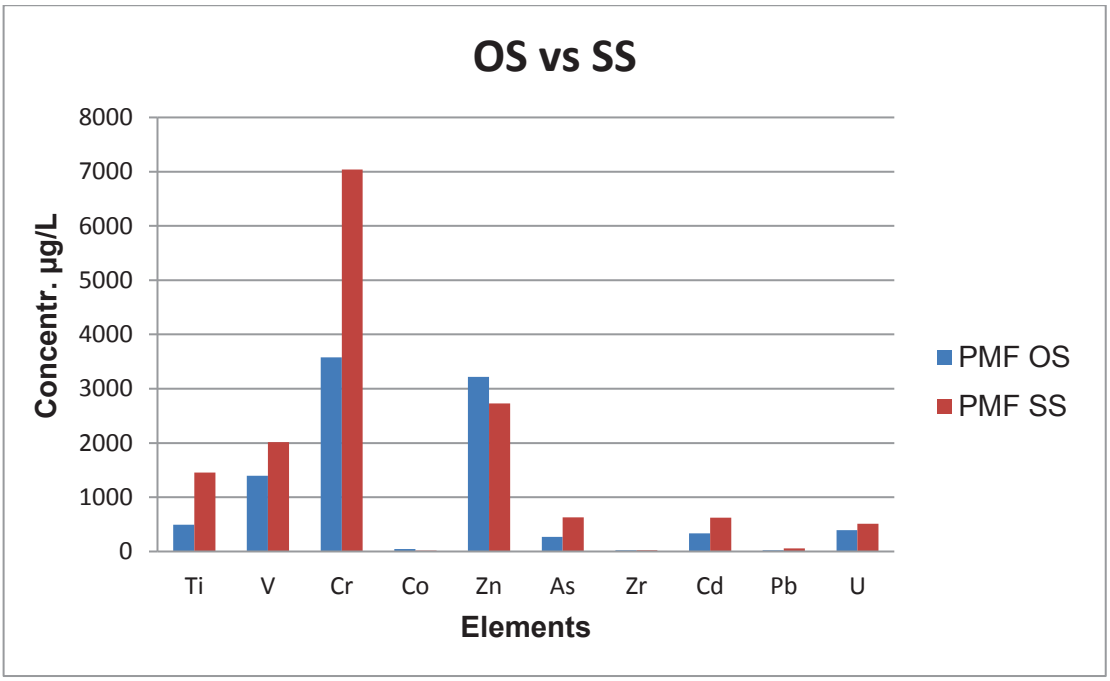

Figure 5.3: Comparison between concentrations of elements in oil shale and spent shale (summation of mobile and less mobile fractions), that were obtained by sequential extraction experiments.

5.4 Column leaching experiment

90 different leachate samples from the 10 days column leaching experiment with distilled water were investigated by ICP-MS for major and trace elements. In the following the concentrations of Ti, V, Cr, Co, Zn, As, Zr, Cd, Pb, and U for OS, SS and SS plus phosphate (triplicate samples) are discussed.

The results are shown in Appendix 5 a, b, c. The appendixes show the concentrations of the above trace elements of the daily leaching, the average of the triplicate samples, standard deviation and median. The summation of the average of ten days column leaching experiments is shown in Table 5.3.

Table 5.3: The total concentration (µg/L) of ten days leaching column experiment with distilled water for (LOS, LSS, LSSP: leaching of oil shale, spent shale, phosphate underneath spent shale column sample respectively).

Material ID	Ti	V	Cr	Co	Zn	As	Zr	Cd	Pb	U
LOS	2.25	163.9	40.0	3.2	56.86	30.77	2.89	5.31	0.44	34.65
LSS	3.73	1920	12.5	0.45	17.61	130.54	0.39	10.6	0.40	1.83
LSSP	1.45	892.3	116.6	0.07	15.92	3.06	0.24	2.74	0.28	0.44

The results in Table 5.3 show that Co, Zn, Zr, and U concentrations from LOS column are higher than those from other columns, The major source of the leachate elements in the column experiment is the elements that are bounded to liquid phase and carbonates. Elements in these two fractions are mobile and highly potential labile at neutral pH conditions. This is clear from the sequential extraction experiment result. At the beginning of the leaching test, these elements showed a high concentration in leachate water from the LOS columns, but then the concentration decreased very rapidly. Moreover, the concentration of above mentioned elements are less in leachate water from the LSSP columns and LSS columns. It is assumed that the lower concentrations of Zr, Co, Zn and U are in spent shale. These elements leave the retort and become a part of the shale oil because they are volatized elements. The concentration of Uranium is slightly higher in water that leachate from LOS than from LSS samples. However it is clearly associated with phosphorous more than the bituminous organic matter (Hamarneh, 1998) as shown in Fig. 5.4.

Co, Zn, Zr and U are more easily mobilized by distilled water from oil shale in comparison to spent shale. Only Co is retained additionally by phosphate. The leaching rate from oil shale gets steady state after about 3 days, for Co, Zn and Zr and after 5 days for U.

The result of the experiment indicates that the phosphates layer underneath the spent shale reduce the mobility, and thus reduce the level of the metals leached from the spent shale.

Phosphate layers can act as accumulation zone for leached trace elements from the above layers due to its low permeability.

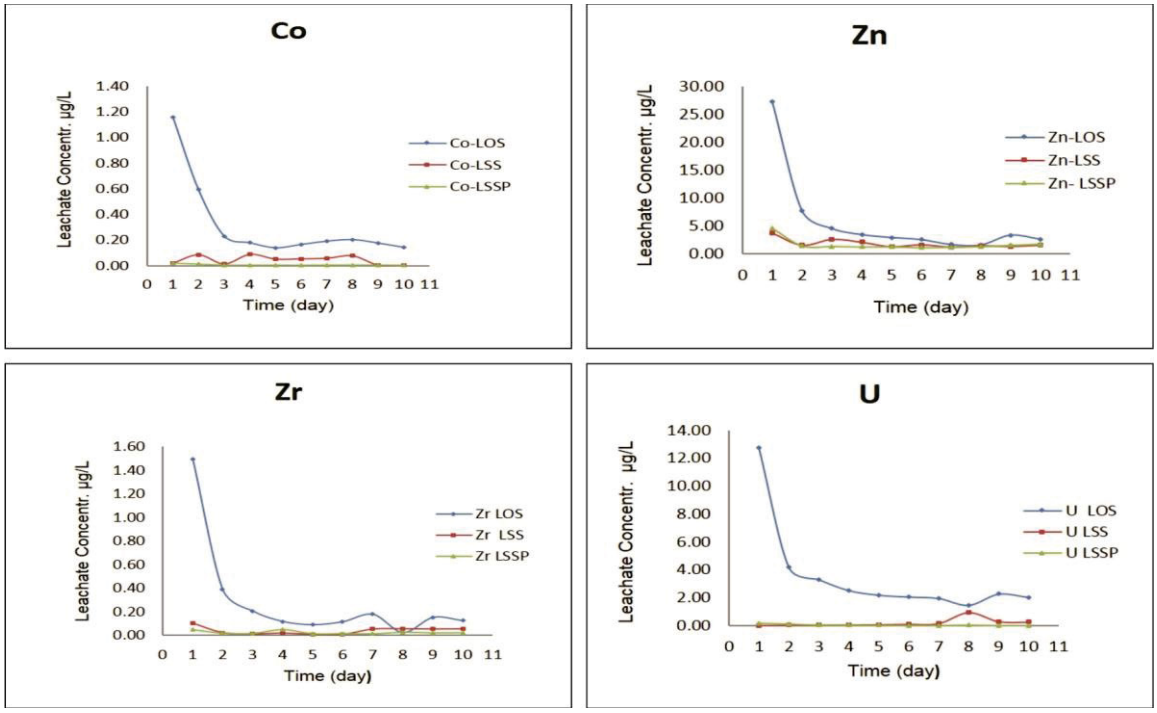

Figure 5.4: Concentrations of CO, Zn, Zr, and U over time from the three different leaching columns (LOS = leaching of oil shale column sample, LSS= leaching of spent shale column sample LSSP = leaching the column of phosphate underneath spent shale samples.

On contrary, Ti, V, As, and Cd do show significantly higher leachability for spent shale. Leaching of Ti form oil shale is considerably low and reaches steady state conditions after 3 days. However, Ti is leached more easily from spent shale and reaches steady state conditions only after 7 days. PO_4 helps to reduce the mobility of Ti from spent shale, which is probably due to sorption of Ti on phosphate.

V is contained in oil shale at rather higher concentrations (163.9µg/L) compared to other trace elements. After retorting the concentration is much higher and it becomes more mobile through distilled water. The concentration gets steady state after about 10 days (Fig. 5.5). This is probably due to anadyl (VO^{2+}) formation (Gütlein, 2013). However, this would require a reduction of V from the oxidation state 5 to 4 during the retorting process. In the presence of PO_4 the mobility of V is lower, but, still much higher than from oil shale. Thus it can be said that V will be readily mobilized from spent shale after retorting of oil shales.

Cd behaves very similar to V. On contrary, As from spent shale is slightly increasing over the 10 days of the experiment which is true for oil shale as well, although at a lower level. Phosphate is reducing the leaching rate significantly and more effective in comparison to the other trace elements. Slawson, (1979) concluded that most of the associated with oil shale processing are found in retort water, spent shale, and with raw shale oil.

Cadmium concentration leachates from LSS is more than that leachates from LOS, generally, it is considered a very low concentration in regards of environmental impact.

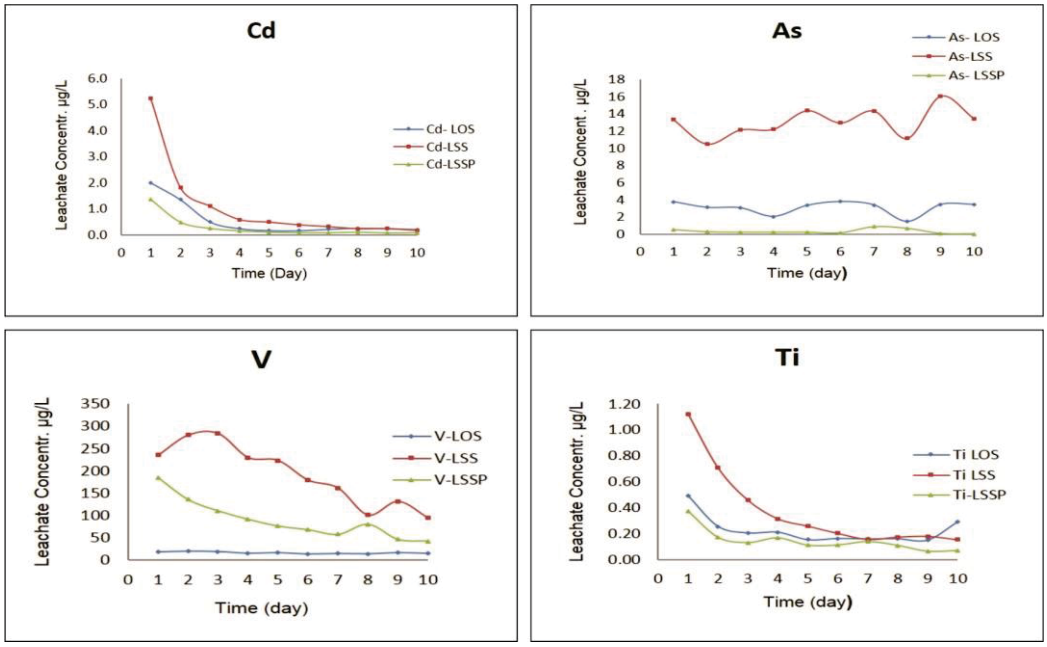

Figure 5.5: Leachate concentrations of Ti, V, As, and Cd over time from the three different leaching columns. (LOS = leaching of oil shale column sample, LSS= leaching of spent shale column sample LSSP = leaching the column of phosphate underneath spent shale samples.

The results depicted Figure 5.6 reveal that the leachate concentration of Pb from the OS in the columnar experiment is higher than SS, one possible explanation is that concerting the OS to SS led to immobilize the Pb in the form of oxide. This result is in harmony with Ibrahim and Jaber (2007). In case of utilizing phosphate underneath spent shale (PSS), it shows a slight reduction in leaching concentration of Pb in comparison with SS.

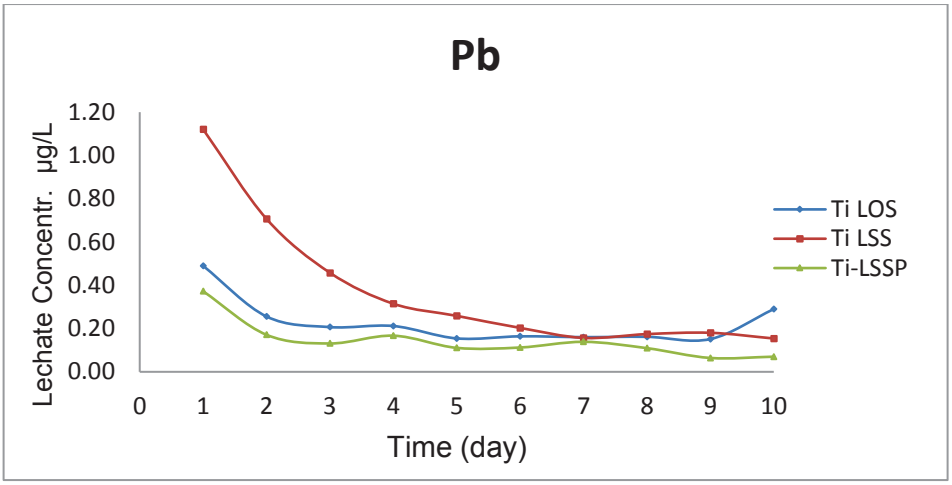

Figure 5.6: Leachate concentration versus time for Pb concentration from the three different columns (LOS: leaching of oil shale column sample, LSS: leaching of spent shale column sample, LSSP: leaching the column of phosphate underneath spent shale samples).

The results presented in Figure 5.7 show that the leachate concentration of Cr from OS is relatively low (< 12µg/L). Moreover, converting OS to SS led to a slight reduction in leachate concentration of Cr.

However, using the phosphate underneath the SS led to a significant increase in leachate concentration of Cr. It seems that the phosphate rock act as a source for Cr in this experiment and not as sorbent. (El-Sheikh et al., 2013).

Ibrahim and Jaber (2007) concluded from their study that there is no detectable release of metals from the ash to percolating water. Al-Harahsheh et al. (2012) suggested that none of the collected spent shale samples exhibited any significant metal release, and low concentration of trace elements comparatively with the EPA limits of drinking water. They explained this by the high alkalinity of the ash.

The results obtained in this study are in agreement with the above investigations. Furthermore, the ten days records for the leaching of the trace elements from each column show that the concentrations are below the MCL´s of the EPA for drinking water and the Jordanian standard specification for drinking water (JS286/1997).

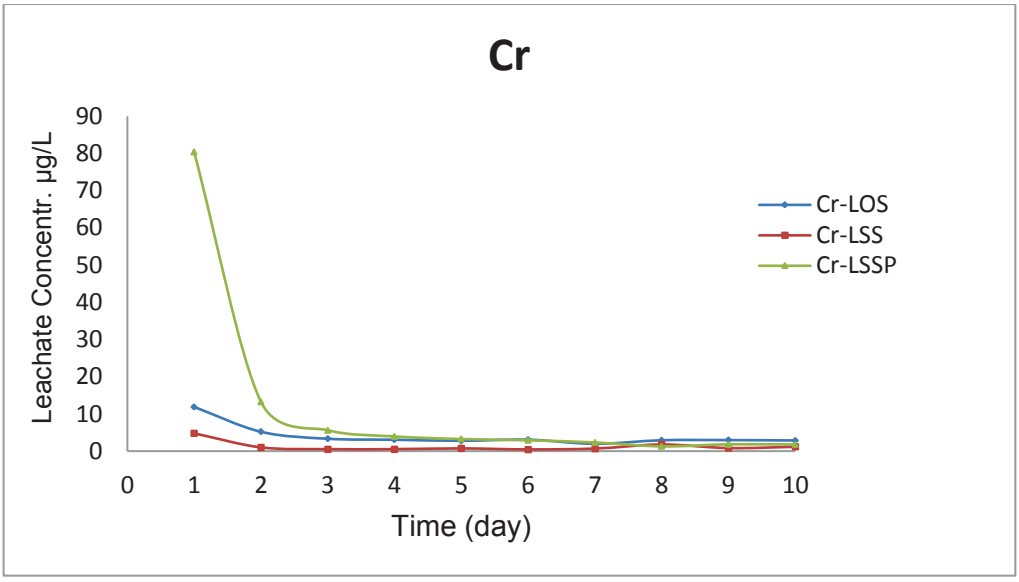

Figure 5.7: Leachate concentration of Cr at versus time, the leachates are from three different leaching columns, (LOS: leaching of oil shale column sample, LSS: leaching of spent shale column sample, LSSP: leaching the column of phosphate underneath spent shale samples).

5.5 Immobilization of trace element in spent shale

Many remediation methods may be used to reduce contaminant mobility and its bioavailability. Immobilization or stabilization of toxic trace elements and metals from spent shale can be achieved by changing their chemical state using certain kind of soil amendments.

In this study, SS was encapsulated in baked Kaolin. In order to evaluate the immobilization potential of trace elements in SS and OS incorporated in baked Kaolin. Kaolin was added to the spent shale samples and oil shale samples in different ratios (Table 4.2). Two leaching standard methods were investigated. Solid-Liquid partitioning as a function of Liquid-Solid ratio (S\L) (M1316), and Solid-Liquid partitioning as a function of pH (M1313) were conducted.

A comparison between the results obtained from column leaching experiment and the results that were obtained from immobilization methods for the OS and SS samples will be discussed in the next chapter.

5.5.1 Solid-Liquid- Partitioning as a Function of S\L Ratio.

This method was applied at the natural pH of the solid material at various Solid to liquid ratios (1:10, 1:5, 1:2, 1:1, and 1:0.5).

The Solid- Liquid partitioning methods (M1316) was applied at natural pH (10.50) of the solid material and at various Solid/ Liquid ratios (S/L): (1:10, 1:5, 1:2, 1:1 and 1:0.5), complete results are in Appendix.6.a, 6.b.

Figure 5.8 shows the leachate concentrations of trace elements from baked Kaolin mixed with various ratios of SS (5%, 15% and 25%), pure baked Kaolin was used as a control sample.

The results of the leachate concentration of trace elements from the pure kaolin (control) show low concentrations (< 10µg/L) at all S/L ratios except for Ti , V, and Cr.

However, the concentration of these metals are still very low in comparison with its concentration in Kaolin before baking at 1000 ºC, moreover, it is lower than the maximum acceptable limits of the Jordanian Standard Specifications for waste water.

It is obvious that optimum S/L ratio for Cr, V, As, and Cd and (Ti, Zn, Pb, Co and U) are 1:5 and 1:2, respectively (Fig 5.8). Moreover, the results revealed that the leachate concentrations of Co, Zn, and U from SS are less than OS.

On contrary, the leachate concentrations of Cd and As in SS are higher than in OS. Furthermore, incorporation of SS in baked Kaolin led to significant reduction in the mobility of all these elements (Co, Zn, U, Cd, and As). The immobilization efficiency of SS in baked Kaolin for Co, Zn, U Cd and As are up to 99.6, 95.6, 99.64, 88.4 and 95.6 % respectively

The leachate concentrations of Ti, V, Cr, and Zr from SS in baked Kaolin were higher than leachate concentrations from SS. A possible explanation is high metal contents in the used kaolin.

Concentrations of Pb from OS, SS, and SS in baked Kaolin are very low (< 0.3 µg/L).

Moreover, V is a highly mobile element (Brookins 1988), the solubility of V is strongly controlled by its oxidation state. Its solubility is highest in toxic environments (Wanty and Goldhaber 1992), that is similar to the experimental conditions, the sorption of TI, V, and Cr by kaolin is very weak. However, the concentrations of these metals are still very low and they do not perform a serious threat to the groundwater.

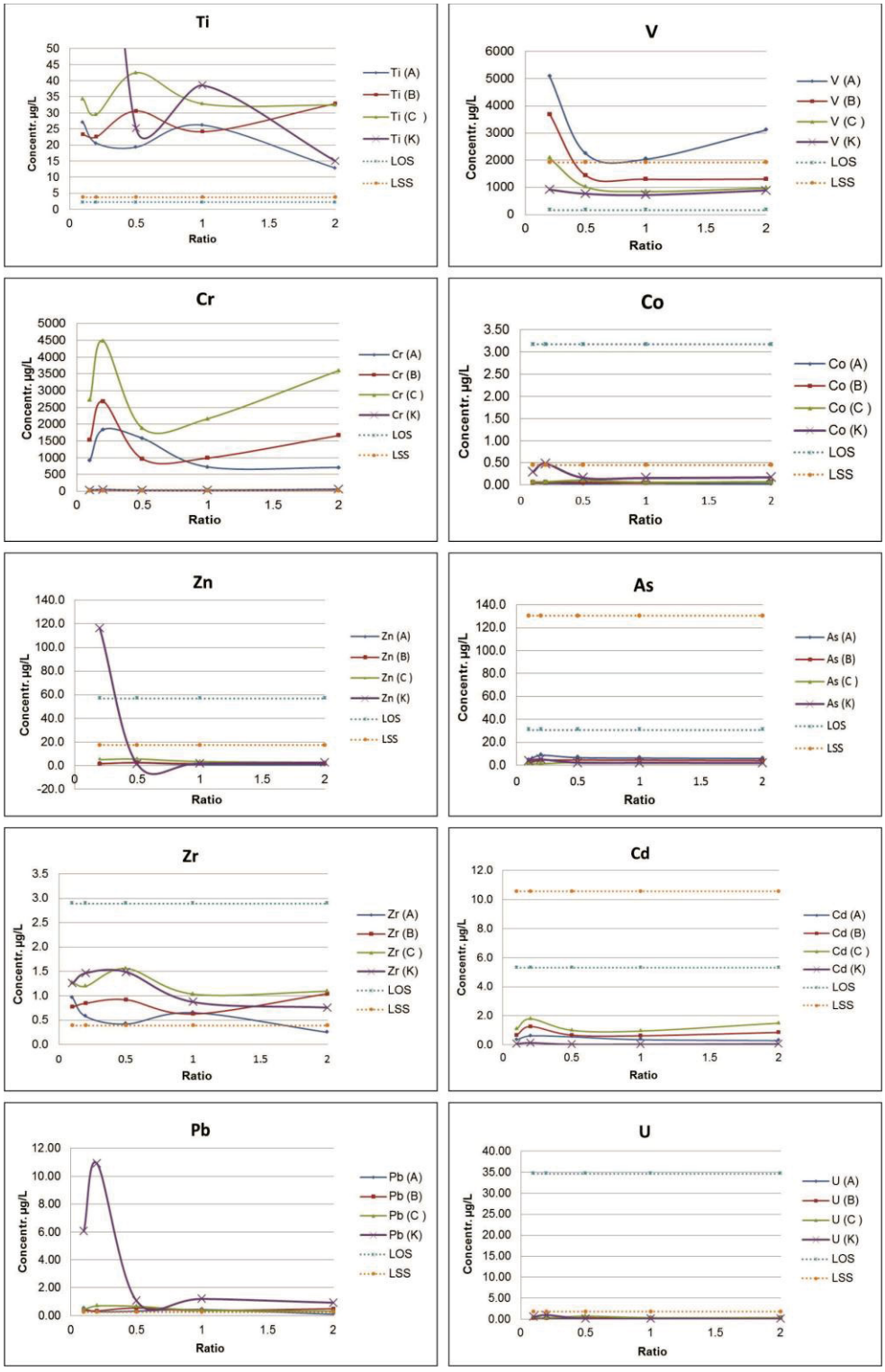

Figure 5.8: : Leachate concentrations of the Solid-Liquid partitioning as a function of liquid-solid ratio (M1316) for SS incorporated in backed-Kaolin at various ratios(A= 95% SS, B= 85% SS, , and C= 75% SS), and the Solid-Liquid ratios are: (1:10, 1:5, 1:2, 1:1, and 1:0.5), LOS and LSS are the total concentrations(µg/L) of oil shale and spent shale column samples over ten days leaching column experiment.

5.5.2 Liquid-Solid Partitioning as a function of pH

The results show that the optimum pH is 4 for the elements Ti, Cr, Zn, Zr, Pb, Co, Cd, and U (Appendix 7.a, 7.b). For V the optimum pH is 12. Moreover, the optimum leachability for As is at pH 6 and 12.

Figures 5.9 show that the SS leachate concentrations of Co, Zn, Zr, Pb Cr and U are significantly reduced in comparison with OS.

On the contrary the leachate concentrations Ti, V, As, and Cd from SS are increased. One possible explanation is in the high pH (10.5) of the SS (at this pH the elements Co, Zn, Zr, Pb, Cr are not soluble and precipitate in the form of hydroxide (Dulski, 1996).

Two parameters control the results: the ratio of spent shale to kaolin and the pH of the solution. The analysis of leachates from kaolin samples under different pH show that the mobility of Co increases under acidic and reducing conditions (Salminen, et al., 2005). A decrease of mobility of Co on the spent shale samples can be seen by increasing the pH. The competition with H^+ may cause a decrease of sorption of Cobalt at low pH. On contrary, Thomson at al., (1999) suggested that the increase of the solution´s acidity may be due to the reaction of Al $(OH)_3$ components of the clay with sulfuric acid producing $Al_2(SO_4)_3$ complexes and thus cause decrease in Co sorption, This is in agreement with the results of this study.

Generally, by increasing the pH of the solution, the mobility of Co is decreasing. It was observed that Zn is highly sorbing at alkaline pH. The mobility of Zn is greater under acidic and reduction conditions (Salminen, et al., 2005).

Sorption of As increases with increasing of Al, Fe- oxides and with increase of clay minerals content in soil (Elkhatib et al., 1984);, sorption as well increases on amorphous Fe- hydroxide, amorphous Al hydroxide, kaolin and montmorillonite (Manning and Goldberg 1996), As is highly adsorbed on oxides and clays at low pH.(Goldberg, 2002), and that is in agree with the results obtained on this research study (Fig 5.9).

Cd is most mobile under oxidizing conditions and when pH is below 8. Under this condition the release of Cd from rock is increasing (Brookins 1988). In this experiment, the mobility of Cd is decreasing with increasing the alkalinity, besides that Kaolin behaves as a good immobilization agent for Cd in the spent shale. Kabata-Pendias (2001) stated that the activity of Cd is strongly affected by the pH, however, it is more mobile in acidic soil, and the Cd compounds are precipitated in the alkali soil, which supports the above result.

Generally, it is supposed that Zr is very slightly mobile in soils due to sorbing to highly insoluble oxides, which are highly resistance to weathering, such as silicates and chloride

(Kabata-Pendias, 1993). Zirconium oxide is insoluble in acidic, alkali solutions, and almost in water and thus Zr is not much mobile at all.

The mobility or bioavailability of Zr depends on its chemical speciation, some of these minerals are soluble (e.g. zirconium oxychloride), whereas, most of the others are insoluble in water (Prisyagina et al. 2008). In contrast to this Whitfield (2011) and Bern et al (2011) emphasized that Zr is mobile in soils. However, in strong acidic solutions, some species (e.g. polynuclear hydrolysis) are formed and control the solubility and mobility of Zr.

Generally, soil pH affects desorption reactions, sorption and mobility of Zr in the soil (Davydov et al. 2006, Zou et al. 2009). The result of the experiments in this research shows that the mobility of Zn increases under high acidity condition (Fig 5.9)

The solubility of Pb increases with increasing acidity. Usually, this mobilization is slower than its accumulation in soil with rich organic layers (Kabata, 2011). Illites show a greater affinity to sorb Pb than other clay minerals, (Hildebrand and Blume,1974). The sorption of Pb depend on the ligands in the formation of hydroxy complexes of Pb, (Farrah and Pickering ,(1980). They suggested Pb sorption on kaolinite as cation exchange processes. (Fig 5.9) shows the increasing of Pb mobility by decreasing pH values.

Hamarneh, 1998 indicates that most of the U in the spent shale samples is associated with phosphorous content in the oil shale and not with bituminous organic matter. The results show that the mobility of U is slightly higher at pH 8 and pH 5 (Fig 5.9).

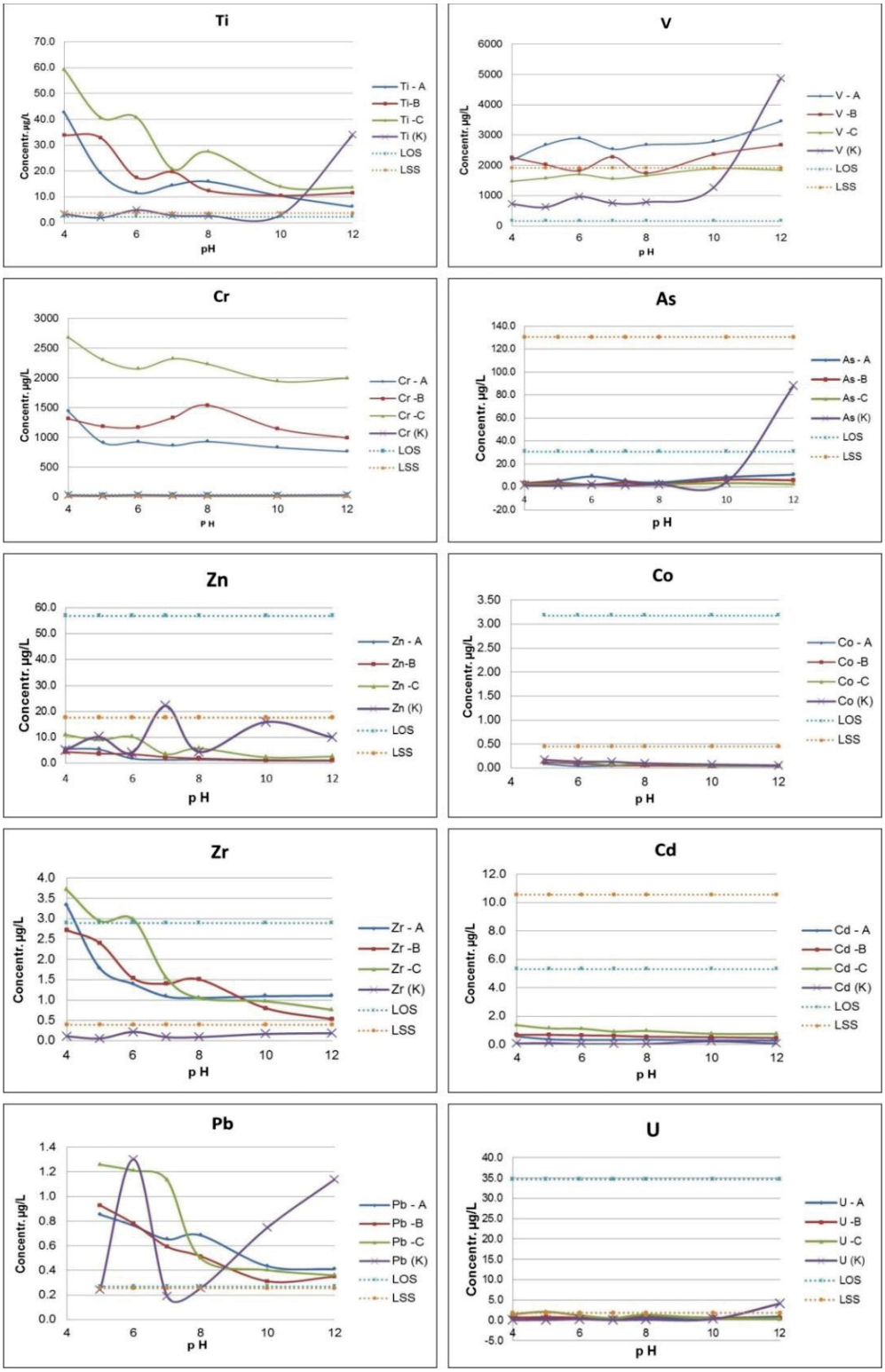

Figure 5.9: Leachate concentrations by using Liquid-Solid Partitioning as a function of pH. (M1313), for SS in backed-Kaolin at various ratios (A= 95% SS, B= 85% SS, and C= 75% SS,), and Solid-Liquid ratios (1:10, 1:5, 1:2, 1:1, and 1:0.5), LOS and LSS are the total concentrations (µg/L) of oil shale and spent shale over ten days leaching column experiment.

5.6 Results of risk assessment by DRASTIC

The DRASTIC index in El Lajjun area was determined through the range and rating for each factor:

- **Groundwater depth** (Factor D): The depth to the groundwater table in the catchment of the study is ranges from 22 to 170 m. However, the water table for the intermediate aquifer (B2/A7) in El-Lajjun area ranges from about 21 to 75 m. The range and rating used in the origin model (Aller et al., 1987) were not convenient to meet the characteristics of the study area, because water depths occur with wide ranges. Only two wells depths are < 30m. Thus, empirical values for range and rating were adapted (table 4.7) with respect to the characteristics of the study area. Finally, a new modified range and rating were used in this study (table 4.7).

  The depth to water table was determined from groundwater well data sets for the B2/A7 Aquifer, which was collected from (MWI) open file. After that, the data was drawn to give the final depth to water map as shown in Fig (5.10).

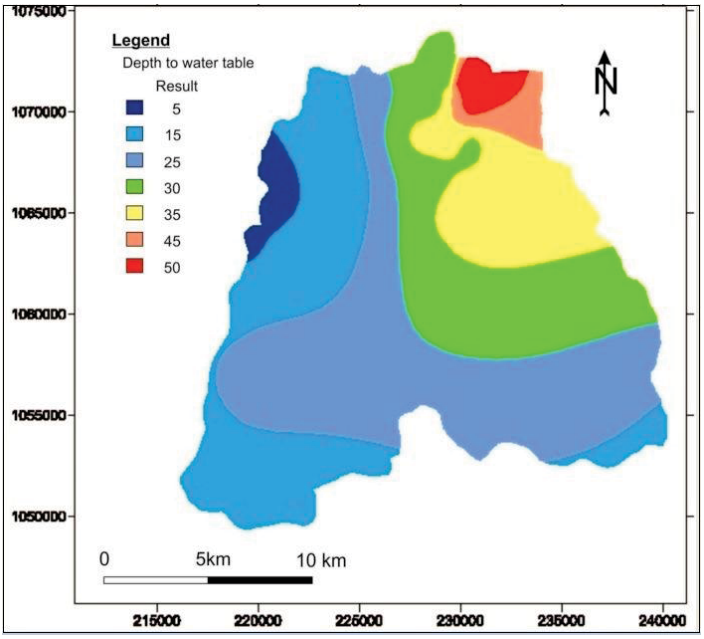

Figure 5.10: Map index of depth to groundwater table of the study area.

- **Groundwater Recharge** (Factor R): El-Naqa (1993) estimated the mean annual evaporation volume over the WadiMujib catchment area with 88% of the

precipitation. WJA estimated the evaporation with about 92.3%, the runoff with about 4.5%, and the infiltration with 3.2% of the precipitation.

- The annual rainfall over the catchment of the study area is around 190 mm/year in average (Table 3.5). Assuming an infiltration of about 3.2% of precipitation, then the groundwater recharge is 6.1 mm/year (0.61 cm/year). Figure 5.10, shows the recharge map over the study area, the rating value is 1, the weight is 3 and thus the DRASTICA index is 4. In consequnce the map has an uniform value of 4.

- **Aquifer media** (Factor A): The aquifer media type was obtained from the geological map scale 1:5000 done by NRA and well data from open file of MWI. The aquifer properties and medias were determined. The common media of B2A7 aquifer is karstic limestone, which has a rating of 10 and a weight of 3, ending with a uniform DRASTIC index of 30.

- **Soil Media** (Factor S): The soil map of Jordan was used in this study. The map was prepared by the Ministry of Agriculture (MOA, 1993). According to this map, there are two types of soil media in study area; Loam and clay loam which reflect values of 6 and 10, respectively (Fig 5.11).

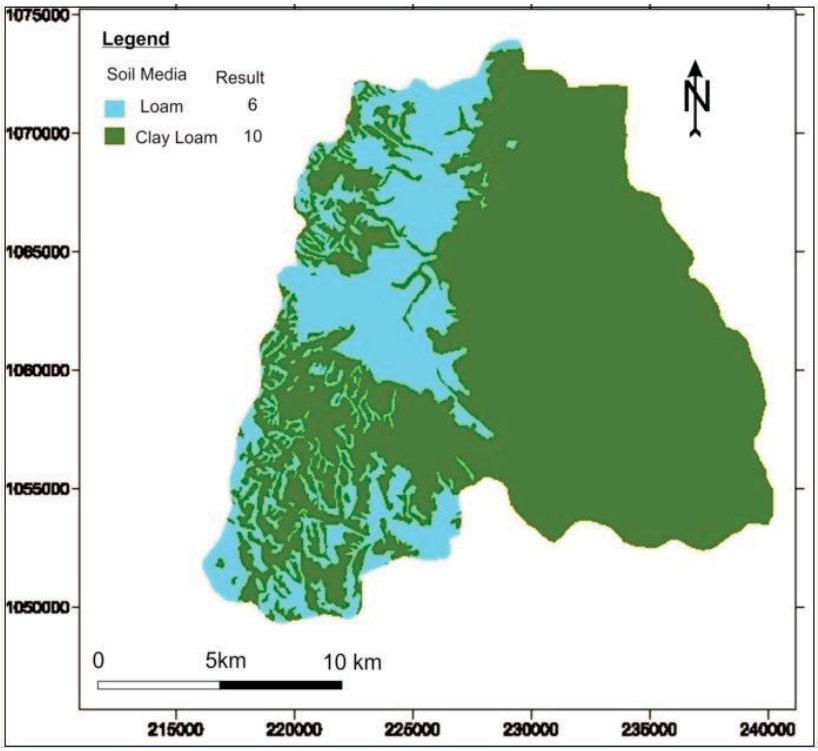

Figure 5.11L Soil media map of the study area.

- **Topography (Slope %) (Factor T):** Land surface elevations for the catchment area were derived from a digital elevation model (DEM) for Adir and Karak area from l: 50,000 scale maps. Most of the area has steep slope (slope > 18 %), which provides a high runoff capacity, and less probability of contaminate infiltration. The slope was classified, rated and finally slope index map were created as shown in Fig (5.12).

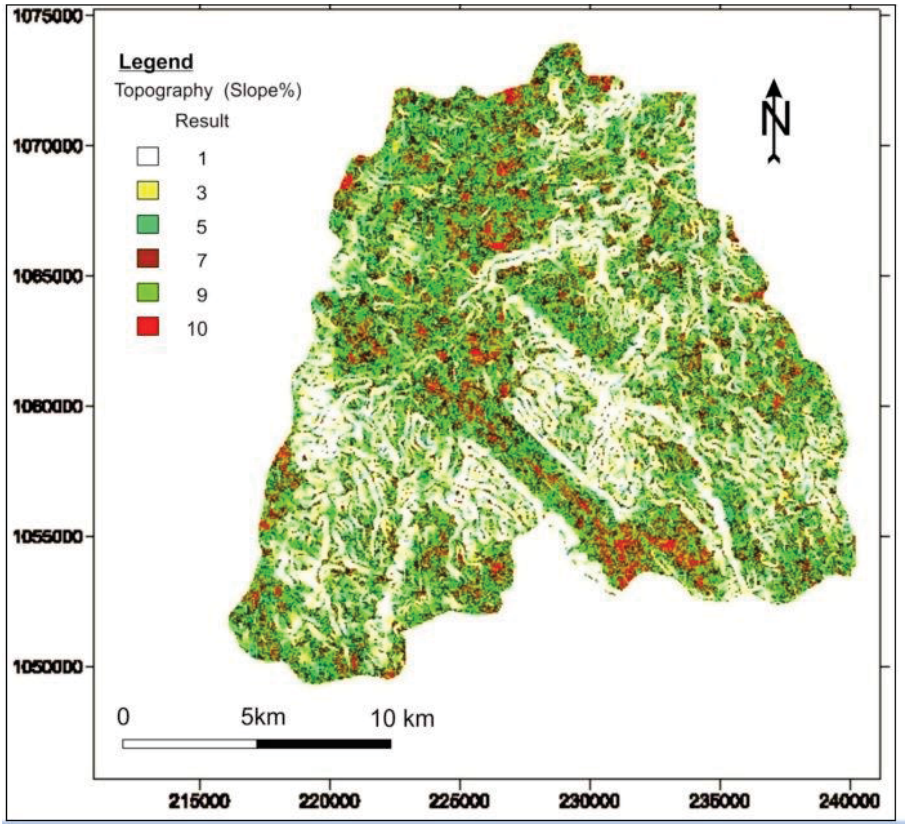

Figure 5.12: Topographic map for the study area.

Vodose Zone Impact (Factor I): It is defined as the zone above the water table which is unsaturated, or discontinuously saturated with water. The geological maps of Adir and Karak area, scale 1:50:000, were used (NRA). The lithology data were obtained from groundwater well data (MWI): bedded limestone and sandstone, massive limestone and basalt rocks (Fig 5.13).

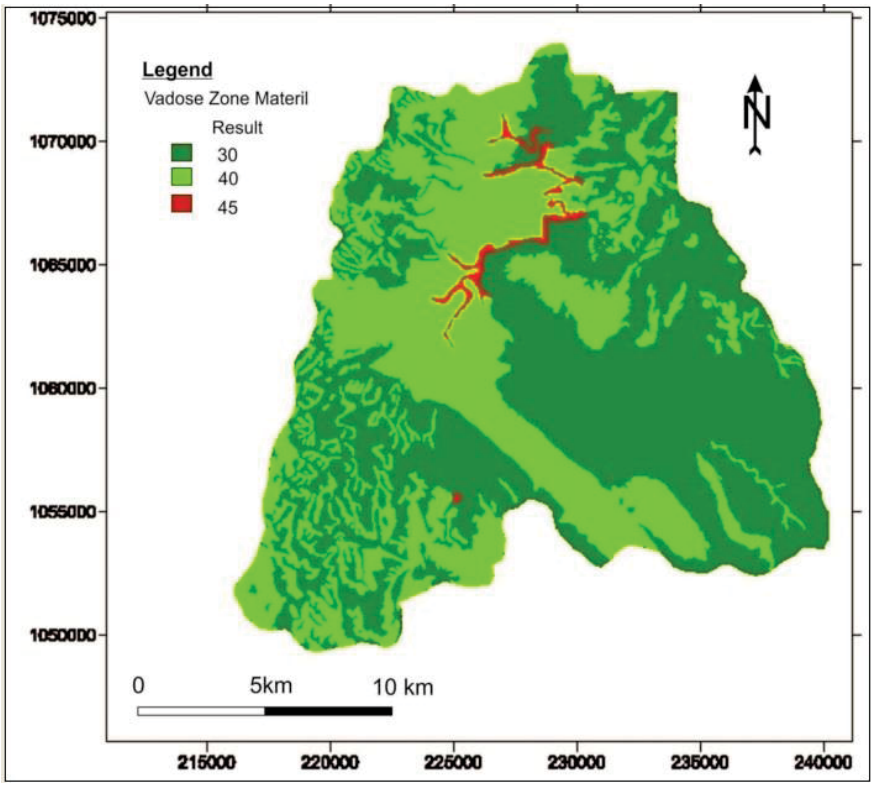

Figure 5.13: Vadose zone impact map of the study area.

- **Hydraulic Conductivity (Factor C):** Hydraulic conductivity is one of the most important factors and controls the rate of groundwater movement in the saturated zone and the degree and fate of contaminants. Hydraulic conductivity values used in this study were derived from pumping test data and from the study of (BGR, 1997). They calculated the hydraulic conductivity for the aquifer of B2A7. Due to karst features, joints, caves, the hydraulic conductivity of the aquifer varies from 0.864 m/day to 8.64 m/day. However, high average value exists in El-Lajjun graben and in the faulted areas in south western and southern parts of the catchments. The resulting map of the hydraulic conductivity index shown in Figure 5.14.

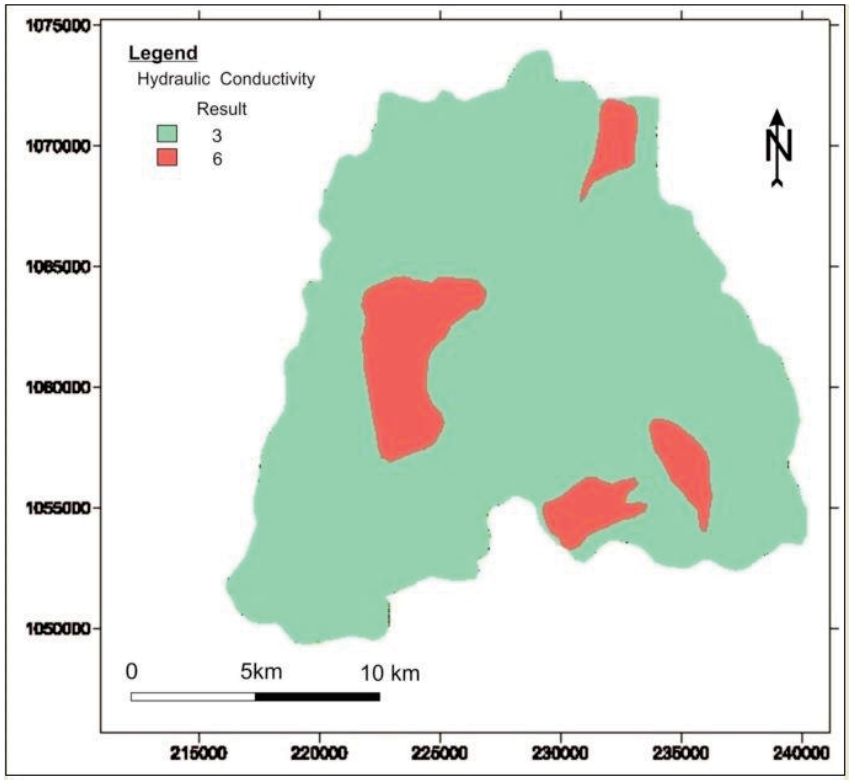

Figure 5.14: Hydraulic conductivity map of the study area. The higher hydraulic conductivity values are located in highly faulted and fractured areas in the catchment area (presented in red).

- **DRASTIC Index Calculation**

  DRASTIC Index for the study area is calculated and shown in Table 5.4.

Table 5.4: Summary of DRASTIC index calculations.

DRASTIC Factor	Range	Rating	Weight	Result
Depth to Water Table (m)	1-30	10	5	30
	30-60	9	5	45
	60 -90	7		35
	90-120	6	5	30
	120-140	5	5	25
	140-150	3	5	15
	> 150	1	5	5
Recharge (cm)	0- 2 (0.6 cm)	1	4	4
Aquifer Media	Karst Limestone	10	3	30
Soil Media	Loam	5	2	10
	Clay Loam	3	2	6
Topographic (Slope %)	0-2	10	1	10
	2-4	9	1	9
	4-6	7	1	7
	6- 8	5	1	5
	8- 10	3		3
	>18	1	1	1
Vadose Zone Material	Bedded Limestone, Sanstone	6	5	30
	Sand and Gravel With Signification Silt	6	5	30
	Sand and Gravel	8	5	40
Conductivity	Basalt	9	5	45
	0-4.1	1	3	3
	4.1-12.3	2	3	6
DRASTIC index	**Value**		**Class**	
	1-100 (83 - 10)		Low	
	101-140 (101 – 140)		Moderate	
	141-200 (141 – 150)		High	

The vulnerability map of El Lajjun catchment area was obtained using the seven hydrogeological data layers in Arc View GIS software. The score of DRASTIC ranges between (83 to 150). Taking into consideration the determined ratings and weighs (table 5.6). These values were reclassified into three main classes according to DRASTIC method classification index (Aller et al., 1987).The study area's vulnerability was classed as low (1-100), moderate(101-140), and high (141-200) as shown in Fig. (5.15).

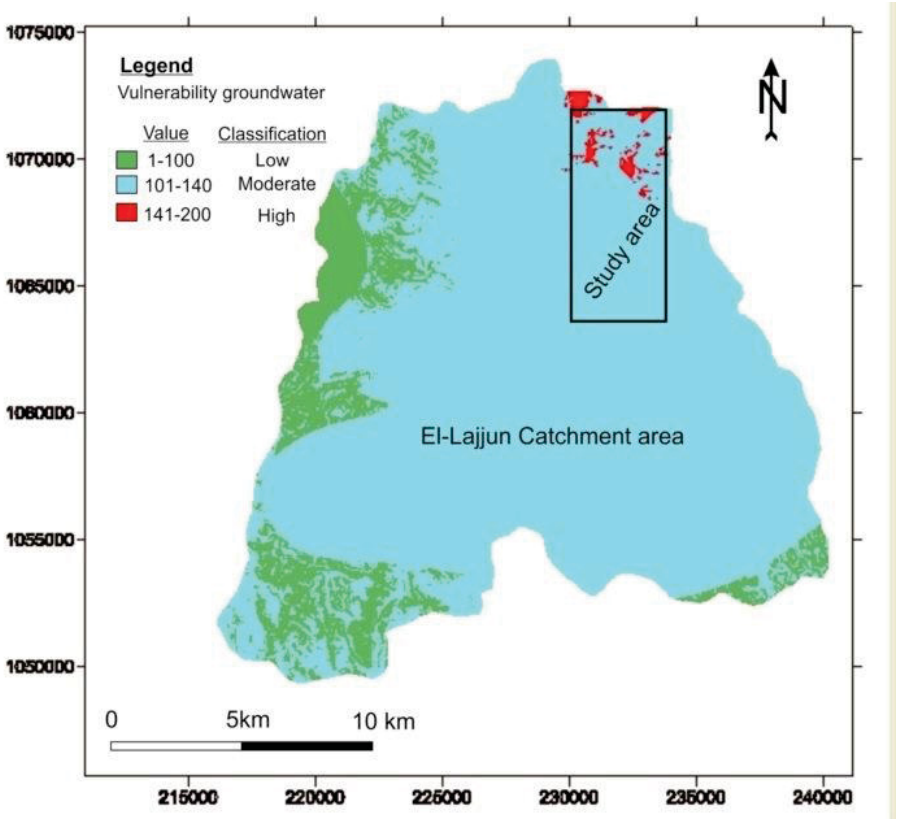

Figure 5.15: DRASTIC Vulnerability index map of the study area, the area with high vulnerability index presented in red.

The high groundwater vulnerability risk zones of the catchment of the study area is limited. They were mainly located in the northeastern corner of El-Lajjungraben and around El-Lajjun village, where the water table is relatively shallow (less than 60 m). The area is highly faulted and fractured (Fig 5.16) which makes the hydraulic conductivity relatively high (about 8.46 m/day) (BGR, 1997). The narrow western and south-western zones of the catchment are within the low vulnerability class. The rest of the catchment area is classified as moderate vulnerable.

Margane and other in 2005, classified El-Lajjun area as high to very high vulnerable. They applied a GLA method which is a kind of rating method. However, the GLA-method only takes the unsaturated zone into consideration. However their results gave an indication about the groundwater vulnerability, which is in agreement with the results obtained by this research study.

Al-Adamat and others in 2010, applied DRASTIC method using GIS to assess groundwater vulnerability to pollution in El-Lajjun area. Their result showed that the area is moderate to low vulnerable. However, it is worth mentioning that they did not take the factor of hydraulic conductivity into consideration.

The result also shows that El-Lajjun area is at the upper margin of moderate and lower margin of high vulnerability. The depth to the water table is the main effective and sensitive factor. However, the depth is relatively shallow, and there is a high possibility to the oil shale mining in the study area to decrease the depth to water table by removing the vadose zone and the overburden, which is existing over the intermediate aquifer (B2/A7). Decreasing the depth to the water table will directly affect the vulnerability values in El-Lajjun areas, and thus the DRASTIC Index value will be within the high vulnerability class. The water table of the intermediate aquifer (B2A7) in some localities is within the lower part of oil shale beds (Fig 5.16). In the last years, the water table was lowered due to extensive pumping, but is still very close to the base oil shale bed, and to the ground surface as well.

For any future oil shale utilization project, it is highly recommended to be cautious of hitting the B2/A7 aquifer during the mining process to avoid groundwater contamination. In case of storing spent shale in the ground, it is highly recommended to store it in isolated and lined impervious layers to avoid groundwater contamination.

The water table of the deep sandstone aquifer (Kurnub/Ram group) in El-Lajjun area is relatively deep. Moreover, there are at least two geological formations acting as aquitards. These formations (A1-6) are forming the main aquitard, which separates the two main aquifer systems in the study area. It consists mainly of about 270 m of marl and marly limestone. However, the area is highly fractured and therefor a slight possibility for groundwater contamination with the surface pollutants exists (Fig 5.16).

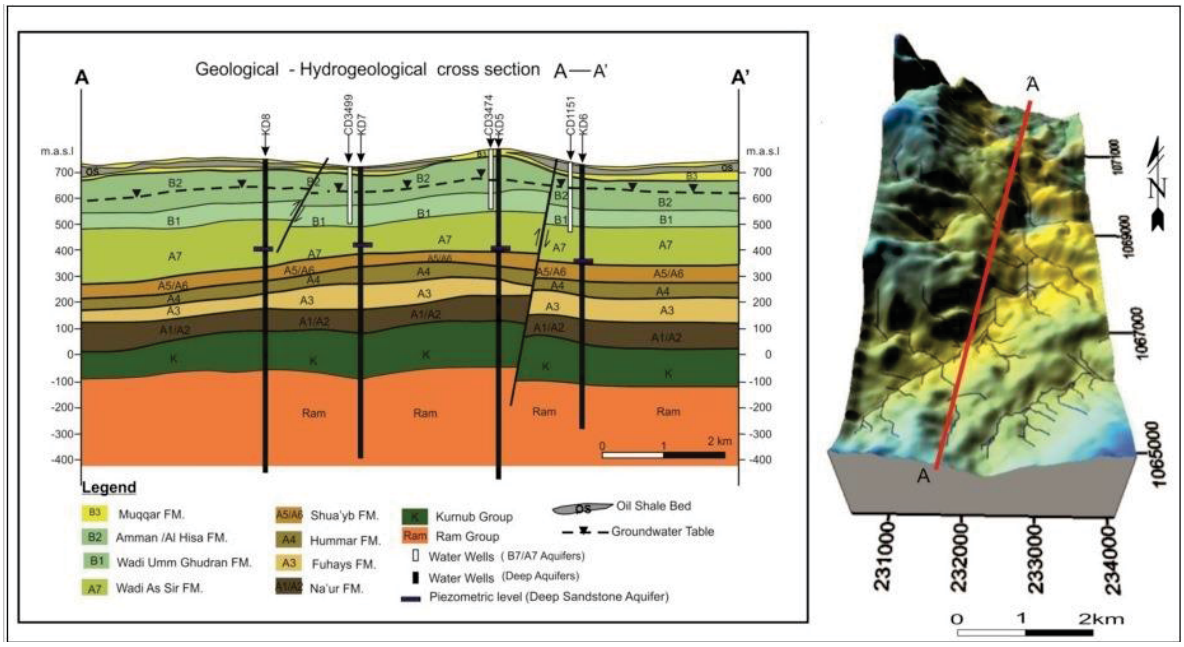

Figure 5.16: Geological –hydrogeological cross section (A-A´), the section built from the data obtained from groundwater wells of the intermediate and deep aquifer for El-lajjun.

5.7 Rainfall – runoff calculations results

The equation (S = (1000 / CN) – 10) is used in this study for the runoff model.

Soil was originally assigned by hydrological soil groups (HSGs). Four groups (A, B, C, D) were defined based on measured rainfall, runoff, and infiltrometer data (Musgrave, 1955). The soils type in the study area are of Group C, where they have moderate high runoff potential when thoroughly wet; the soil in this group has clay (20 to 40 %) and sand (> 50%) and have loam, silt loam sandy clay loam and silty clay loam textures (Mockus,1972). The moisture condition in a soil prior to a storm event is referred to as the Antecedent Runoff Condition (ARC). The Natural Resources Conservation Service (NRCS) developed three antecedent runoff conditions: ARC I (Dry Condition): soils are dry but surface cracks are not evident, ARC II (Average Condition where soils are not dry or saturated, and ARC III (Wet Condition) where soils are saturated or near saturation due to heavy rainfall or light rainfall and low temperatures within the last 5 days (USDA-NRCS, 2004).

The soil type in the study area is of Group C according to the classification tables of the Soil Conservation Services. This gives a CN value of 74, inch is applied in equation (S = (1000 / CN) – 10) to obtain ARCII,

S= (1000/74) - 10

S= 3.51 inches.

The following runoff equation was used to obtain the values for dry, normal, and wet conditions.

Q = (P - 0.2 S)2 / (P + 0.8 S)

With a rainy day value of 20 the average storm rainfall becomes 3.8 inches. Substituting the obtained values of s and p in the runoff equation gives

Q= 1.44 inches.

The same calculations can be repeated for ARCI and ARCIII. Results are shown in table 5.5.

Table 5.5: Calculated components of the rainfall under different conditions according to Antecedent Runoff Condition (ARC).

ARC	Rainfall (inches)	CN	S	Runoff %	Runoff
ARCI	Dry	55	0.44	11.6	7.74 * 10^6
ARCII	3.8	74	1.44	36.9	25.60 * 10^6
ARCIII	Wet	88	2.53	66.6	44.99 * 10^6

Precipitation in (10^6 m^3) for each storm is given as follows:

P = A (km^2)* P (mm)

= 700 * 9.65

= 67.55 * 10^6 m^3.

The infiltration amounts are very small and rarely can reach the aquifer thought the oil shale beds beneath the surface, but there is weak possibility to infiltrate through the highly fractured and faulted beds. Therefore, the contamination may not take place in the normal conditions.

5. 8 Result of Hydrochemical data analysis

5.8.1 Groundwater aquifer trace elements

Five repetitive samples were collected from groundwater wells taped from Intermediate aquifer (B2/A7), and from the deep sandstone (Kurnub/Ram) aquifer. The results show that the mean level of most elements determined in the water samples ware within the Jordanian standards as well as the World Health Organization standards for drinking water (Appendix 8.a.b.c).

5.8.2 Total dissolved solids

TDS was calculated from the chemical analysis of major elements (Freeze and Cherry 1979), the type of water according to classification proposed by Caroll (1962) are presented too, it is clear from the TDS values that the two aquifers (B2/A7) and the deeps and stone aquifer (Kurnub/Ram) are almost fresh water, the deep sandstone aquifer has lower TDS value than that of B2/A7. The electrical conductivity (EC) measurements for the intermediate aquifer (B2/A7) ranges between 1066 to 1362 µS/cm in average is 1224 µS/cm, in the lower sandstone aquifer ranges between 701 to1256 µS/cm in average about 874.5 µS/cm, the TDS value for the B2/A7 aquifer ranges between 463.1 to 589.5mg/l in average (518.3mg/l) and the average of the pH is 7.4,whilethe TDS for the lower sandstone aquifer (KURNUB/Ram) ranges between 266.6 to 533.2 mg/l in average 354.1mg/l and the average of the pH is 7.2 (Appendix 9).

Chapter 6 CONCLUSIONS AND RECOMMENDATION

6.1 Conclusion

This study focuses on the environmental impact assessment of trace elements concentrations in spent shale, which is the major residual from the utilization of oil shale.

The X-ray diffraction (XRD) results for a representative oil shale samples indicate that mineralogy of El-Lajjun oil shale, as a whole, is uniform with depth, and consists of Calcite and Quartz as major constituents, and of Apatite, Dolomite, Feldspar and Pyrite as minor or trace constituents.

Fisher assay results indicate that the oil shale in the study area, and generally in Jordan, is rich in organic matter and that spent shale will be the main residual product of the extraction techniques. It is relatively high in average (81.5 %).

The results of the SS sequential extraction show different distribution pattern of trace elements on six fractions in comparison with OS. Moreover, the accumulation of elements concentrations in SS mobile and potential labile fractions is higher than the same elements in OS. The only exception is Zn (it is 15% less in SS in comparison to OS). This is probably due to the fact, that Zn has a high affinity to organic matter (Wedepohl, 1978). It could be that the Zn was separated with the oil vapor and shale gas from the solids during the pyrolysis process.

The results of sequential extraction experiment indicate that the concentration of trace elements and trace elements are richer in oil shale and in the spent shale than the earth crust. However, this is mainly because these elements are associated with hydrocarbons content of oil shale.

The results of column leaching experiment show that Co, Zn, Zr, and U concentrations from LOS column are higher than those from the LSSP columns and LSS columns. These elements leave the retort and become a part of the shale oil due to their volatility.

The concentration of U is slightly higher in water that leachate from LOS than from LSS samples. However, it is clearly associated with phosphorous more than the bituminous organic matter (Hamarneh, 1998).

The result of the experiment indicates that the phosphates layer underneath the spent shale reduce the mobility, and thus reduce the level of the metals leached from the spent shale, and that is due to its low permeability. Except in the case of Cr, which increased, It seems that the phosphate rocks act as a source for Cr in this experiment and not as sorbent (El-Sheikh et al., 2013). Finally, the ten days records for the leaching of the trace elements from each column show that the concentrations are below the MCL´s of the EPA for drinking water and the Jordanian standard specification for drinking water (JS286/1997).

Spent Shale was encapsulated in baked Kaolin in order to evaluate the immobilization potential of trace elements in SS and OS. Kaolin was added to the spent shale samples and oil shale samples in different ratios. Two leaching standard methods were investigated. Solid-Liquid partitioning as a function of Liquid-Solid ratio (S\L) (M1316), and Solid-Liquid partitioning as a function of pH (M1313) were carried out. A comparison between the results obtained from column leaching experiment and the results that were obtained from immobilization methods for the OS and SS samples is as follows:

In the M1316 experiment, distilled water was used, and the L/S ratio was 1:10, 1:5, 1:2, 1:1, and 1:0.5. It is obvious that optimum S/L ratio for Cr, V, As, and Cd and Ti, Zn, Pb, Co and U are 1:5 and 1:2, respectively. Moreover, the results revealed that the leachate concentrations of Co, Zn, and U from SS are less than OS, which means that incorporation of SS in baked Kaolin led to significant reduction in the mobility of elements (Co, Zn, U, Cd, and As). The immobilization efficiencies of SS in baked Kaolin for Co, Zn, U Cd and As are up to 99.6, 95.6, 99.64, 88.4, and 95.6 % respectively

The leachate concentrations of Ti, V, Cr, and Zr from SS in baked Kaolin were higher than leachate concentrations from SS. A possible explanation is high metal contents in the used kaolin. Concentrations of Pb from OS, SS, and SS in baked Kaolin are very low. Moreover, V is a highly mobile element (Brookins 1988) and its solubility is strongly controlled by its oxidation state. The solubility of V is highest in toxic environments (Wanty and Goldhaber 1992) that is similar to the experimental conditions. The sorption of TI, V, and Cr by kaolin is very weak. However, concentrations of these metals are still very low and they do not perform a serious threat to the groundwater.

In the M1313 experiment, different pH values (4, 5, 6, 7, 8, 10, 12) were used. The results show that the SS leachate concentrations of Co, Zn, Zr, Pb, Cr and U are significantly

reduced in comparison with OS. On the contrary, the leachate concentrations Ti, V, As, and Cd from SS are increased. One possible explanation is in the high pH (10.5) of the SS (at this pH the elements Co, Zn, Zr, Pb, Cr are not soluble and precipitate in the form of hydroxide (Dulski, 1996).

It was recognized that the concentration of the trace elements and heavy metals that were measured in the immobilization methods still below the maximum level as per the EPA for drinking water, and Jordanian standards for drinking water (JS286/1997) as well.

GIS model and the DRASTIC method were used for determining the vulnerability of the groundwater (intermediate aquifer (B2/A7)) in El- Lajjun catchment area. The aquifer vulnerability map, as a result, shows that the area is divided into three zones: low (risk index (10-100); intermediate (risk index 101–140) and high groundwater vulnerability (risk index 141-200). The highly risk areas are limited and are mainly located in the northeastern corner of El-Lajjun graben and around El- Lajjun village, where the water table is relatively shallow (less than 60 m), and the area is highly faulted and fractured. This makes the hydraulic conductivity relatively high (about 8.46 m/day) (BGR, 1997).

The water table of the deep sandstone aquifer (Kurnub/Ram group) in El-Lajjun area is relatively deep. Moreover, there are at least two geological formations act as aquitard. These formations are forming the main aquitard, which separates the two main aquifer systems in the study area. Although, the area is highly fractured and still there is a very weak possibility for groundwater contacted with the surface pollutants.

The results of the rainfall – runoff calculations for the catchment of the study showed that the infiltration amounts of water are very small and rarely can reach the oil shale beds beneath the surface. Therefore, the contamination may not take place at normal conditions.

6.2 Recommendations

As a result of this study the following investigations are highly recommended to be carried out in the area of interest:

1. The immobilization methods applied in this study reduced the mobility of Co, Zn, Zr, Cd, Pb, and U, but there is no satisfied effective on the mobility of Ti, V, Cr; it is recommended in further investigations using other amendment for immobilization of toxic elemenst.
2. Chemical and isotopic research related to the intermediate and deep sandstone aquifers is recommended, however, the investigations should focus on the isotopic signature to assess the hydraulic connection between the two aquifers.
3. Details studies on the spent shale and its possibilities in industrial uses are recommended, since huge quantities of this material are expected after retorting.
4. Most of oil shale extraction technologies, especially power generation require considerable amounts of water, therefore, detailed water studies should be considered carefully.

Chapter 7 SUMMARY

Many research studies have been performed about the oil-shale in Jordan, related to origin, geology, geochemistry, mineralogy and chemistry. This study focuses on the environmental impact assessment of trace elements concentrations in spent shale, which is the main residual from the utilization of oil shale.

The study area El-Lajjun covers 28 km^2, located central Jordan, approximately 110 km south of Amman; and belongs mainly to the Wadi Mujib catchment, it is considered to be one of the most important catchments in Jordan.

Wadi El-Lajjun catchment area (370 km^2) consist of two main aquifer systems: The intermediate Aquifer System (Amman Wadi As Sir Aquifer) (B2/A7), and the deep sandstone aquifer (Kurnub/Ram Group Aquifer). The B2/A7 aquifer is part of the Upper Cretaceous aquifer and is considered as the main source of fresh water in Jordan.

The upper Cretaceous sedimentary rocks are the most dominant formations in the study area.They are composed mainly of marl, chalky marl, oil shale, limestone, chert, phosphorite, silicified limestone and massive limestone, in addition to alluvial gravels of Pleistocene age.

The Cretaceous-Palaeogene rocks in Jordan are divided into four lithostratigraphical groups; Kurnub, Ajlun, Belqa and Batn Al Ghul. The Kurnub sandstone group consists mainly of continental silicicalstics. The Ajlun Group comprises predominantly marine carbonate platform sediments and six formations; in upward sequence these are; Naur (A1-2), Fuhays (A3), Hummar (A4), Shuayb (A5/6), Wadi As Sir Formation (A7) and Khuraij Formation, neither the Kurnub Group nor the Ajlun Group are exposed in the study area, but they are recorded in some of the deep boreholes within the catchment area.

The Dead Sea Transform Fault (DST), Karak-Al Fayha Fault System and Siwaqa Fault are the nearest faults zones to the study area, the study area is bounded by two major faults, trending NNW-SSE forming major, elongated graben (i.e Lajjun Graben), the graben is marked by a broad topographic low consisting of down faulted Muwaqqar Chalk Marl formation overlain by Pleistocene gravels.

The study area is located within the Highlands Topographic region, which is one of the three elongated distinctive topographic provinces in Jordan.

The study area is characterized by the Saharan Mediterranean bioclimatic zone, the climate is characterized by the relatively short rainfall period during the cool winter season between November and March while the summer season is characterized by an extensive drought.

The Hydrogeology of the study area is controlled by the geological setting, which also controls the piezometery, occurrence and movement of the groundwater, and the distribution of productive areas in the aquifers.

The main aquifers in El-Lajjun catchment area consist of two main aquifer systems: The intermediate Aquifer System (Amman Wadi As Sir Aquifer) (B2/A7), and the deep sandstone aquifer (Kurnub/Ram Group Aquifer), the (B2/A7) aquifer is of the Upper Cretaceous age, and consists of limestone, chert, and marly limestone, this considered as the main source of fresh water in Jordan, the Kurnub/Ram Group Aquifer, consists of the sandstone of the Lower Cretaceous and older ages, The B2/A7 aquifer is underlain by the (A1\6) sequence, consisting predominantly of marl, marly limestone and limestone. This sequence is regarded as an aquitard, it hydraulically separates the B2/A7 aquifer from the underlying Kurnub/Ram Group aquifer.

There are many water wells drilled previously in El-Lajjun water field by the Ministry of Water and Irrigations (MWI), and by privet sector, many of these wells penetrating the intermediate aquifer (B2/A7), some others of deep sandstone aquifer of (Kurnub/Ram) of 1000m depth. These wells were drilled to supply Amman the capital city for domestic water.

Oil shale is generally defined as sedimentary rocks that contain an organic material in its inorganic matrix, the inorganic material is mainly composed of dolomite and limestone,

The Oil shale deposits of Jordan have been investigated since the 1960's. These investigations focused on economic and environmental methods for utilizing oil shale, resources for power generation and/or retorting. El-Lajjun oil shale was deposited in sedimentary basin; it is comprise massive beds of brown-black, kerogen-rich, bituminous chalky marl, which were deposited in shallow marine environment.

The shale oil extraction is a technical industrial process to decompose the oil shale and to convert its kerogen into shale oil by hydrogenation, pyrolysis process or by a thermal dissolution.

Several classifications of extraction technologies have been created, these classifications

are based on; process principles, heating methods, heat carrier, location of extraction and others, the classification with respect to location distinguishes between off-site, on-site, and in situ.

The In-situ technology is below-ground heating processing for oil shale by thermal injection of a hot fluid through the ground into the bed rock that contains oil shale. The surface retorting, also known as over-ground retorting (ex-situ processing); the process of which the shale oil extracted after the raw materials have been mined and transported to the processing facilities. Generally, the method depends on internal combustion technologies and that means to heat the oil shale materials within a vertical or horizontal reactor for the decomposition at high temperatures (pyrolysis).

Several oil shale ex-situ thermal processes for oil shale thermal decomposition have been developed and patented worldwide of commercial processes include Galoter, Fushun, Alberta Taciuk, Kiviter and Pertosix Lurgi-Ruhrgas or TOSCO II.

Recently, Government of Jordan gave rights to an international oil shale companies to mine and process oil shale in El Lajjun Area, and will apply the proven oil shale extraction technology of the Alberta Taciuk process (ATP).

The proposed oil shale utilization processes; mining, products and byproducts, could have serious repercussions on the surrounding environment if these issues are not investigated and treated accordingly.

Many reconnaissance filed trips have been carried out to El-Lajjun area. All pervious data regarding; the geology, lithology of drilled boreholes and their chemical and mineralogical results were collected and reviewed.

Ten representative oil shale (OS) rock samples (with total weight about 20 kg) were collected from different localities of oil shale exposures in the study area. A standardized laboratory Fischer Assay test has been done on the OS samples, for determining oil shale characteristics, and to obtain spent shale (SS), which will be used in this research study. Sequential extraction procedure was used to evaluate the changes in the mobility and distribution of the main trace elements and heavy metals: Ti, V Cr, Co, Zn, As Zr, Cd, Pb and U. Detailed column leaching experiment has been done; to simulate the leaching behavior of the above elements under actual field conditions, and possibilities influence on the groundwater in the study area have been evaluated. The records for the leaching of

the trace elements show that the concentrations are below the MCL´s of the EPA for drinking water and the Jordanian standard specification for drinking water

An immobilization method was used to reduce the mobilization and bioavailability of the trace elements fraction that are contained in the spent shale, by using Kaolin as soil amendment. Two methods were applied to evaluate this immobilization method, they are; solid-Liquid partitioning as a function of liquid-solid ratio, and Liquid-solid partitioning as a function of pH. A comparison between the results obtained from column leaching experiment and the results that were obtained from immobilization methods for the OS and SS samples, indicated that the immobilization method reduced the mobility of the trace element expect, Ti, V, and Cr, however, it is still lower than the maximum acceptable limits of the Jordanian Standard Specifications for waste water. The Inductively coupled plasma mass spectrometry (ICP-MS) was used to determine all the experiment results.

The catchment of the study area (Wadi El-Lajjun catchment) is ungauged; therefore, the SCS runoff curve number method is used for predicting direct runoff from rainfall excess, the results of the method calculations showed that the infiltration amounts of water are very small , (approximately 0.6 cm/year), and rarely can reach the groundwater through the oil shale beds beneath the surface, therefore, the contamination may not take place due to normal conditions.

The DRASTIC approach was used to assess the groundwater vulnerability of the B2/A7 aquifer to pollution by oil shale utilization. The aquifer vulnerability map shows that the area is divided into three zones: low (risk index (10-100); intermediate (risk index 101–140) and high groundwater vulnerability (risk index 141-200), the highly risk area is limited, and were mainly located in the northeastern corner of El-Lajjun graben, where the hydraulic conductivity is relatively high, and the area is highly fractured and faulted.
The water table of the deep sandstone aquifer (Kurnub/Ram group) in El-Lajjun area is relatively deep, moreover, the aquifer is confined however, and there are at least two geological formations above act as aquitard. Although, the area is highly fractured and still there is a very weak possibility for groundwater contacted with the surface pollutants.

Finally, it is recommended for detailed chemical and isotopic specialized research related to the intermediate and deep sandstone aquifers. However, the investigations should focus on the isotopic signature to assess the hydraulic connections between the aquifers.

Details studies on the spent shale, and its possibilities in industrial uses is recommended because huge quantities of this material are expected after retorting. Most of oil shale extraction technologies, especially power generation require considerable amounts of water, therefore, detailed water studies should be considered carefully.

8 REFERENCES

- **Abed, A. M., 1982**. Depositional environments of the early Cretaceous Kurnub (Hathira) Sandstones, north Jordan. Sedimentary Geology, 31: 267-279.
- **Abed, A. M., 2000.** Geology of Jordan. Jordanian Geologists Association, Amman, 571p.
- **Abed, A. M., Arouri, K., Amireh, B. S. and Al-Hawari, Z. ,** 2009."Characterization and genesis of some Jordanian oil shales" Dirasat, Vol. 36, No.1, p.7-17.
- **Abu Ajamieh, M., 1980.** An assessment of the El Lajjun oil shale deposit., Nat. Res. Auth., Amman, 82p.
- **Abu Saad, L. and Andrews, I.J.**,1993. A database of stratigraphic information from deep boreholes in Jordan. Geology Directorate, Subsurface Geology Division, Natural Resources Authority, Subsurface Geology Bulletin, 6.
- **Abu-Qubu, J., Rimawi, O., Abu-Hamatteh, Z.S.H., Merkel, B. and Dunger, V.,** 2016 Groundwater modeling of wadi wala dam area the heedan wellfield in Jordan
- **Agrar- und Hydrotechnic**. ,1977. National Water Master Plan of Jordan. Groundwater Resources, Vol. 3. Unpublished report, Ministry of Planning, Amman.
- **Al-Adamat, R., Al-Harahsheh, A. and Al-Farajat, M.,** 2010. The Use of GIS and Leachability Tests to Investigate Groundwater Vulnerability to Pollution from Oil Shale Utilization at Lajjoun Area/Southern Jordan. Institute of Earth and Environmental Sciences.
- **Al-Adamat. RAN., Foster. IDL., Baban. SMJ**. 2003. Groundwater vulnerability and risk mapping for the Basaltic aquifer of the Azraq basin of Jordan using GIS, remote sensing and DRASTIC. Appl Geogr. 23:303–324.
- **Al-Harahsheh, A., Al-Otoom, A., Al-Harahsheh, M., Allawzi, M., Al-Adamat, R., Al-Farajat, M. and Al-Ayed, O.,** 2012. The Leachability Propensity of El-Lajjun Jordanian Oil Shale Ash. Jordan Journal of Earth and Environmental Sciences.(Special Publication, Number 2), 4, pp.29-34.
- **Aller, L., Bennett, T., Lehr, J. H., Petty, R.J., and Hackett G.,** 1987, DRASTIC: A standardized system for evaluating ground water pollution potential using hydrogeologic settings: NWWA/EPA Series, EPA-600/2-87-035.

- **Altun, N. E., Hiçyilmaz, C., Hwang, J. Y., Suatbaǵci, A. and Koķ, M.V.** 2006. "Oil shale in the world and Turkey; reserves, current situation and future prospects: a review" Oil Shale Journal. Vol. 23, No. 3, .p. 211-227.
- **Altz-Stamm, A**., 2012. Jordan's water resource challenges and the prospects for sustainability. GIS for Water Resources.
- **Amireh, B**. ,1979. "Geochemistry and petrography of some Jordanian oil shale", M.Sc. Thesis, Amman-Jordan.
- **Andrews, I. J.,**1992. Cretaceous and Paleocene Lithostratigraphy in the subsurface of Jordan. Subsurface Geology Bulletin No. 5. NRA, Amman, Jordan.
- **Andrews, R.G.** 1954**.** The use of relative infiltration indices in computing runoff (unpublished). Soil Conservation Service, Fort Worth, Texas, 6pp.
- **Arzu Firat, E. and Fatma, G.,** 2013. DRASTIC-based methodology for assessing groundwater vulnerability in the Gümüshaciköy and Merzifon basin (Amasya, Turkey). Earth Sciences Research Journal, 17(1), pp.33-40.
- **Bai, Z.G., Dent, D.L., Olsson, L. and Schaepman, M.E**., 2008. Proxy global assessment of land degradation. Soil use and management, 24(3), pp.223-234.
- **Barberi, F., Capaldi, G., Gasperini, P., Marinelli, G., Santacroce, R., Scandone, R., Treuil, M. and Varet, J., 1979.** Recent basaltic volcanism of Jordan and its implications on the geodynamic evolution of the Afro-Arabian Rift System, Atti. Conv. Lincei., **47**: 667-83.
- **Barjous, M. O., 1986.** The geology of Siwaqa Area, Map Sheet No. 3252-IV, Nat. Res. Auth., Geol. Dir., Geol. Map. Div., Bulletin **4**, Amman.
- **Bartis, J.T., LaTourrette, T., Dixon, L., Peterson, D.J. and Cecchine, G.,** 2005. Oil shale development in the United States: prospects and policy issues. Rand Corporation.
- **Bell, M.J., Harch, G. and Wright, G.C**., 1991. Plant population studies on peanut (Arachis hypogaea L.) in subtropical Australia. 1. Growth under fully irrigated conditions. Animal Production Science, 31(4), pp.535-543.
- **Bell, P.R.F., Krol, A.A. and Greenfield, P.F.,** 1986. Factors controlling the leaching of major and minor constituents from processed Rundle oil shale. Water Research, 20(6), pp.741-750.
- **Bender, F., 1968.** Geologie Von Jordanien. Bietrage Zur Regionalen geologie Der Erde. Bortitrager, Band **7**: 230p, Berlin, Stuttgart.

- **Bender, F., 1974.** Geology of Jordan. Contribution to the Regional Geology of the World. Gebrueder Borntraeger, 196p, Berlin.
- **Bender, H., Giesel, W., Hueser, M., Klinge, H., Knop, R.-M., Rashdan, J. &Schelke, K. (1987)**: Possibilities of and Constraints to Groundwater Development for the Water Supply of the Envisaged Oilshale Processing Plant. –Jordanian-German Technical Cooperation Project El Lajjun Oilshale Feasibility Study Phase I, prepared for Central Water Authority, BGR archive no. 101584, 128 p; Hannover.
- **Bern CR, Chadwick OA, Hartshorn AS, Khomo LM, Chorover J.,** 2011 A mass-balance model to separate and quantify colloidal and solute redistributions in soil. Chem Geol 282:113–119.
- **Besieso**, M. 2007. Jordan's Commercial Oil Shale Strategy.27th Oil Shale Symposium. Colorado School of Mines, Colorado, USA.
- **BGR**., 1987 Possibilities and constraints to groundwater development for the water supply of the envisaged oil shale processing plants. Internal report of WAJ, 1987
- **BGR/CWAJ**., 1987 Al Lajjun Oilshale Feasibility Study Phase I, Possibilities of and constraints to groundwater development for the water supply of the envisaged oilshale processing plant, Final Report, Amman-Jordan.
- **Blake, M.A**., 1939. Some results of crosses of early ripening varieties of peaches. In Proc. Amer. Soc. Hort. Sci (Vol. 37, pp. 232-241). Clapp, D.B. and Morton, A.A., 1936. The condensation of certain aromatic methyl ketones. Journal of the American Chemical Society, 58(11), pp.2172-2172.
- **Brendow, K**.,2009. Oil shale – a local asset under global constrain. Oil Shale. A Scientific-Technical Journal (Estonian Academy Publishers) 26 (3): 357–372.
- **BRGM**., 2006. Investigations of updating groundwater mathematical model(s) for the Saq and overlying aquifers (Vol. 12). Bureau de Recherches Géologiques et Minières. Unpublished report, Ministry of Water and Electricity, Riyadh.
- **Burdon, D. J., 1959.** Handbook of the Geology of Jordan: to accompany and explain the three sheets of 1:250,000 Geological Map, East of the Rift, A. M. Quennell, Govt. Hashemite Kingdom of Jordan, 82p, Benham, Colchester.
- **Burkart, M.R., Kolpin, D.W., Jaquis, R.J. and Cole, K.J.**(1999) Agrichemicals in ground water of the Midwestern USA: relations to soil characteristics. Journal of Environmental Quality, 28:1908–1915.
- **Burnham, A.K. and McConaghy, J.R.,** 2006. Comparison of the acceptability of various oil shale processes. United States. Department of Energy.

- **Cameron. E., Peloso. GF**. 2001. An application of fuzzy logic to the assessment of aquifers' pollution potential. Env Geol 40:1305– 1315.
- **Cane, R. F.,** 1976. The origin and formation of oil shale. In Oil Shale (Vol. 5, pp. 27-60). Elsevier Amsterdam.
- **Carroll, D.**, 1962. Rainwater as a chemical agent of geologic processes: a review. US Government Printing Office.
- **Charalambous, A.N**., 2016. The fossil Ram sandstone aquifer of Jordan: hydrogeology, depletion and sustainability. Quarterly Journal of Engineering Geology and Hydrogeology, pp.2015-060.W
- **Civita,M.(**1994)- Aquifer Vulnerability maps To pollution,Pitagora Ed.,Bologna.
- **Clapp, F.G., 1936.** Geology and bitumens of the Dead Sea area, Palestine and Transjordan. AAPG Bulletin, 20(7), pp.881-909.
- **D.S. Kosson, H.A. van der Sloot, F. Sanchez and A.C. Garrabrants.,** 2002. An Integrated Framework for Evaluating Leaching in Waste Management and Utilization of SecondaryMaterials," Environmental Engineering Science, 19(3) 159-204.
- **Davydov YP, Davydov DY, Zemskova LM**., 2006.Speciation of Zr(IV) radionuclides in solutions. Radiochemistry 48:358–364.
- **Diabat, A. and Masri, A., 2002.** The state of paleostress along the Siwaqa Fault (Central Jordan) based on fault-slip data, 15th Iraqi Geological Congress, Baghdad.
- **Dubertret, 1932.** Les forms structurales de la Syria et de la Palestine; leur origine. Comptes Rendus Acad., Sci. France, **195**: 65-67.
- **Dulski, T. R. (1996)**. A manual for the chemical analysis of metals. ASTM International. ISBN 0-8031-2066-4 p. 100
- **Dyni, John R.,** 2010. Oil Shale. In Clarke, Alan W.; Trinnaman, Judy A. Survey of energy resources (22 ed.). World Energy Council. pp. 93–123.
- **EASAC.** ,2007. "A study on the EU oil shale industry viewed in the light of the Estonian experience. A report submitted to the Committee on Industry Research and Energy of the European Parliament by European Academies Science Advisory Council (EASAC)."
- **Elenurm, T.,** 2008. Applying cross-cultural student teams for supporting international networking of Estonian enterprises. Baltic Journal of Management, 3(2), pp.145-158.
- **Elkhatib, E.A., O.L. Bennett, and R.J. Wright.**. 1984a. Kinetics of arsenite sorption in soils. Soil Sci. Soc. Am. J. 48:758–762.

- **El-Sheikh, A.H., Al-Degs, Y.S., Sweileh, J.A. and Said, A.J.,** 2013. Separation and flame atomic absorption spectrometric determination of total chromium and chromium (III) in phosphate rock used for production of fertilizer. Talanta, 116, pp.482-487.
- **EN12457, 2001** Characterization of Waste – Leaching – Compliance Test for Leaching of Granular Waste Materials and Sludges, Comité Européen de Normalisation, Brussels, Belgium,.
- **Estonian oilshale group tests new technology in Canada** ,*BNN. 2002* F. Sanchez, D.S. Kosson, R. Keeney, R. DeLapp, L. Turner and P. Kariher., 2008. Characterization of Coal Combustion Residues from Electric Utilities Using Wet Scrubbers for Multi-Pollutant Control," EPA-600/R-08/077, U.S. Environmental Protection Agency, Washington DC.
- **EXACT 2000** Temporal Trends for Water Resources Data in areas of Israeli, Jordanian, and Palestinian Interest. Compiled by the U.S.Geological Survey, Authorized and Released by the Executive Action Team, Middle East Water Data Banks Project, 2000.
- **F. Sanchez, R. Keeney, D.S. Kosson and R. DeLapp**., 2006, Characterization of Mercury-Enriched Coal Combustion Residues from Electric Utilities Using Enhanced Sorbents for Mercury Control," EPA-600/R-06/008, U.S. Environmental Protection Agency,Washington DC.
- **Farrah**, **H., Hatton, D. and Pickering, W.F**., 1980. The affinity of metal ions for clay surfaces. Chemical Geology, 28, pp.55-68.
- **Forbes, R. J**., 1970. A short history of the art of distillation: from the beginnings up to the death of Cellier Blumenthal. Brill. . pp. 41–42.
- **Francu, J., B. Harvie, B. Laenen, A. Siirde and M. Veiderma**, 2007. A study on the EU oil shale industry viewed in the light of the Estonian experience. A report by EASAC to the Committee on Industry, Research and Energy of the European Parliament.
- **Freeze**, **R. A. and Cherry, J. A. (Eds)** (1979). Groundwater. (New Jersey: Prentice-Hall.
- **Freund, R., Garfunkel, Z., Zak, I., Goldberg, M., Weissbrod, T., Derin, B., Bender, F., Wellings, F.E. and Girdler, R.W.,** 1970. The shear along the Dead Sea Rift [and discussion]. Philosophical Transactions of the Royal Society of London A: Mathematical, Physical and Engineering Sciences, 267(1181), pp.107-130.

- **Fritch, T. G.; McKnight, C. L., Yelderman, J. C., Arnold, J. G.,** 2000. An Aquifer Vulnerability Assessment of the Paluxy Aquifer, Central Texas, USA, using GIS and a modified DRASTIC approach. J. Environ. Manage., 25: 337–345.
- **Garfunkel, Z.,** 1981**.** Internal structure of the Dead Sea leaky transform (rift) in relation to plate kinematics, Tectonophysics **80:** 81-108.
- **Gary L. Baughman, compiler**, 1978. Synthetic fuels data handbook (2nd ed.): Denver, Cameron Engineers, Inc., p. 438.
- **Ghrair, A**., 2009. PhD thesis 2009: Immobilization of Heavy Metals in Soil by Amendment of Nanoparticulate Zeolitic Tuff, Institute of Soil Science and Land Evaluation University of Hohenheim, Stuttgart, Germany (unpublished)
- **Girdler, R.W.,** 1983. Processes of planetary rifting as seen in the rifting and break up of Africa. Tectonophysics, 94(1-4), pp.241-252.
- **Goldberg, S.,** 2002. Competitive adsorption of arsenate and arsenite on oxides and clay minerals. Soil Science Society of America Journal, 66(2), pp.413-421
- **Goldscheider, N., Hunkeler, D. and Rossi, P**., 2006. Review: microbial biocenoses in pristine aquifers and an assessment of investigative methods. Hydrogeology Journal, 14(6), pp.926-941.
- **Gonzalez-Alcaraz, M. N., Conesa, H. M., & Alvarez-Rogel, J.** 2013. Phytomanagement of strongly acidic, saline eutrophic wetlands polluted by mine wastes: the influence of liming and Sarcocornia fruticosa on metals mobility. Chemosphere, 90(10), 2512–2519.
- **Gütlein, A., Kersten, M., Feinstein, S. and Illner, P.,** 2013. Mobility of Cr and V in spent oil shale: impact of thermal treatment. Procedia Earth and Planetary Science, 7, pp.413-416.
- **Hamarneh, Y.,** 1998. Oil Shale Resources Development in Jordan. NRA, 82p.
- **Hutton, A.C. (1987**)."Petrographic classification of oil shales". International Journal of Coal Geology, V. 8, No. 3, pp. 203–231.
- **Hutton, A.C., 1991**."Classification, organic petrography and geochemistry of oil shale". Eastern Oil Shale Symposium, University of Kentucky Institute for Mining and Minerals Research, United States of America V. 1, pp. 163–172
- **Ibrahim, K. M. and J. O. Jaber .,**2007. Geochemistry and environmental impacts of retorted oil shale from Jordan." Environmental Geology 52: 979-984.
- **Ibrahim, K., 1987.** Geochemistry and petrology of some of the basaltic outcrops in central Jordan, M.Sc. Thesis, University of Jordan, Amman, 164p.

- **Ibrahim, K., 1993.** The geological frame-work for the Harat Ash Shamm Basaltic Super Group and its volcanotectonic evolution. Nat. Res. Auth., Geol. Dir., Map. Div., Bulletin **25**, Amman.
- **Ibrahim, K.,** 1996**.** The regional geology of Al-Azraq area, Map Sheet 3553-I. NRA, Geol. Dir., Map. Div. Bulletin **36**, Amman.
- **Ibrahim, K., Masri, A. and Khalil, B., 1994.** Jabal Shihan Volcano, volcanistratigraphy and petrology, Nat. Res. Auth., Geol. Dir., Geol. Map. Div., Unpub. Rep., 13p, Amman.
- **Ionides, G., and Blake, G. S.,** 1939**.** Report on the water resources of Trans-Jordan and their Development. Incorporating report on geology, soil, mineral and hydrogeological correlations, London: Crown Agents for the Colonies.
- **Jaber, J. O., Sladek, T. A., Mernitz, S., & Tarawneh, T. M**. ,2008. Future policies and strategies for oil shale development in Jordan. JJMIE, 2(1), 31-44.
- **Jaber, J.O., Probert, S.D. and Williams, P.T.** 1999. Evaluation of oil yield from Jordanian oil shales. Energy, 24(9), pp.761-781.
- **Jamrah A., Futaisi AA., Rajmohan N., Al-Yaroubi S.** (2007). Assessment of groundwater vulnerability in the coastal region of Oman using DRASTIC index method in GIS environment. Environ Monit Assess. doi:10.1007/s10661-007-0104-6.
- **Johnson, Harry R.; Crawford, Peter M.; Bunger, James W**. 2004. Strategic significance of America's oil shale resource. Volume II: Oil shale resources, technology and economics. Office of Deputy Assistant Secretary for Petroleum Reserves; Office of Naval Petroleum and Oil Shale Reserves; United States Department of Energy. pp. 13–16; A2; B3–B5
- **Johnson, R.B. and Onwuegbuzie, A.J**., 2004. Mixed methods research: A research paradigm whose time has come. Educational researcher, 33(7), pp.14-26.
- **Jordan Climatological Data Hand Book,** 1922/1923 –1997/1998, Meteorological Department, Amman, 2014.
- **Jordan Climatological Data Hand Book,** 1922/1923 –1997/1998, Meteorological Department, Amman, 2000

Jordan, Geol. Jahrb, C38, PP. 39-53.

- **Jury, W. A. and Ghodrati**, M. 1989. Overview of organic chemical environmental fate and transport modeling approaches. In: Reactions and Movement of Organic

Chemicals in Soils. Special Publication No. 22. Madison, WI, Soil Science Society of America and American Society ofAgronomy.

- **Jury, W.A. and Ghodrati, M**. (1987) Overview of Organic Chemical Environmental Fate and Transport Modeling Approaches. Reactions and Movement of Organic Chemicals in Soils. Proceedings of a Symposium of the Soil Science Society of America and the American Society of Agronomy, Atlanta, Georgia. SSSA Special Publication No. 22. Soil Science Society of America: 271-304.
- **Kabala, C., & Singh, B. R.** ,2001. Fractionation and mobility of copper, lead and zinc in soil profiles in the vicinity of copper smelter. Journal of Environmental Quality, 30(2), 485–492.
- **Kabata-Pendias A**., 1993 Behavioural properties of trace metals in soils. Appl Geochem 8:Supplement 2, 3–9.
- **Kalinski, R. J., Kelly, W. E., Bogardi, I., Ehrman, R. L., Yamamoto, P. O.**, 1994.Correlation between DRASTIC Vulnerabilities and Incidents of VOC Contamination of Municipal Wells inNebraska. Ground Water, 32(1): 31–34.

  Karst Studies, 74 (2), 221–234
- **Kent, K.M.** 1966. Estimating runoff from rainfall in small watersheds. Paper H9, 6th Western National Meeting, AGU, Los Angeles, CA, pp. 1–19.
- **Kesten, D., Weber, M., Haberland, C., Janssen, C., Agnon, A., Bartov, Y., Rabba, I. and DESERT Group,** 2008**.** Combining satellite and seismic images to analyse the shallow structure of the Dead Sea Transform near the DESERT transect. International Journal of Earth Sciences, 97(1), pp.153-169.
- **Khalil, B.,** 1988**.** Geological map of Ar Rabba area, Map Sheet No. 3152-IV, 1:50,000 National Geolo-gical Mapping Project, Nat. Res. Auth., Geol. Dir., Geol. Map. Div., Amman.
- **Khalil, B.,** 1992**.** The geology of Ar Rabba, Map Sheet No. 3152-IV, Nat. Res. Auth., Geol. Dir., Geol. Map. Div., Bulletin **22**, 105p, Amman.
- **Knox, A. S., Paller, M. H., Nelson, E. A., Specht, W. L., Halverson, N. V., & Gladden, J. B.** ,2006.Metal distribution and stability in constructed wetland sediment. Journal of Environmental Quality, 35(5), 1948–1959.
- **Koel, Mihkel.,** 1999. Estonian oil shale . Oil Shale. A Scientific-Technical Journal (Estonian Academy Publishers) (Extra).

- **Kök, A.G., Fisher, M.L. and Vaidyanathan, R**., 2008. Assortment planning: Review of literature and industry practice. In Retail supply chain management (pp. 99-153). Springer US.
- **Kottek, M., Grieser, J., Beck, C., Rudolf, B. and Rubel, F**., 2006. World map of the Köppen-Geiger climate classification updated. Meteorologische Zeitschrift, 15(3), pp.259-263.
- **Kumpiene, J.,** 2010. Trace element immobilization in soil using amendments. In Trace Elements in Soils (pp. 353-380). John Wiley and Sons Ltd. Chichester.
- **Liive, Sandor** .,2007. Oil Shale Energetics in Estonia . Oil Shale. A Scientific-Technical Journal (Estonian Academy Publishers) 24 (1): 1–4.
- **Lunge, G**.,1887, Coal-tar and ammonia Publisher: Gurney and Jackson, London.
- **Luo, Y.M. and Christie, P**., 1998. Bioavailability of copper and zinc in soils treated with alkaline stabilized sewage sludges. Journal of Environmental Quality, 27(2), pp.335-342.
- **Ma, L. Q., & Rao, G. N.** ,1997. Chemical fractionation of cadmium, copper, nickel and zinc in contaminated soils. Journal of Environmental Quality, 26(1), 259–264.
- **Margane, A., Subah, A., Khalifa, N. and Almomani, T.,** 2005. Groundwater Vulnerability Mapping in the Karak–Lajjun Area. In Proceedings of UNESCO-IHP Jordan Workshop on Aquifer Vulnerability.
- **Masri, A., 1996.** Geological map of Dihban (Wadi Al Mujib) area, Map Sheet No. 3152-I, 1:50,000 National Geological Mapping Project, Nat. Res. Auth., Geol. Dir., Geol. Map. Div., Amman.
- **Masri, A., 2010.** The Geology of Batn Al Ghul (Jabal Al Harad) area, Map Sheet No. 3149-II, Nat. Res. Auth., Geol. Dir., Geol. Map. Div., Bulletin **72**, Amman.
- **Masri, A., Memesh, A., Moumani, K., Dini, S., 2014.** Lithostratigraphic correlation of Phanerozoic rocks in southern Jordan and northwest Saudi Arabia. Ministry of Energy and Mineral Resources (Amman)-Saudi Geological Survey (Jeddah) Special Publication, 65p.
- **Massone H, Mauricio MQ, Martínez D.** (2010.) Enhanced groundwater vulnerability assessment in geological homogeneous areas: a case study from the Argentine Pampas. Hydrogeology Journal, 18: 371–379.
- **Mckenzie, D., Davies, D., and Molnar, P., 1970.** Plate tectonics of the Red Sea and East Africa. Nature, **226**: 243-248.

- **Melloul AJ., Collin M**. (1998). A proposed index for aquifer waterquality assessment: the case of Israel's Sharon region. J Environ Manage 54(2):131–142.
- **Ministry of Water and Irrigation**., 2001. Open files of wells Databank, Amman-Jordan website www.mwi.gov.jo.
- **MOA** – Ministry of Agriculture. (1993). National soil map and land use project. The soils of Jordan. Hunting Technical services Ltd. In association with Soil Survey and Land. Research Center. Vol. 3 Level 1.
- **Mockus, V. 1949**. Estimation of total (and peak rates of) surface runoff for individual storms. Exhibit A of Appendix B, Interim Survey Report, Grand (Neosho) River Watershed, USDA Soil Conservation Service.
- **Mockus, V**., 1972. Estimation of direct runoff from storm rainfall. Chapter 10, Section 4 (Hydrology), National Engineering Handbook. Soil Conservation Service, US Dept.
- ***Moody, Richard ,*** *2007. Oil & Gas Shales, Definitions & Distribution In Time & Space. In The History of On-Shore Hydrocarbon Use in the UK, Geological Society of London.*
- **Naqa, A., Hammouri, N., Kuisi, M**., 2006. GIS-based Evaluation of Groundwater Vulnerability in the Russeifa Area, Jordan. Revista Mexicana de Ciencias Geológicas, 23(3): 277-287.
- **National Research Council (NRC),** 1993. Groundwater Vulnerability Assessment Predicting Relative Contamination Potential under Conditions of Uncertainty. Committee for Assessing Ground Water Vulnerability, National Academy Press, Washington, D. C. 210p.
- **NWMP.** ,1977. National Water Master Plan of Jordan, National resources Authority in cooperation with GTZ, HKJ, 1977.
- **NWMP. ,**2003. National Water Master Plan of Jordan, Surface Water-Main Report, The Ministry of Water and Irrigation in cooperation with GTZ, HKJ, 2003.
- **Odut, Steven; Taciuk, Gordon W.; Barge, John; Stamatis, Vicki; Melo, Daniel**.,2008, Alberta Taciuk Process (ATP) Technology – Recent Developments and Activities .28th Oil Shale Symposium. Golden, Colorado: UMATAC Industrial Processes.
- **Opik, I., Golubev, N., Kaidalov, A., Kann, J. and Elenurm, A**., 2001. Current status of oil shale processing in solid heat carrier UTT (Galoter) retorts in Estonia. Oil Shale, 18(2), pp.99-107.

- **Õpik, Ilmar** ,1999, Black scenario of oil shale power generating in Estonia. Oil Shale. A Scientific-Technical Journal (Estonian Academy Publishers) 16 (3): 193–196.
- **Parker, D. H.,** 1970**.** The hydrology of the Mesozoic-Cenozoic aquifers of the western highlands and plateau of east Jordan. Investigation of the sandstone aquifer of east Jordan, Technical report No. **2**, United Nations Development Project/ Food and Agricultural Organization, Project **212**, 4 volumes, 424p.
- **Patten, James W**.,2007. Red-Leaf Resources. Presentation at the Utah Energy Summit .Utah Energy Summit.
- **Picard, L.,** 1943**.** Structure and Evolution of Palestine. Bulletin **4,** Geol. Dept. Hebrew University of Jerusalem.
- **Powell, J. H.,** 1989a**.** Stratigraphy and Sedimentation of the Phanerozoic rocks in Central and South Jordan, Part A: Ram and Khrayim groups, Natural Resources Authority. Geol. Dir., Map. Div., Bulletin **11a**., Amman.
- **Powell, J. H.,** 1989b**.** Stratigraphy and sedimen-tation of the Phanerozoic rocks in central and southern Jordan, **Part B**: Kurnub, Ajlun and Belqa groups, Nat. Res. Auth., Geol. Dir., Geol. Map. Div., Bull. **11**: 161p, Amman.
- **Powell, J.H., and Khalil, B.M.,** 2011**.** Evolution of Cretaceous to Eocene alluvial and carbonate platform sequences in central and south Jordan. GeoArabia, V. **16**, No. 4, p. 29-82, Gulf PetroLink, Bahrain.
- **Prisyagina NI, Kovalenko NI, Ryzhenko BN, Starshinova NP**., 2008. Experimental determination of ZrO 2 solubility in alkaline fl uoride solutions at 500°C and 1000 bar. Geochem Int 46:1164–1167
- **PURGA, J**., 2004. Toward an understanding of minority student retention at azusa pacific university (california) (Doctoral dissertation).
- **Qian Jialin; Wang Jianqiu** .,2006. World oil shale retorting technologies . International Oil Shale Conference. China University of Petroleum (Amman, Jordan: Jordanian Natural Resources Authority).
- **Quennell, A. M., 1951**. The geology and mineral resources of (former) Transjordan. Colon. Geol. Mm. Resource, **2**: 85-115, London.
- **Quennell, A. M., 1956.** Geological map of Jordan (East of the Rift Valley) 1: 250,000. Department of Lands and Survey, Hashemite Kingdom of Jordan.

- **Rao, P.S.C., Hornsby**, A.C. and Jessup, R.E. (1985) Indices for ranking the potential for pesticide contamination in groundwater. Proceedings of Soil Crop Science Society Florida; 1–24
- **Rinklebe, J. and Shaheen, S.M**., 2014. Assessing the mobilization of cadmium, lead, and nickel using a seven-step sequential extraction technique in contaminated floodplain soil profiles along the central Elbe River, Germany. Water, Air, & Soil Pollution, 225(8), pp.1-20.
- **Runnels, R.T., Kulstad, R.O., McDuffee, C. and Schleicher, J.A**., 1952. Oil shale in Kansas. University of Kansas Publications.
- **Salameh, E. and Banayan, H**.,1993.Water Resources of Jordan and their future potentials. FES and RSCN, Amman Department of Meteorology: Publications and files of the Department of Meteorology/Amman.
- **Salameh, E. and Udluft**, P. (1985): The hydrodynamic pattern of the central part of
- **Salminen, R., Batista, M.J., Bidovec, M., Demetriades, A., De Vivo, B., De Vos, W., Duris, M., Gilucis, A., Gregorauskiene, V., Halamić, J. and Heitzmann, P.,** 2005. Geochemical atlas of Europe, part 1, background information, methodology and maps. Geological survey of Finland.
- **Seckler, D., Barker, R. and Amarasinghe, U.,** 1999. Water scarcity in the twenty-first century. International Journal of Water Resources Development, 15 (1/2): 29.
- **Segev, A., Lyakhovsky, V. and Weinberger, R.,** 2014**.** Continental transform–rift interaction adjacent to a continental margin: The Levant case study. Earth-Science Reviews, 139, pp.83-103.
- **Senchugov, K., Kaidalov, A., Shaparenko, L., Popov, A., Kindorkin, B., Lushnyak, B. & Marguste, M.,** 1997. Utilization of rubber waste in mixture with oil shale in destructive thermal processing using the method of solid heat carrier. Oil Shale, 14(1), 59-66.
- **Sener E., Sener S., Davraz A**. (2009). Assessment of aquifer vulnerability based on GIS and DRASTIC methods: a case study of the Senirkent-Uluborlu Basin (Isparta, Turkey). Hydrogeology Journal, 17: 2023–2035.
- **Shawabkeh, 1990.** Geological map of Adir area, Map Sheet No. 3152-II, 1:50,000 National Geological Mapping Project, Nat. Res. Auth., Geol. Dir., Geol. Map. Div., Amman.

- **Shawabkeh,** 1991**.** The Geology of Adir area, Map Sheet No. 3152-II, Nat. Res. Auth., Geol. Dir., Geol. Map. Div., Bulletin **18**, 31p., Amman.
- **Sherman, L.K.** 1942. The unit hydrograph method. In Physics of the Earth, IX, Hydrology, O.E.Meinzer, ed., National Research Council, McGraw-Hill, NY.
- **Slawson, G.C. and Yen, T.F. eds.,** 1979. Compendium reports on oil shale technology (Vol. 1). Environmental Protection Agency, Office of Research and D evelopment, Environmental Monitoring and Support Laboratory.
- **Speers, G.C**.,1969. El-Lajjun Oil shale Deposit. Jordan Report EPR/R 7005. British Petroleum Co. Exploration and Production Research Division 15p Plus Data Appendix.
- **Speight, J.G.**, 2007. The Chemistry and Technology of Petroleum, fourth ed. CRC Press, Boca Raton, Florida.
- **Speight, James G**., 2008. Synthetic Fuels Handbook: Properties, Process, and Performance. McGraw-Hill. pp. 13; 182; 186.
- **Stanfield**., K. E., and Frost, C. I., 1946 and 1949* Method of assaying oil shale by a Modified Fischer retorts U. S. Bur. Mines Rept. Inv. 3977 and 4477.
- **Tesoriero, A.J., Inkpen, E .L and Voss, F.D**. (1998). Assessing ground-
- **Tessier, A., Campbell, P.G. and Bisson, M.,** 1979. Sequential extraction procedure for the speciation of particulate trace metals. Analytical chemistry, 51(7) pp.844-851.
- **Thompson, H.A., Parks, G.A. and Brown, G.E**., 1999. Dynamic interactions of dissolution, surface adsorption, and precipitation in an aging cobalt (II)-clay-water system. Geochimica et Cosmochimica Acta, 63(11), pp.1767-1779.
- **Ueno, M., Brookins, J., Beckman, B. and Fisher, J.W.,** 1988. A1 and A2 adenosine receptor regulation of erythropoietin production. Life sciences, 43(3), pp.229-237
- **UNEP,** 1992 jordan
- **UNEP**. World Atlas of Desertification, UNEP and Edward Arnold, 1992.
- **US OTA**, 1980. An Assessment of Oil Shale Technologies, Volume I. Report PB80-210115. Office of Technology Assessment. Congress of the United States, Washington, DC.
- **USDA-NRCS (United States Department of Agriculture**- Natural Resources Conservation Service). **(2004)** "Estimated direct runoff from storm rainfall. National Engineering handbook Hydrology, Chapters 10, Part 630", Washington, DC,

- **Usman, A. R. A., and A. Ghallab.**, 2006. Heavy-metal fractionation and distribution in soil profiles short-term-irrigated with sewage wastewater. Chemistry and Ecology 22:267–278.
- **Usman, A.R.A., Kuzyakov, Y. and Stahr, K.,** 2004. Dynamics of organic C mineralization and the mobile fraction of heavy metals in a calcareous soil incubated with organic wastes. Water, Air, and Soil Pollution, 158(1), pp.401-418.
- **Van Beynen P.E., Brinkmann R. & van Beynen K.,** 2012. A sustainability index for karst environments. J. Cave
- **Vías, JM, Andreo, B, Perles, MJ & Carrasco, F** (2005): A comparative study of four schemes for groundwater vulnerability mapping in a diffuse flow carbonate aquifer under Mediterranean climatic conditions. Environmental Geology, vol. 47, no. 4 pp. 586–595.
- **Volkov, E.; Stelmakh, G**.,1999). The stages of research on creating commercial units for processing the oil shale fines. Development of the process "Galoter" in 1944-1999". Oil Shale. A Scientific-Technical Journal (Estonian Academy Publishers) 16 (2): 161–185.
- **Water Authority of Jordan**., 2010. Open files of the Water Authority of Jordan/Amman.

water vulnerability using logistic regression. Proceedings for the Source Water Assessment and Protection 98 Conference, Dallas, TX; 157– 65.

- **WEC (World Energy Council).** 2007. Deciding the Future: Energy Policy Scenarios to 2050. London (UK)
- **Whit fi eld CJ**., 2011 Evaluation of elemental depletion weathering rate estimation methods on acid-sensitive soils of north-eastern Alberta, Canada. Geoderma 166:189–197
- **Worrall, F., Koplin, D**., 2004. Aquifer Vulnerability to Pesticide Pollution Combining Soil, Land-use and Aquifer Properties with Molecular Descriptors. J. Hydrol., 293: 191-204.
- **Yen, T.F. and Chilingarian**, G.V., 1976. Oil shale.Clapp, F.G., 1936. Geology and bitumens of the Dead Sea area, Palestine and Transjordan. AAPG Bulletin, 20(7), pp.881-909.
- **Zeien, H., Brümmer, G.W., 1989**. Chemische Extraktion zur Bestimmung von Schwermetallbindungsformen in Böden. Mitt. Dtsch. Bodenkundl. Ges 59,505e510.

- **Zhong, X., Zhou, S., Zhu, Q., & Zhao, Q.** ,2011. Fraction distribution and bioavailability of soil heavy metals in the Yangtze River Delta—a case study of Kunshan City in Jiangs Province, China. Journal of Hazardous Materials, 198(1), 13–21.
- **Zou Z, Qiu R, Zhang W, Dong H, Zhao Z, Zhang T, Wei X, Cai X**., 2009 The study of operating variables in soil washing with EDTA. Environ Pollut 157:229–236.

9 APPENDIXES

Appendix .1: Main wells penetrating the B2/A7 aquifer and Kurnub/Ram Group Aquifer.

Appendix.2: shows the sample identifications for the experiment of Liquid-solid partitioning as a function of liquid-solid ratio (Method 1316).

Appendix 3: shows the sample identifications for the experiment of Liquid-solid partitioning as a function of pH (Method 1313).

Appendix 4: Sequential extraction results of oil shale and spent shale samples,

Appendix 5 : Column leaching Experiments results for, (LOS: leaching of oil shale

Appendix 6.a : The concentrate of elements obtained from the (Solid-Liquid Partitioning as a Function of S\L Ratio) method experiment (method 1316) for the spent shale,

Appendix 6.b: Plots of the concentrate of elements obtained from the (Solid-Liquid Partitioning as a Function of S\L Ratio) method experiment (method 1316) for the spent shale,

Appendix 7.a: The concentrate of elements obtained from the Liquid-Solid Partitioning as a Function of Extract p H, method experiment (method 1313).

Appendix 7. Plots of the concentrate of elements obtained from the Liquid-Solid Partitioning as a Function of Extract p H, method experiment, (method 1313).

Appendix 8 : Groundwater analyses for a representative water samples taped from the intermediate aquifer (B2A7), the deep sand stone aquifer of (Kurnub/Ram) aquifer, the analyses include the concentrations of the REE and heavy metals by using ICP-MS, the concentration values are in ppb.

Appendix 9: chemical analysis results for groundwater representative samples (mg/l)

Appendix .1: Main wells penetrating the B2/A7 aquifer and Kurnub/Ram Group Aquifer.

STATION ID	North	East	Aquifer	Altitude (m)	Well Depth (m)	Yield (m^3/h)	SWL (m)
CD1145	1061580	220940	B2/A7	980	267.0	28.0	99.8
CD1146	1062016	220756	B2/A7	988	220.0	270.0	80.0
CD1147	1061680	221480	B2/A7	989	215.0	58.0	80.5
CD1160	1065485	234581	B2/A7	762	200.0	39.0	59.9
CD1203	1055794	220084	B2/A7	1073	247.0	55.0	128.5
CD1218	1062280	225100	B2/A7	910	220.0	55.0	141.7
CD1220	1058350	224600	B2/A7	950	300.0	35.0	72.0
CD1221	1066000	224450	B2/A7	910	252.0	65.0	159.8
CD1222	1066400	225210	B2/A7	910	306.0	67.0	159.6
CD1224	1064190	224900	B2/A7	900	238.0	43.0	145.0
CD1225	1052740	225750	B2/A7	1040	250.0	51.0	133.5
CD1228	1062850	223450	B2/A7	920	297.0	30.0	145.9
CD1229	1063500	221600	B2/A7	950	280.0	22.0	170.0
CD3225	1070584	226189	B2/A7	885	378.0	19.0	138.2
CD3256	1061900	220650	B2/A7	990	313.0	40.0	149.5
CD3257	1061300	222200	B2/A7	950	332.0	17.0	144.0
CD3403	1067300	228600	B2/A7	840	310.0	62.0	125.4
CD3419	1056309	244628	B2/A7	846	265.0	78.0	111.8
CD3508	1061431	233944	B2/A7	872	260.0	21.0	79.8
CD3531	1061516	222640	B2/A7	927	250.0	70.0	143.0
CD3579	1061841	223553	B2/A7	916	332.0	25.0	137.3
CD3456	1069600	232200	B2/A7	750	235.0	52.0	55.6
CD3458	1069630	232917	B2/A7	712	203.0	80.0	54.8
CD3462	1065382	233284	B2/A7	752	300.0	55.0	64.5
CD3479	1071188	232628	B2/A7	770	225.0	55.0	87.6
CD3499	1068378	232653	B2/A7	695	196.0	50.0	72.7
CD3331	1072275	233355	B2/A7	691	205.0	50.0	95.0
CD1193	1069360	231400	B2/A7	784	250.0	70.0	72.2
CD3453	1069627	232930	RAM	712	1050.0	90.0	372.0
CD3455	1068945	233590	RAM	682	1040.0	115.0	342.2
CD3459	1069079	231763	RAM	718.0	1050.0	89.0	376.0
CD3411	1070019	234775	RAM	665.0	1001.0	61.0	310.7
CD3412	1065368	233248	RAM	755.0	1011.0	41.0	398.1
CD3415	1071192	232632	RAM	770.0	1045.0	105.0	352.5
CD3416	1072271	233351	RAM	691.0	995.0	120.0	332.8
CD3417	1068364	232682	RAM	702.0	1020.0	40.0	340.2
CD3418	1066544	232406	RAM	721.0	980.0	105.0	366.0

Appendix.2: shows the sample identifications for the experiment of Liquid-solid partitioning as a function of liquid-solid ratio (Method 1316).

No	Sample ID	pH	EC (µs/cm)
1	M16 SS A - 1	10.24	505
2	M16 SS A - 2	10.2	755
3	M16 SS A - 3	10.33	372
4	M16 SS A - 4	10.25	370
5	M16 SS A - 5	10.40	580
6	M16 SS B - 1	10.25	789
7	M16 SS B - 2	10.2	1202
8	M16 SS B - 3	10.2	544
9	M16 SS B - 4	10.3	580
10	M16 SS B - 5	10.3	740
11	M16 SS C - 1	10.5	1153
12	M16 SS C - 2	10.4	1630
13	M16 SS C - 3	10.4	814
14	M16 SS C - 4	10.5	930
15	M16 SS C - 5	10.7	1300
16	M16 OS A - 1	8.4	820
17	M16 OS A - 2	8.2	1340
18	M16 OS A - 3	8.0	657
19	M16 OS A - 4	8.10	690
20	M16 OS A - 5	7.85	907
21	M16 OS B - 1	9.96	1305
22	M16 OS B - 2	10.08	1655
23	M16 OS B - 3	10.02	664
24	M16 OS B - 4	9.95	654
25	M16 OS B - 5	10.2	1150
26	M16 OS C - 1	10.4	1800
27	M16 OS C - 2	10.25	2.33Ms/cm
28	M16 OS B - 3	10.1	877
29	M16 OS C - 4	10.2	972
30	M16 OS C - 5	10.4	1255
31	M16 K - 1	80.02	19.2
32	M16 K - 2	6.5	40
33	M16 K - 3	6.6	17.8
34	M16 K - 4	6.9	20
35	M16 K - 5	6.7	43

Appendix 3: shows the sample identifications for the experiment of Liquid-solid partitioning as a function of pH (Method 1313).

No	Samples ID	pH	EC (µs/cm)
1	M13 SS A pH4	10.27	525
2	M13 SS A pH 5	10.3	520
3	M13 SS A pH6	10.28	510
4	M13 SS A pH7	10.28	522
5	M13 SS A pH8	10.3	525
6	M13 SS A pH10	10.4	508
7	M13 SS A pH12	11.48	1880
8	M13 SS B pH4	10.35	799
9	M13 SS B pH 5	10.4	820
10	M13 SS B pH6	10.3	814
11	M13 SS B pH7	10.3	795
12	M13 SS B pH8	10.3	789
13	M13 SS B pH10	10.3	744
14	M13 SS B pH12	11.55	2.10 ms/cm
15	M13 SS C pH4	10.4	1730
16	M13 SS C pH 5	10.5	1140
17	M13 SS C pH6	10.5	1090
18	M13 SS C pH7	10.55	1140
19	M13 SS C pH8	10.56	1120
20	M13 SS C pH10	10.5	1055
21	M13 SS C pH12	11.6	2.44 ms/cm
22	M13 OS A pH4	8.3	1730
23	M13 OS A pH 5	8.13	1140
24	M13 OS A pH6	8.3	1090
25	M13 OS A pH7	8.4	1140
26	M13 OS A pH8	8.0	1120
27	M13 OS A pH10	7.88	1055
28	M13 OS A pH12	11.50	2.44 ms/cm
2930	M13 OS B pH4	10.0	798
31	M13 OS B pH 5	10.08	787
32	M13 OS B pH6	10.1	808
33	M13 OS B pH7	9.95	780
34	M13 OS B pH8	10.0	820
35	M13 OSB pH10	10.2	473
36	M13 OSB pH12	11.6	2.11ms/cm
37	M13 OS C pH4	10.3	1750
38	M13 OS C pH 5	10.35	1740
39	M13 OS C pH6	10.33	1707
40	M13 OS C pH7	10.5	1770
41	M13 OS C pH8	10.36	1680
42	M13 OSC pH10	10.3	1533
43	M13 OSC pH12	11.5	3.17 ms/cm
44	M13 K pH4	7.4	31.4
45	M13 K pH 5	7.5	49

46	M13 K pH6	8.2	149
47	M13 K pH7	7.4	26
48	M13 K pH8	7.8	30
49	M13 K pH10	7.7	99
50	M13 K pH12	10.9	1120

Appendix 4: Sequential extraction results of oil shale and spent shale samples, showing the averages, slandered deviation, and the median.

Where:

- Fx OS (SS) net : is the result of subscription blank value of Fx from Fx
- Fx OS (SS) AVRG: is the average of the triplicates measurements of oil shale (spent shale).
- Fx OS (SS) STDV: is the slandered deviation for the oil shale and (spent shale) measurements.
- Fx OS (SS) MED: is the median for the oil shale and (spent shale) measurements.
- Fx OS (SS) (Fx-F1): is the subscription the value of F1 measurement from each Fx value measurement, that because the concentration of the elements that obtained in (F1) will be included in the next fractionation (F2, F3, F4, F5 and F6).
- All the concentration measurements as in (ppb).by using ICP

Appendix 4 a : Sequential extraction results of oil shale samples, showing the averages, slandered deviation, and the median.

Fraction, sample ID	**Ti**	**V**	**Cr**	**Co**	**Zn**
(detection limit, undiluted sample)	**0.1**	**0.1**	**0.1**	**0.01**	**1**
F1 blank (1:10)	3.19	< 1	1.65	0.20	12.81
F1 OS1 (1:10)	4.11	54.87	9.00	3.27	123.20
F1 OS2 (1:10)	3.67	41.95	9.98	4.24	124.30
F1 OS3 (1:10)	3.69	49.80	9.19	4.31	111.50
F1 OS AVRG	3.83	48.87	9.39	3.94	119.67
F1 OS net	0.63	48.87	7.75	3.74	106.86
F1 OS STDV	0.25	6.51	0.52	0.58	7.09
F1 OS MED	3.69	49.80	9.19	4.24	123.20
F2 blank (1:100)	< 10	< 10	12.15	< 1	< 100
F2 OS1 (1:100)	28.69	409.80	1768.00	22.88	1920.00
F2 OS2 (1:100)	27.74	380.40	1703.00	23.85	1942.00
F2 OS3 (1:100)	30.93	387.50	1700.00	24.03	1933.00
F2 OS AVRG	29.12	392.57	1723.67	23.59	1931.67
F2 OS net	29.12	392.57	1711.52	23.87	1931.67
F2 OS (F2-F1)	28.49	343.69	1703.77	20.13	1824.81
F2 OS STDV	1.64	15.34	38.42	0.62	11.06
F2 OS MED	28.69	387.50	1703.00	23.85	1933.00

F3 blank (1:5)	< 0.5	< 0.5	< 0.5	< 0.5	< 5
F3 OS1 (1:5)	26.54	151.30	252.60	6.37	460.20
F3 OS2 (1:5)	27.33	167.00	258.30	7.29	332.00
F3 OS3 (1:5)	18.90	126.80	239.90	7.06	220.60
F3 OS AVRG	24.26	148.37	250.27	6.91	337.60
F3 OS net	24.26	148.37	250.27	6.91	337.60
F3 OS (F3-F1)	24.26	148.37	250.27	6.91	338.60
F3 OS STVD	4.66	20.26	9.42	0.48	119.90
F3 OS MED	26.54	151.30	252.60	7.06	332.00
F4 blank (1.10) (Int. Std in H2O)	< 1	< 1	< 1	< 0.1	41.12
F4 OS1 (1.10)	7.65	189.80	315.80	9.95	976.20
F4 OS2 (1.10)	7.04	216.40	320.10	8.90	702.60
F4 OS3 (1.10)	6.85	220.70	285.10	8.54	564.50
F4 OS AVRG	7.18	208.97	307.00	9.13	747.77
F4 OS net	7.17	208.97	307.00	9.13	706.65
F4 OS (F4-F1)	6.54	160.09	299.25	5.39	599.79
F4 OS STVD	0.42	16.74	19.09	0.73	209.53
F4 OS MED	7.04	216.40	315.80	8.90	702.60
F5 blank (1:20)	6.61	< 2	3.15	0.45	< 20
F5 OS1 (1:20)	762.90	889.20	2574.00	17.74	1301.00
F5 OS2 (1:20)	901.70	950.80	2589.00	16.82	836.50
F5 OS3 (1:20)	782.10	940.60	2701.00	16.22	1015.00
F5 OS AVRG	815.57	926.87	2621.33	16.93	1050.83
F5 OS net	815.57	926.87	2618.18	16.48	1050.83
F5 OS (F5-F1)	814.93	877.99	2610.44	12.74	943.98
F5 OS STVD	75.21	33.02	69.40	0.77	234.31
F5 OS MED	782.10	940.60	2589.00	16.82	1015.00
F6 blank (1:20)	< 2	< 2	3.79	0.52	< 20
F6 OS1 (1:20)	362.50	663.70	1245.00	11.75	156.30
F6 OS2 (1:20)	382.40	681.10	1317.00	11.09	67.66
F6 OS3 (1:20)	332.40	604.60	1233.00	8.81	< 20
F6 OS AVRG	359.10	649.80	1265.00	10.55	111.98
F6 OS net	359.10	649.80	1261.21	10.03	111.98
F6 OS (F6-F1)	358.47	600.93	1253.47	6.29	5.12
F6 OS STDV	25.17	40.10	45.43	1.54	62.68
F6 OS MED	362.50	663.70	1245.00	11.09	111.98
F7 OS 1	8988	77000	570000	46000	599000
F7 OS 2	9665	79000	579000	56000	839000

F7 OS 3	8520	64000	548000	48000	804000
F7 OS AVRG	9058	73333	565667	50000	747333
F7 OS STVD	576	8145	15948	5292	129647
F7 OS MED	8988	77000	570000	48000	804000

Fraction, sample ID	**As**	**Zr**	**Cd**	**Pb**	**U**
(detection limit, undiluted sample)	**0.2**	**0.01**	**0.01**	**0.01**	**0.001**
F1 blank (1:10)	< 2	0.19	< 0.1	0.01	< 0.01
F1 OS1 (1:10)	5.39	0.55	8.81	0.12	30.95
F1 OS2 (1:10)	7.37	0.63	8.13	0.23	29.22
F1 OS3 (1:10)	5.28	0.53	9.31	0.16	29.94
F1 OS AVRG	6.02	0.57	8.75	0.17	30.04
F1 OS net	6.02	0.37	8.75	0.16	30.04
F1 OS STDV	1.18	0.05	0.59	0.05	0.87
F1 OS MED	5.39	0.55	8.81	0.16	29.94
F2 blank (1:100)	< 20	< 1	< 1	2.45	< 0.1
F2 OS1 (1:100)	37.59	1.29	225.50	14.37	232.00
F2 OS2 (1:100)	39.33	1.39	229.50	12.83	224.50
F2 OS3 (1:100)	31.00	1.52	226.70	15.40	227.50
F2 OS AVRG	35.97	1.40	227.23	14.20	228.00
F2 OS net	35.97	1.40	227.23	11.76	228.00
F2 OS (F2-F1)	29.96	1.03	218.48	11.60	197.96
F2 OS STDV	4.39	0.12	2.05	1.29	3.77
F2 OS MED	37.59	1.39	226.70	14.37	227.50
F3 blank (1:5)	< 1	< 0.05	< 0.05	< 0.05	< 0.05
F3 OS1 (1:5)	7.79	4.07	57.72	0.60	46.69
F3 OS2 (1:5)	9.45	8.61	38.20	0.58	48.30
F3 OS3 (1:5)	5.97	6.31	22.03	0.75	39.64
F3 OS AVRG	7.74	6.33	39.32	0.64	44.88
F3 OS net	7.74	6.33	39.32	0.64	44.88
F3 OS (F3-F1)	7.74	6.33	39.32	0.64	44.88
F3 OS STVD	1.74	2.27	17.87	0.09	4.61
F3 OS MED	7.79	6.31	38.20	0.60	46.69
F4 blank (1.10) (Int. Std in H2O)	< 2	< 0.1	< 0.1	< 0.1	< 0.01
F4 OS1 (1.10)	14.51	0.56	104.00	7.74	37.52
F4 OS2 (1.10)	15.64	3.23	68.73	7.48	39.58
: F4 OS3 (1.10)	15.82	0.15	54.37	8.05	35.86

F4 OS AVRG	15.32	1.31	75.70	7.76	37.65
F4OS net	15.32	1.31	75.70	7.76	37.65
F4 OS (F4-F1)	9.31	0.94	66.95	7.60	7.62
F4 OS STVD	0.71	1.67	25.54	0.29	1.86
F4 OS MED	15.64	0.56	68.73	7.74	37.52
F5 blank (1:20)	< 4	1.48	< 0.2	0.08	0.03
F5 OS1 (1:20)	249.30	8.93	8.40	0.51	259.10
F5 OS2 (1:20)	236.00	5.60	9.98	0.32	282.70
F5 OS3 (1:20)	227.90	6.75	9.79	0.47	260.50
F5 OS AVRG	237.73	7.09	9.39	0.43	267.43
F5 OS net	237.73	5.61	9.39	0.36	267.41
F5 OS (F5-F1)	231.72	5.23	0.64	0.20	237.37
F5 OS STVD	10.80	1.69	0.86	0.10	13.24
F5 OS MED	236.00	6.75	9.79	0.47	260.50
F6 blank (1:20)	< 4	0.87	< 0.2	1.93	< 0.02
F6 OS1 (1:20)	190.80	17.62	< 0.3	< 0.2	99.37
F6 OS2 (1:20)	208.00	11.38	< 0.4	< 0.2	96.98
F6 OS3 (1:20)	210.70	9.30	< 0.5	< 0.2	91.45
F6 OS AVRG	203.17	12.77	<0.5	<0.2	95.93
F6 OS net	203.17	11.89	<0.5	<0.2	95.93
F6 OS (F6-F1)	197.15	11.52	<0.5	<0.2	65.90
F6 OS STDV	10.79	4.33	0.01	0.01	4.06
F6 OS MED	208.00	11.38	0.01	0.01	96.98
F7 OS 1	221000	30000	112000	34000	25000
F7 OS 2	219000	42000	115000	38000	14000
F7 OS 3	210000	33000	101000	41000	19000
F7 OS AVRG	216667	35000	109333	37667	19333
F7 OS STVD	5859	6245	7371	3512	5508
F7 OS MED	219000	33000	112000	38000	19000

Appendix 4 b: Sequential extraction results of spent shale samples, showing the averages, slandered deviation, and the median.

Fraction, sample ID	Ti	V	Cr	Co	Zn
	ppb	ppb	ppb	ppb	ppb
(detection limit, undiluted sample)	0.1	0.1	0.1	0.01	1
F1 blank (1:10)	3.19	0.05	1.65	0.20	12.81
F1 SS1 (1:10)	3.59	127.10	6.64	0.10	27.33
F1 SS2 (1:10)	3.49	126.80	13.08	0.47	32.21

F1 SS3 (1:10)	3.67	128.50	7.76	0.14	30.26
F1 SS AVRG	3.58	127.47	9.16	0.24	29.93
F1 SS net	0.39	127.10	7.51	0.04	17.12
F1 SS STDV	0.09	0.91	3.44	0.20	2.46
F1 SS MED	3.49	126.80	6.64	0.20	27.33
F2 blank (1:100)	0.05	0.05	12.15	< 1	< 100
F2 SS1 (1:100)	57.69	577.60	2130.00	6.51	1196.00
F2 SS3 (1:100)	60.59	619.20	2110.00	6.15	1017.00
F2 SS3 (1:100)	58.02	603.80	2210.00	6.11	1057.00
F2 SS AVRG	58.77	598.40	2120.00	6.33	1106.50
F2 SS net	58.72	598.35	2107.85	6.33	1106.50
F2 SS (F2-F1)	58.33	471.25	2100.34	6.30	1089.38
F2 SS STDV	1.59	21.03	52.92	0.22	93.95
F2 SS MED	58.02	603.80	2130.00	6.15	1057.00
F3 blank (1:5)	3.56	0.05	< 0.5	0.07	< 5
F3 SS1 (1:5)	233.50	284.60	272.70	1.10	45.45
F3 SS2 (1:5)	224.00	276.60	253.50	0.98	47.76
F3 SS3(1:5)	231.30	280.30	277.40	0.82	37.78
F3 SS AVRG	229.60	280.50	267.87	0.97	43.66
F3 SS net	226.04	280.50	267.87	0.90	43.66
F3 SS (F3-F1)	225.65	153.40	260.35	0.86	26.54
F3 SS STDV	4.97	4.00	12.66	0.14	5.22
F3 SS MED	231.30	280.30	272.70	0.98	45.45
F4 blank (1.10) (Int. Std in H2O)	< 1	< 1	< 1	< 0.1	41.12
F4 SS1 (1.10)	13.43	299.00	329.50	2.10	540.60
F4 SS2 (1.10)	10.43	328.90	304.70	2.24	532.30
F4 SS3 (1.10)	11.43	316.50	296.60	2.26	552.90
F4 SS AVRG	11.76	314.80	310.27	2.20	541.93
F4 SS net	11.76	314.80	310.27	2.20	500.81
F4 SS (F4F1)	11.37	187.70	302.75	2.16	483.69
F4 SS STDV	1.53	15.02	17.14	0.08	10.36
F4 SS MED					
F5 blank (1:20)	6.61	< 2	3.15	0.45	< 20
F5 SS1 (1:20)	700.20	1019.00	3418.00	4.96	1585.00
F5 SS2 (1:20)	757.00	958.70	3226.00	4.30	859.80
F5 SS3 (1:20)	785.70	946.00	3159.00	4.31	909.20
F5 SS AVRG	747.63	974.57	3267.67	4.52	1118.00
F5 SS net	741.02	974.57	3264.52	4.07	1118.00

F5 SS (F5-F1)	740.63	847.47	3257.00	4.04	1100.88
F5 SS STDV	43.51	39.00	134.43	0.38	405.19
F5 SS MED	757.00	958.70	3226.00	4.31	909.20
F6 blank (1:20)	< 2	< 2	3.79	0.05	< 20
F6 SS1 (1:20)	358.80	341.80	1070.00	0.55	< 20
F6 SS2 (1:20)	476.90	411.00	1169.00	0.29	< 20
F6 SS3 (1:20)	419.70	314.60	1131.00	< 0.2	< 20
F6 SS AVRG	418.47	355.80	1123.33	0.42	<20
F6 SS NET	418.47	355.80	1119.55	0.37	<20
F6 SS (F6-F1)	418.08	228.70	1112.03	0.34	<20
F6 SS STDV	59.06	49.70	49.94	0.18	
F6 SS MED	419.70	341.80	1131.00	0.42	
F7 SS1	10700	89000	773000	14000	1250000
F7 SS2	7498	91000	781000	18000	1159000
F7 SS3	8146	85000	788000	15000	983000
F7 SS AVRG	8781	88333	780667	15667	1130667
F7 SS STDV	1693	3055	7506	2082	135736
F7 SS MED	8146	89000	781000	15000	1159000

Fraction, sample ID	**As**	**Zr**	**Cd**	**Pb**	**U**
(detection limit, undiluted sample)	**0.2**	**0.01**	**0.01**	**0.01**	**0.001**
F1 blank (1:10)	< 2	0.19	< 0.1	0.58	< 0.01
F1 SS1 (1:10)	75.39	0.28	4.58	< 0.1	22.19
F1 SS2 (1:10)	73.56	0.22	4.52	< 0.1	22.03
F1 SS3 (1:10)	73.02	0.27	4.90	< 0.1	23.03
F1 SS AVRG	73.99	0.26	4.67	<0.1	22.42
F1 SS net	73.99	0.06	4.67	<0.1	22.42
F1 SS STDV	1.24	0.03	0.20	<0.1	0.54
F1 SS MED	74.48	0.22	4.55	<0.1	22.11
F2 blank (1:100)	< 20	< 1	< 1	2.45	< 0.1
F2 SS1 (1:100)	172.30	4.05	273.30	24.08	178.20
F2 SS3 (1:100)	175.80	4.74	251.70	23.29	186.90
F2 SS3 (1:100)	172.10	4.70	252.40	22.90	171.40
F2 SS AVRG	174.05	4.40	262.50	23.69	182.55
F2 SS net	174.05	4.40	262.50	23.69	182.55
F2 SS (F2-F1)	100.06	4.33	257.83	23.69	160.13
F2 SS STDV	2.08	0.39	12.27	0.60	7.77
F2 SS MED	172.30	4.70	252.40	23.29	178.20

F3 blank (1:5)	< 1	< 0.05	< 0.05	0.02	0.01
F3 SS1 (1:5)	138.90	1.65	14.83	0.73	48.58
F3 SS2 (1:5)	136.90	1.46	16.38	0.78	47.40
F3 SS3(1:5)	133.30	1.71	9.94	0.59	47.31
F3 SS AVRG	136.37	1.61	13.72	0.70	47.76
F3 SS net	136.37	1.61	13.72	0.68	47.75
F3 SS (F3-F1)	62.38	1.54	9.05	0.68	25.34
F3 SS STDV	2.84	0.13	3.36	0.10	0.71
F3 SS MED	136.90	1.65	14.83	0.73	47.40
F4 blank (1.10) (Int. Std in H2O)	< 2	< 0.1	< 0.1	< 0.1	< 0.01
F4 SS1 (1.10)	129.00	21.85	178.20	26.69	38.03
F4 SS2 (1.10)	116.60	22.12	178.90	26.98	36.45
F4 SS3 (1.10)	138.50	2.99	183.30	33.73	37.78
F4 SS AVRG	128.03	15.65	180.13	29.13	37.42
F4 SS net	128.03	15.65	180.13	29.13	37.42
F4 SS (F4F1)	54.04	15.59	175.47	29.13	15.00
F4 SS STDV	10.98	10.97	2.76	3.98	0.85
F4 SS MED					
F5 blank (1:20)	< 4	1.48	< 0.2	5.78	0.03
F5 SS1 (1:20)	290.30	< 0,2	214.60	14.63	279.60
F5 SS2 (1:20)	273.10	< 0,2	159.80	8.61	279.60
F5 SS3 (1:20)	267.90	< 0,2	157.40	10.06	285.20
F5 SS AVRG	277.10	<0.2	177.27	11.10	281.47
F5 SS net	277.10	<0.2	177.27	5.32	281.44
F5 SS (F5-F1)	203.11	<0.2	172.60	5.32	259.02
F5 SS STDV	11.72		32.35	3.14	3.23
F5 SS MED	273.10		159.80	10.06	279.60
F6 blank (1:20)	< 4	0.87	< 0.2	1.93	< 0.02
F6 SS1 (1:20)	199.50	4.18	7.36	< 0.2	43.40
F6 SS2 (1:20)	211.90	3.24	5.32	< 0.2	60.02
F6 SS3 (1:20)	213.20	3.53	4.26	< 0.2	50.96
F6 SS AVRG	208.20	3.65	5.65	<0.2	51.46
F6 SS net	208.20	2.78	5.65	<0.2	51.46
F6 SS (F6-F1)	134.21	2.71	0.98	<0.2	29.04
F6 SS STDV	7.56	0.48	1.58		8.32
F6 SS MED	211.90	3.53	5.32		50.96
F7 SS1	633000	212000	125000	15000	22373

F7 SS2	484000	181000	98000	18000	21455
F7 SS3	523000	187000	135000	15000	24153
F7 SS AVRG	546667	193333	119333	16000	22660
F7 SS STDV	77268	16442	19140	1732	1372
F7 SS MED	523000	187000	125000	15000	22373

Appendix 5 : Column leaching Experiments results for, (LOS: leaching of oil shale column sample (Appendix 5.a), (LSS: leaching of spent shale column sample Appendix 5.b) and (LSSP: leaching the column of phosphate underneath spent shale samples(Appendix 5.c).

The tables include; the average, slandered deviation, median and the summation of the average of ten days Column leaching Experiments.

Where:

- AVRG: is the average of the triplicates samples measurements.
- STDV: is the slandered deviation sample measurement.
- MED: is the median sample measurement.
- All the concentration measurements as in (µm/l).by using ICP-MS.

Appendix 5.a : Column leaching Experiments results for Oil shale samples.

	Ti	V	Cr	Co	Zn	As	Zr	Cd	Pb	U
Detection limit	**0.1**	**0.1**	**0.1**	**0.01**	**1**	**0.2**	**0.010**	**0.01**	**0.01**	**0.00**
Sample ID										
LOS 1:1	0.62	18.72	11.82	1.77	30.21	4.26	2.26	2.64	0.02	15.87
LOS 2:1	0.35	15.50	9.14	0.61	28.16	2.98	0.75	1.10	0.01	9.69
LOS 3:1	0.50	21.09	14.65	1.09	23.41	4.05	1.47	2.23	0.02	12.69
LOS 1 AVRG	0.49	18.44	11.87	1.16	27.26	3.76	1.49	1.99	0.01	12.75
LOS 1 STVD	0.14	2.81	2.75	0.58	3.49	0.69	0.76	0.80	0.00	3.09
LOS 1 MED	0.50	18.72	11.82	1.09	28.16	4.05	1.47	2.23	0.02	12.69
LOS 1:2	0.42	19.79	5.33	1.08	9.76	3.92	0.66	2.61	0.02	4.39
LOS 2:2	0.14	19.78	3.43	0.25	4.10	1.79	0.17	0.48	0.02	3.46
LOS 3:2	0.20	20.69	6.84	0.45	9.06	3.58	0.33	0.95	0.05	4.70
LOS 2 AVRG	0.26	20.09	5.20	0.59	7.64	3.09	0.39	1.35	0.03	4.18
LOS 2 STDV	0.15	0.52	1.71	0.44	3.08	1.15	0.25	1.12	0.02	0.64
LOS 2 MED	0.20	19.79	5.33	0.45	9.06	3.58	0.33	0.95	0.02	4.39
LOS 1:3 6	0.28	24.12	3.28	0.36	5.64	4.76	0.36	0.66	0.03	3.97
LOS 2:3 6	0.17	16.96	2.26	0.15	2.66	1.38	0.10	0.35	0.02	2.42
LOS 3:3 6	0.17	16.45	4.43	0.18	5.07	3.01	0.17	0.48	0.04	3.48
LOS 3 AVRG	0.21	19.18	3.33	0.23	4.45	3.05	0.21	0.50	0.03	3.29
LOS 3 STDV	0.07	4.29	1.08	0.11	1.58	1.69	0.13	0.16	0.01	0.79
LOS MED	0.17	16.96	3.28	0.18	5.07	3.01	0.17	0.48	0.03	3.48
LOS 1:4 6	0.31	16.91	4.92	0.22	3.65	2.34	0.20	0.20	0.04	3.19
LOS 2:4 6	0.22	15.59	1.66	0.16	2.98	1.10	0.07	0.27	0.03	2.00
LOS 3:4 6	0.12	13.91	2.60	0.16	3.46	2.68	0.09	0.25	0.02	2.35
LOS 4 AVRG	0.21	15.47	3.06	0.18	3.36	2.04	0.12	0.24	0.03	2.51
LOS 4 STDV	0.10	1.50	1.68	0.04	0.34	0.83	0.07	0.03	0.01	0.61
LOS 4 MED	0.22	15.59	2.60	0.16	3.46	2.34	0.09	0.25	0.03	2.35
LOS 1:5 6	0.14	18.10	3.94	0.16	2.34	5.61	0.14	0.08	0.02	2.63

LOS 2:5 6	0.15	15.02	1.40	0.12	2.03	1.04	0.05	0.20	0.02	1.71
LOS 3:5 6	0.17	16.58	2.99	0.13	4.13	3.34	0.09	0.21	0.04	2.21
LOS 5 AVRG	0.15	16.57	2.78	0.14	2.83	3.33	0.09	0.16	0.02	2.18
LOS 5 STDV	0.01	1.54	1.28	0.02	1.14	2.29	0.04	0.07	0.01	0.46
LOS 5 MED	0.15	16.58	2.99	0.13	2.34	3.34	0.09	0.20	0.02	2.21
LOS 1:6	0.16	13.54	4.63	0.19	2.73	7.78	0.14	0.09	0.05	2.90
LOS 2:6	0.17	15.40	1.42	0.15	1.77	1.11	0.05	0.16	0.02	1.56
LOS 3:6	0.17	12.04	3.19	0.16	2.86	2.43	0.16	0.23	0.01	1.69
LOS 6 AVRG	0.16	13.66	3.08	0.17	2.46	3.77	0.12	0.16	0.03	2.05
LOS 6 STDV	0.01	1.68	1.61	0.02	0.59	3.53	0.06	0.07	0.02	0.74
LOS 6 MED	0.17	13.54	3.19	0.16	2.73	2.43	0.14	0.16	0.02	1.69
LOS 1:7	0.17	14.77	3.32	0.11	1.82	6.89	0.09	0.06	0.03	2.53
LOS 2:7	0.15	14.92	1.22	0.12	1.50	1.03	0.04	0.14	0.01	1.29
LOS 3:7	0.16	14.43	1.36	0.34	1.43	2.25	0.41	0.44	0.01	2.02
LOS 7 AVRG	0.16	14.71	1.97	0.19	1.58	3.39	0.18	0.21	0.02	1.95
LOS 7 STDV	0.01	0.20	0.96	0.11	0.17	2.52	0.17	0.16	0.01	0.51
LOS 7 MED	0.16	14.77	1.36	0.12	1.50	2.25	0.09	0.14	0.01	2.02
LOS 1:8	0.18	15.01	2.42	0.16	1.10	0.78	0.02	0.08	0.01	0.01
LOS 2:8	0.13	14.71	1.23	0.11	1.40	0.98	0.04	0.15	0.01	1.19
LOS 3:8	0.18	12.40	5.11	0.35	1.95	2.61	0.01	0.53	0.03	3.17
LOS 8 AVRG	0.16	14.04	2.92	0.20	1.48	1.45	0.02	0.25	0.02	1.46
LOS 8 STDV	0.03	1.17	1.62	0.10	0.35	0.82	0.01	0.20	0.01	1.30
LOS 8 MED	0.18	14.71	2.42	0.16	1.40	0.98	0.02	0.15	0.01	1.19
LOS 1:9	0.16	18.99	2.19	0.07	1.83	5.42	0.04	0.06	0.04	1.89
LOS 2:9	0.13	14.81	1.16	0.11	2.06	1.06	0.04	0.15	0.03	1.14
LOS 3:9	0.17	16.46	5.54	0.36	5.91	3.84	0.37	0.52	0.04	3.75
LOS 9 AVRG	0.15	16.75	2.96	0.18	3.26	3.44	0.15	0.24	0.04	2.26
LOS 9 STDV	0.02	2.11	2.29	0.16	2.29	2.21	0.19	0.25	0.01	1.35
LOS 9 MED	0.16	16.46	2.19	0.11	2.06	3.84	0.04	0.15	0.04	1.89
LOS 1:10	0.41	14.74	2.38	0.06	1.89	6.12	0.04	0.07	0.05	2.09
LOS 2:10	0.13	14.80	1.14	0.10	1.70	1.04	0.04	0.16	0.04	1.08
LOS 3:10	0.33	15.38	5.07	0.26	3.98	3.17	0.30	0.38	0.06	2.90
LOS 10 AVRG	0.29	14.97	2.86	0.14	2.53	3.44	0.13	0.21	0.05	2.02
LOS 10 STDV	0.12	0.29	1.64	0.09	1.03	2.08	0.12	0.13	0.01	0.75
LOS 10 MED	0.33	14.80	2.38	0.10	1.89	3.17	0.04	0.16	0.05	2.09
The total average of ten days leaching from LOS Column	2.25	163.86	40.03	3.18	56.86	30.77	2.89	5.31	0.44	34.65

Appendix 5 a: Column leaching Experiments results for spent shale samples										
	Ti	**V**	**Cr**	**Co**	**Zn**	**As**	**Zr**	**Cd**	**Pb**	**U**
Detection limit	0.1	0.1	0.1	0.01	1	0.2	0.010	0.01	0.01	0.001
Samples ID										
LSS 1:1	0.88	215.30	1.89	0.02	2.55	20.86	0.17	5.80	0.03	0.01
LSS 2:1	1.20	224.00	6.25	0.02	5.10	10.26	0.09	4.64	0.02	0.01
LSS 3:1	1.29	266.10	6.20	0.02	3.43	8.91	0.05	5.28	0.02	0.02
LSS 1 AVRG	1.12	235.13	4.78	0.02	3.69	13.34	0.10	5.24	0.02	0.01
LSS 1 STDV	0.22	27.17	2.51	0.00	1.30	6.55	0.06	0.58	0.00	0.00
LSS 1 MED	1.20	224.00	6.20	0.02	3.43	10.26	0.09	5.28	0.02	0.01
LSS 1:2	0.32	251.00	0.20	0.05	1.18	15.33	0.02	0.73	0.06	0.01
LSS 2:2	0.50	199.80	1.16	0.15	1.88	8.97	0.01	1.25	0.03	0.01
LSS 3:2	1.30	389.30	1.67	0.05	1.31	7.18	0.04	3.48	0.03	0.05
LSS 2 AVRG	0.71	280.03	1.01	0.08	1.46	10.49	0.02	1.82	0.04	0.02
LSS 2 STDV	0.52	98.03	0.75	0.06	0.37	4.28	0.02	1.46	0.02	0.02
LSS 2 MED	0.50	251.00	1.16	0.05	1.31	8.97	0.02	1.25	0.03	0.01
LSS 1:3	0.26	275.20	0.14	0.01	2.86	17.49	0.01	0.39	0.03	0.02
LSS 2:3	0.28	156.90	0.97	0.01	2.06	9.87	0.01	0.55	0.02	0.03
LSS 3:3	0.83	418.80	0.49	0.02	2.65	9.03	0.02	2.36	0.02	0.03
LSS 3 AVRG	0.46	283.63	0.53	0.01	2.52	12.13	0.01	1.10	0.02	0.02
LSS 3 STDV	0.32	131.15	0.41	0.00	0.42	4.66	0.00	1.10	0.00	0.01
LSS 3 MED	0.28	275.20	0.49	0.01	2.65	9.87	0.01	0.55	0.02	0.03
LSS 1:4	0.16	237.60	0.17	0.09	2.00	17.30	0.02	0.26	0.02	0.03
LSS 2:4	0.23	127.40	0.91	0.08	2.23	10.72	0.03	0.32	0.02	0.06
LSS 3:4	0.55	324.00	0.52	0.09	1.80	8.65	0.02	1.18	0.02	0.05
LSS 4 AVRG	0.31	229.67	0.54	0.09	2.01	12.22	0.02	0.58	0.02	0.05
LSS 4 STDV	0.21	98.54	0.37	0.01	0.22	4.52	0.01	0.51	0.00	0.02
LSS 4 MED	0.23	237.60	0.52	0.09	2.00	10.72	0.02	0.32	0.02	0.05
LSS 1:5	0.19	269.70	0.20	0.05	1.01	22.35	0.01	0.32	0.01	0.04
LSS 2:5	0.16	112.60	0.99	0.05	0.76	11.04	0.02	0.26	0.02	0.10
LSS 3:5	0.42	287.50	0.99	0.06	1.76	9.74	0.01	0.88	0.01	0.05
LSS 5 AVRG	0.26	223.27	0.73	0.05	1.18	14.38	0.01	0.49	0.01	0.07
LSS 5 STDV	0.14	96.25	0.45	0.01	0.52	6.94	0.01	0.34	0.00	0.03
LSS 5 MED	0.19	269.70	0.99	0.05	1.01	11.04	0.01	0.32	0.01	0.05
LSS 1:6	0.11	191.80	0.17	0.06	1.46	17.14	0.01	0.23	0.02	0.05
LSS 2:6	0.18	102.80	1.01	0.05	1.77	11.18	0.01	0.24	0.01	0.14
LSS 3:6	0.32	243.10	0.20	0.05	1.46	10.56	0.01	0.69	0.01	0.09
LSS 6 AVRG	0.20	179.23	0.46	0.05	1.56	12.96	0.01	0.38	0.02	0.09
LSS 6 STDV	0.11	70.99	0.48	0.00	0.18	3.63	0.00	0.27	0.00	0.05
LSS 6 MED	0.18	191.80	0.20	0.05	1.46	11.18	0.01	0.24	0.01	0.09
LSS 1:7	0.12	170.10	0.18	0.05	1.65	17.21	0.06	0.27	0.01	0.07
LSS 2:7	0.11	96.37	0.92	0.05	0.34	12.32	0.05	0.22	0.01	0.20
LSS 3:7	0.23	218.20	0.97	0.07	1.34	13.50	0.05	0.45	0.01	0.16
LOSS 7 AVRG	0.16	161.56	0.69	0.06	1.11	14.34	0.05	0.31	0.01	0.14
LSS 7 STDV	0.07	61.36	0.45	0.01	0.68	2.55	0.01	0.12	0.00	0.07
LSS 7 MED	0.12	170.10	0.92	0.05	1.34	13.50	0.05	0.27	0.01	0.16
LSS 1:8	0.14	34.47	2.83	0.09	1.56	6.68	0.06	0.08	0.03	2.23

LSS 2:8	0.14	86.45	0.95	0.06	1.01	11.81	0.05	0.21	0.01	0.23
LSS 3:8	0.25	182.20	1.57	0.08	1.51	14.95	0.06	0.41	0.02	0.27
LOSS 8 AVRG	0.17	101.04	1.78	0.08	1.36	11.15	0.06	0.23	0.02	0.91
LSS 8 STDV	0.06	74.94	0.96	0.02	0.30	4.18	0.01	0.16	0.01	1.15
LSS 8 MED	0.14	86.45	1.57	0.08	1.51	11.81	0.06	0.21	0.02	0.27
LSS 1:9	0.20	138.50	0.24	0.01	0.90	17.11	0.05	0.20	0.02	0.13
LSS 2:9	0.18	89.81	1.03	0.00	1.80	13.14	0.05	0.19	0.05	0.28
LSS 3:9	0.17	166.50	1.18	0.01	1.00	17.96	0.06	0.32	0.02	0.41
LSS 9 AVRG	0.18	131.60	0.82	0.00	1.24	16.07	0.05	0.24	0.03	0.28
LSS 9 STDV	0.02	38.81	0.50	0.00	0.49	2.57	0.00	0.07	0.02	0.14
LSS 1:10	0.15	115.60	1.26	0.01	1.64	15.51	0.06	0.16	0.02	0.15
LSS 2:10	0.17	84.40	1.10	0.01	1.04	12.33	0.05	0.18	0.06	0.28
LSS 3:10	0.14	84.46	1.12	0.01	1.76	12.52	0.06	0.17	0.05	0.28
LSS 10 AVRG	0.15	94.82	1.16	0.01	1.48	13.45	0.05	0.17	0.04	0.24
LSS 10 STDV	0.02	18.00	0.09	0.00	0.39	1.78	0.00	0.01	0.02	0.07
LSS 10 MED	0.15	84.46	1.12	0.01	1.64	12.52	0.06	0.17	0.05	0.28
The total average of ten days leaching from LSS Column	3.73	1919.99	12.49	0.45	17.61	130.54	0.39	10.56	0.40	1.83

Appendix 5.c : Column leaching Experiments results for phosphate underneath spent shale samples.

	Ti	V	Cr	Co	Zn	As	Zr	Cd	Pb	U
Detection limit	0.1	0.1	0.1	0.01	1	0.2	0.010	0.01	0.01	0.001
Sample ID										
LSSP 1:1	0.43	196.5	85.9	0.02	3.74	0.61	0.07	1.40	0.04	0.18
LSSP 2:1	0.38	185.6	64.3	0.02	4.05	0.46	0.03	1.42	0.02	0.16
LSSP 3:1	0.32	172.8	90.9	0.02	5.80	0.47	0.05	1.25	0.06	0.16
LOSSP 1 AVRG	0.37	185.0	80.4	0.02	4.53	0.51	0.05	1.36	0.04	0.17
LSSP 1 STDV	0.06	11.9	14.1	0.00	1.11	0.08	0.02	0.09	0.02	0.01
LSS 1 MED	0.38	185.6	85.9	0.02	4.05	0.47	0.05	1.40	0.04	0.16
LSSP 1:2	0.19	149.6	11.8	0.01	1.40	0.26	0.02	0.54	0.02	0.12
LSSP 2:2	0.19	132.4	7.1	0.01	1.46	0.24	0.01	0.41	0.01	0.14
LSSP 3:2	0.13	125.0	20.9	0.01	1.21	0.23	0.02	0.51	0.04	0.08
LSSP 2 AVRG	0.17	135.7	13.3	0.01	1.35	0.24	0.02	0.49	0.02	0.11
LSSP 2 STDV	0.04	12.6	7.0	0.00	0.13	0.01	0.01	0.07	0.01	0.03
LSSP 2 MED	0.19	132.4	11.8	0.01	1.40	0.24	0.02	0.51	0.02	0.12
LSSP 1:3	0.13	100.4	6.3	0.01	1.27	0.20	0.01	0.26	0.02	0.05
LSSP 2:3	0.12	103.3	4.4	0.01	1.25	0.21	0.01	0.19	0.03	0.03
LSSP 3:3	0.15	127.5	6.2	0.00	1.24	0.20	0.02	0.27	0.02	0.04
LSSP 3 AVRG	0.13	110.4	5.6	0.01	1.25	0.21	0.02	0.24	0.02	0.04
LSSP 3 STDV	0.02	14.9	1.1	0.00	0.02	0.01	0.01	0.04	0.00	0.01
LSSP 3 MED	0.13	103.3	6.2	0.01	1.25	0.20	0.01	0.26	0.02	0.04
LSSP 1:4	0.17	67.1	3.2	0.01	1.20	0.21	0.01	0.15	0.02	0.03

LSSP 2:4	0.13	88.0	3.3	0.01	1.10	0.21	0.01	0.10	0.03	0.02
LSSP 3:4	0.21	118.9	5.3	0.00	1.20	0.21	0.13	0.21	0.04	0.06
LSSP 4 AVRG	0.17	91.4	3.9	0.01	1.16	0.21	0.05	0.15	0.03	0.04
LSSP 4 STDV	0.04	26.0	1.2	0.00	0.06	0.00	0.07	0.05	0.01	0.02
LSSP 4 MED	0.17	88.0	3.3	0.01	1.20	0.21	0.01	0.15	0.03	0.03
LSSP 1:5	0.10	72.4	3.5	0.00	1.00	0.21	0.01	0.12	0.03	0.02
LSSP 2:5	0.11	79.4	2.8	0.01	1.01	0.20	0.01	0.08	0.03	0.01
LSSP 3:5	0.12	76.4	3.4	0.01	1.50	0.21	0.01	0.10	0.03	0.02
LSSP 5 AVRG	0.11	76.1	3.2	0.01	1.17	0.21	0.01	0.10	0.03	0.02
LSSP 5 STDV	0.01	3.5	0.4	0.00	0.28	0.01	0.00	0.02	0.00	0.01
LSSP 5 MED	0.11	76.4	3.4	0.01	1.01	0.21	0.01	0.10	0.03	0.02
LSSP 1:6	0.12	69.3	3.3	0.01	1.00	0.11	0.01	0.10	0.01	0.02
LSSP 2:6	0.11	65.1	2.3	0.00	1.04	0.17	0.02	0.06	0.02	0.01
LSSP 3:6	0.11	69.3	3.1	0.01	1.06	0.09	0.01	0.08	0.01	0.01
LSSP 6 AVRG	0.11	67.9	2.9	0.00	1.03	0.12	0.01	0.08	0.01	0.01
LSSP 6 STDV	0.01	2.4	0.6	0.00	0.03	0.04	0.00	0.02	0.00	0.00
LSSP 6 MED	0.11	69.3	3.1	0.01	1.04	0.11	0.01	0.08	0.01	0.01
LSSP 1:7	0.15	62.4	2.8	0.01	1.09	0.92	0.01	0.10	0.02	0.01
LSSP 2:7	0.13	51.9	1.8	0.00	1.09	0.71	0.01	0.05	0.02	0.01
LSSP 3:7	0.13	58.0	2.4	0.01	1.10	0.92	0.01	0.08	0.03	0.01
LSSP 7 AVRG	0.14	57.4	2.3	0.01	1.09	0.85	0.01	0.08	0.02	0.01
LSSP 7 STDV	0.01	5.3	0.5	0.00	0.01	0.12	0.00	0.02	0.00	0.00
LSSP 7 MED	0.13	58.0	2.4	0.01	1.09	0.92	0.01	0.08	0.02	0.01
LSSP 1:8	0.19	142.9	0.2	0.01	1.12	0.80	0.03	0.17	0.01	0.09
LSSP 2:8	0.18	46.3	1.5	0.01	1.22	0.55	0.02	0.06	0.02	0.01
LSSP 3:8	0.19	51.6	2.1	0.01	1.30	0.62	0.03	0.07	0.02	0.01
LSSP 8 AVRG	0.19	80.3	1.3	0.01	1.21	0.66	0.03	0.10	0.02	0.03
LSSP 8 STDV	0.01	54.3	1.0	0.00	0.09	0.13	0.00	0.06	0.01	0.05
LSSP 8 MED	0.19	51.6	1.5	0.01	1.22	0.62	0.03	0.07	0.02	0.01
LSSP 1:9	0.05	53.2	2.2	0.01	1.66	0.08	0.02	0.06	0.02	0.01
LSSP 2:9	0.07	34.6	1.2	0.01	1.09	0.05	0.02	0.06	0.01	0.01
LSSP 3:9	0.07	50.2	2.0	0.00	1.57	0.03	0.02	0.08	0.02	0.01
LSSP 9 AVRG	0.06	46.0	1.8	0.01	1.44	0.05	0.02	0.07	0.01	0.01
LSSP 9 STDV	0.01	10.0	0.5	0.00	0.31	0.02	0.00	0.01	0.00	0.00
LSSP 9 MED	0.07	50.2	2.0	0.01	1.57	0.05	0.02	0.06	0.02	0.01
LSSP 1:10	0.05	51.5	2.2	0.01	1.74	0.01	0.02	0.08	0.03	0.01
LSSP 2:10	0.70	34.0	1.3	0.00	1.71	0.01	0.02	0.08	0.08	0.01
LSSP 3:10	0.80	41.7	1.9	0.01	1.54	0.01	0.03	0.07	0.04	0.01
LSSP 10 AVRG	0.52	42.4	1.8	0.00	1.67	0.01	0.02	0.08	0.05	0.01
LSSP 10 AVRG	0.41	8.8	0.5	0.00	0.11	0.00	0.01	0.01	0.03	0.00
LSSP 10 AVRG	0.70	41.7	1.9	0.01	1.71	0.01	0.02	0.08	0.04	0.01
The average of ten days leaching from LSSP Column	1.45	892.42	116.55	0.07	15.92	3.06	0.24	2.74	0.26	0.44

Appendix 6.a : The concentrate of elements obtained from the (Solid-Liquid Partitioning as a Function of S\L Ratio) method experiment (method 1316) for the spent shale, all concentration results values are µm/L measured by ICP-MS

Sample ID	Ration	Ti	V	Cr	Co	Zn
m16 SS A-1	0.1	27.06	2845	913.6	0.044	2.13
m16 SSA-2	0.2	20.57	5079	1838.0	0.036	1.90
m16 SSA- 3	0.5	19.33	2246	1582.0	0.031	2.48
m16 SSA-4	1	26.19	2035	724.7	0.037	0.92
m16 SSA- 5	2	12.80	3110	708.3	0.024	0.57
m16 SSB -1	0.1	23.25	2138	1522.0	0.049	1.44
m16 SSB -2	0.2	22.50	3694	2679.0	0.058	1.62
m16 SSB -3	0.5	30.59	1441	967.5	0.058	2.66
m16 SSB -4	1	24.12	1300	990.6	0.045	1.77
m16 SSB -5	2	32.87	1306	1662.0	0.067	1.90
m16 SSC-1	0.1	34.38	1509	2722.0	0.071	3.80
m16 SSC-2	0.2	29.50	2073	4486.0	0.072	5.18
m16 SSC-3	0.5	42.49	1019	1881.0	0.104	5.72
m16 SSC-4	1	32.82	848	2163.0	0.062	3.60
m16 SSC-5	2	32.40	974	3599.0	0.072	2.94
∑ LSS		3.73	1920.0	12.49	0.45	17.61
Sample ID		As	Zr	Cd	Pb	U
m16 SS A-1	0.1	4.593	0.964	0.351	0.508	0.218
m16 SSA-2	0.2	8.661	0.574	0.614	0.282	0.171
m16 SSA- 3	0.5	6.678	0.421	0.550	0.326	0.123
m16 SSA-4	1	6.306	0.654	0.357	0.437	0.158
m16 SSA- 5	2	5.953	0.250	0.292	0.100	0.066
m16 SSB -1	0.1	2.036	0.770	0.667	0.379	0.255
m16 SSB -2	0.2	4.394	0.849	1.265	0.342	0.267
m16 SSB -3	0.5	4.570	0.919	0.668	0.548	0.347
m16 SSB -4	1	4.477	0.628	0.622	0.373	0.220
m16 SSB -5	2	4.200	1.043	0.853	0.491	0.339
m16 SSC-1	0.1	1.561	1.273	1.092	0.438	0.450
m16 SSC-2	0.2	1.347	1.197	1.791	0.693	0.332
m16 SSC-3	0.5	2.552	1.561	1.001	0.665	0.709
m16 SSC-4	1	1.890	1.034	0.949	0.398	0.379
m16 SSC-5	2	1.797	1.093	1.495	0.325	0.330
∑ LSS		130.45	0.39	10.56	0.26	1.83

Appendix 6.b: Plots of the concentrate of elements obtained from the (Solid-Liquid Partitioning as a Function of S\L Ratio) method experiment (method 1316) for the spent shale, all concentration results values are µm/L measured by ICP-MS

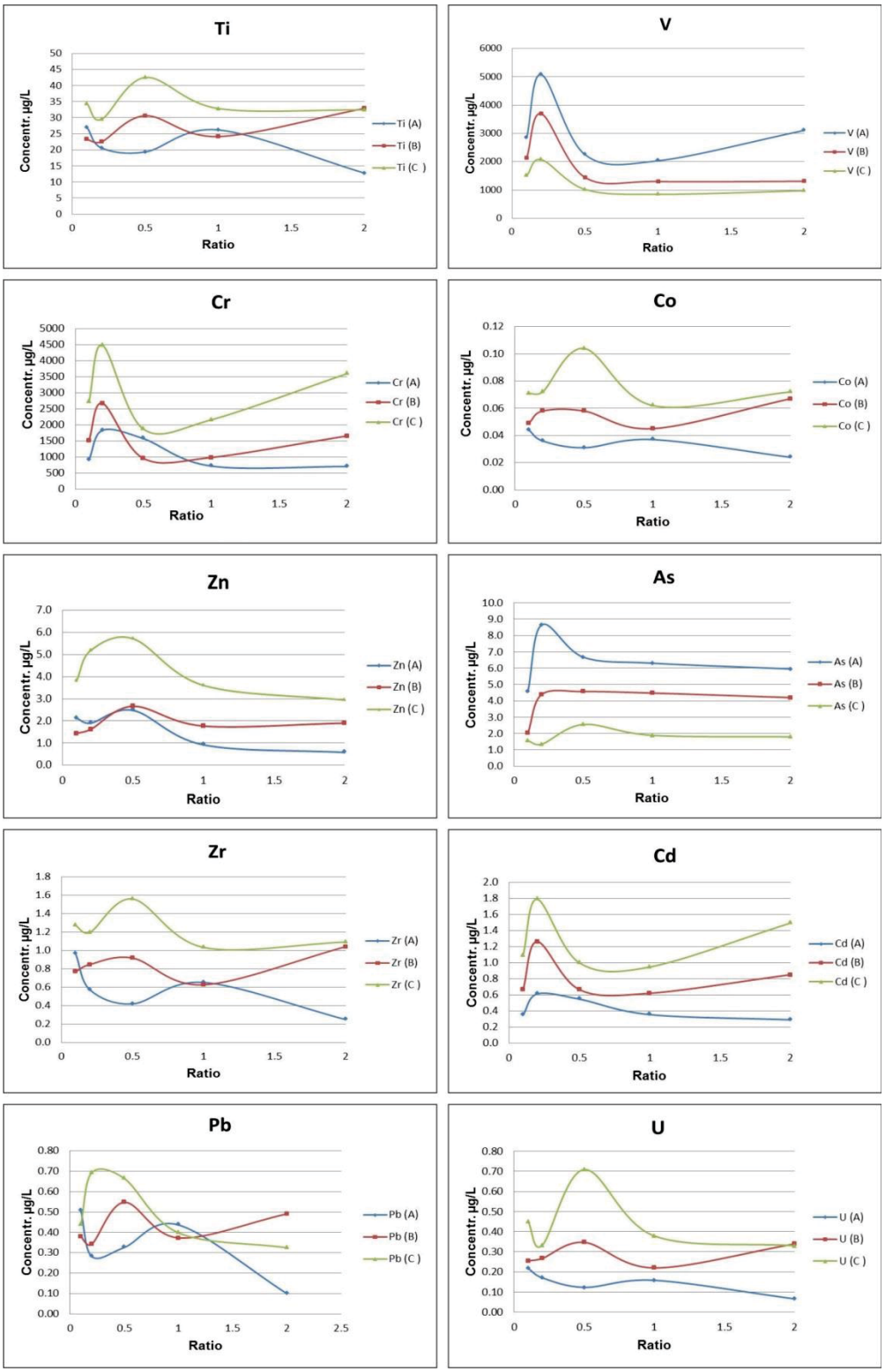

Appendix 7.a: The concentrate of elements obtained from the Liquid-Solid Partitioning as a Function of Extract p H, method experiment, method 1313, all concentration results values are µm/L measured by ICP-MS

Sample ID	pH	Ti	V	Cr	Co	Zn
M13-SSA	4	42.50	2169.0	1438.0	0.14	5.54
M13-SSA	5	19.25	2673.0	911.4	0.09	5.32
M13-SSA	6	11.44	2885.0	925.2	0.04	1.84
M13-SSA	7	14.49	2534.0	864.8	0.05	1.36
M13-SSA	8	15.87	2679.0	930.4	0.05	1.39
M13-SSA	10	10.33	2785.0	831.3	0.04	1.01
M13-SSA	12	6.15	3454.0	764.7	0.04	0.95
Sample ID	**pH**	**As**	**Zr**	**Cd**	**Pb**	**U**
M13-SSA	4	3.43	3.32	0.57	1.93	0.78
M13-SSA	5	5.55	1.78	0.37	0.85	0.35
M13-SSA	6	9.14	1.39	0.33	0.76	0.32
M13-SSA	7	5.33	1.09	0.33	0.65	0.33
M13-SSA	8	4.05	1.05	0.34	0.69	0.51
M13-SSA	10	8.62	1.09	0.30	0.43	0.50
M13-SSA	12	10.68	1.11	0.29	0.41	0.89

Sample ID	pH	Ti	V	Cr	Co	Zn
M13-SSB	4	33.89	2266.0	1314.0	0.17	4.37
M13-SSB	5	32.90	2027.0	1187.0	0.12	3.75
M13-SSB	6	17.43	1824.0	1170.0	0.09	3.49
M13-SSB	7	19.64	2282.0	1333.0	0.06	2.41
M13-SSB	8	12.39	1742.0	1542.0	0.05	1.88
M13-SSB	10	10.49	2355.0	1149.0	0.04	1.28
M13-SSB	12	11.59	2676.0	993.3	0.04	1.17
Sample ID	**pH**	**As**	**Zr**	**Cd**	**Pb**	**U**
M13-SSB	4	3.66	1.72	0.69	0.93	0.56
M13-SSB	5	3.87	2.40	0.69	0.93	0.75
M13-SSB	6	2.21	1.53	0.65	0.78	0.60
M13-SSB	7	3.95	1.40	0.63	0.59	0.46
M13-SSB	8	2.55	3.51	0.56	0.52	1.01

M13-SSB	**10**	6.47	0.80	0.52	0.31	0.60
M13-SSB	**12**	5.94	0.53	0.47	0.35	0.43

Sample ID	**pH**	**Ti**	**V**	**Cr**	**Co**	**Zn**
M13-SSC	**4**	59.14	1475.0	2682.0	0.20	11.01
M13-SSC	**5**	40.72	1579.0	2302.0	0.16	8.98
M13-SSC	**6**	40.75	1701.0	2153.0	0.13	10.20
M13-SSC	**7**	20.74	1563.0	2322.0	0.07	3.54
M13-SSC	**8**	27.48	1661.0	2233.0	0.09	5.67
M13-SSC	**10**	13.98	1892.0	1945.0	0.05	2.31
M13-SSC	**12**	13.62	1845.0	1996.0	0.05	2.60
Sample ID	**pH**	**As**	**Zr**	**Cd**	**Pb**	**U**
M13-SSC	**4**	2.49	3.71	1.37	1.30	1.47
M13-SSC	**5**	2.47	2.94	1.13	1.26	2.08
M13-SSC	**6**	2.24	2.98	1.12	1.21	1.19
M13-SSC	**7**	1.49	1.55	0.92	1.13	0.53
M13-SSC	**8**	2.08	1.05	0.95	0.50	1.34
M13-SSC	**10**	3.50	0.97	0.76	0.40	0.44
M13-SSC	**12**	2.51	0.76	0.76	0.36	0.37

Appendix 7. Plots of the concentrate of elements obtained from the Liquid-Solid Partitioning as a Function of Extract p H, method experiment, method 1313, all concentration results values are µm/L measured by ICP-MS

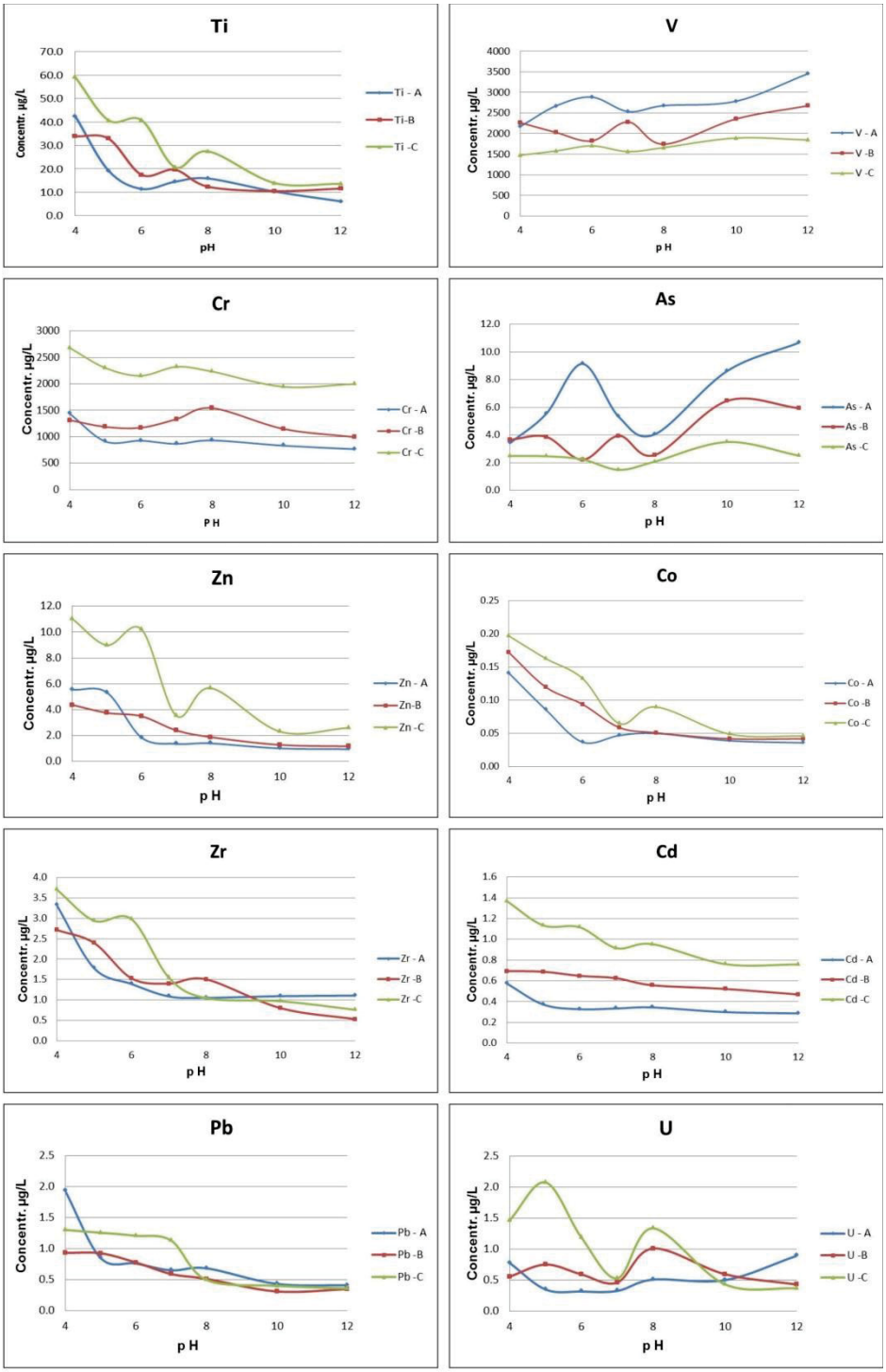

Appendix 8 : Groundwater analyses for a representative water samples taped from the intermediate aquifer (B2A7), the deep sand stone aquifer of (Kurnub/Ram) aquifer, the analyses include the concentrations of the REE and heavy metals by using ICP-MS , the concentration values are in ppb.

Appendix 8 a : groundwater analyses for water samples taped from intermediate aquifer (B2A7)

1. Well ID (CD 1157)

Li	B	Na	Mg	Al	Si	P	S	K	Ca
9.27	230.30	109000	52440	20.16	6773.0	41.57	52850	2643.0	114500
Sc	V	Cr	Mn	Fe	Co	Ni	Cu	Zn	As
0.04	0.15	0.45	23.35	816.30	0.13	4.56	11.78	58.15	0.24
Se	Br	Br	Rb	Sr	Mo	Cd	Sn	Sb	Cs
0.06	643.20	639.50	2.72	1236.0	11.25	0.18	0.13	1.19	0.30
Ba	La	Ce	Pr	Nd	Sm	Eu	Pb	235U	238U
39.98	0.03	0.06	0.01	0.02	0.00	0.01	0.97	0.45	0.17

1. Well ID. CD 3445

Li	**B**	**Na**	**Mg**	**Al**	**Si**	**P**	**S**	**K**	**Ca**
11.81	128.30	79900	31030	9.58	7863.0	51.49	39840	3712.0	94570
Sc	**V**	**Cr**	**Mn**	**Fe**	**Co**	**Ni**	**Cu**	**Zn**	**As**
0.03	19.77	0.29	78.61	860.20	0.45	24.08	16.88	92.42	0.22
Se	**Br**	**Br**	**Rb**	**Sr**	**Mo**	**Cd**	**Sn**	**Sb**	**Cs**
16.41	471.60	468.90	4.67	736.8	25.32	0.96	0.10	1.31	0.43
Ba	**La**	**Ce**	**Pr**	**Nd**	**Sm**	**Eu**	**Pb**	**235U**	**238U**
102.00	0.05	0.07	0.00	0.02	0.00	0.04	0.55	9.11	3.29

1. Well ID : CD1160) (L13)

Li	**B**	**Na**	**Mg**	**Al**	**Si**	**P**	**S**	**K**	**Ca**
9.87	217.10	117300	43750	164.10	6968.0	99.47	46720	4182.0	92680
Sc	**V**	**Cr**	**Mn**	**Fe**	**Co**	**Ni**	**Cu**	**Zn**	**As**
0.03	0.55	1.13	27.64	720.50	0.22	6.03	24.29	29.26	0.77
Se	**Br**	**Br**	**Rb**	**Sr**	**Mo**	**Cd**	**Sn**	**Sb**	**Cs**
0.21	665.50	659.00	3.95	1098.0	36.90	0.10	0.48	2.89	0.72
Ba	**La**	**Ce**	**Pr**	**Nd**	**Sm**	**Eu**	**Pb**	**235U**	**238U**
40.23	0.32	0.59	0.06	0.24	0.05	0.06	1.25	0.66	0.24

Appendix 8 b. : groundwater analyses for water samples taped from The deep sandstone aquifer (Kurnub/Ram Aquifer)

Well ID KD1

Li	B	Na	Mg	Al	Si	P	S	K	Ca
13.12	173.80	102700	42780	261.90	7905.00	93.23	84310	4531	113600
Sc	**V**	**Cr**	**Mn**	**Fe**	**Co**	**Ni**	**Cu**	**Zn**	**As**
0.06	0.36	0.88	55.15	1100	13.64	37.06	20.11	31.04	0.95
Se	**Br**	**Br**	**Rb**	**Sr**	**Mo**	**Cd**	**Sn**	**Sb**	**Cs**
0.83	577.3	573.3	4.73	1129.00	89.98	0.08	0.13	0.70	0.58
Ba	**La**	**Ce**	**Pr**	**Nd**	**Sm**	**Eu**	**Pb**	**235U**	**238U**
66.87	0.10	0.16	0.01	0.03	0.01	0.07	1.21	1.05	0.38

Well ID KD7

Li	B	Na	Mg	Al	Si	P	S	K	Ca
9.28	162.50	76180	41520	512.80	7838.00	143.80	67970	2954	105600
Sc	**V**	**Cr**	**Mn**	**Fe**	**Co**	**Ni**	**Cu**	**Zn**	**As**
0.13	1.17	1.10	27.62	1197	0.34	2.40	18.92	67.44	0.54
Se	**Br**	**Br**	**Rb**	**Sr**	**Mo**	**Cd**	**Sn**	**Sb**	**Cs**
0.11	506.5	502.8	2.63	1177.00	54.53	0.04	0.15	1.25	0.37
Ba	**La**	**Ce**	**Pr**	**Nd**	**Sm**	**Eu**	**Pb**	**235U**	**238U**
47.42	0.87	1.60	0.18	0.65	0.12	0.04	1.37	1.15	0.42

Appendix 9: chemical analysis results for groundwater representative samples (mg/l)

chemical analysis results for groundwater samples taped from the intermediate aquifer (B2/A7) (mg/l)

well ID	HCO3	Ca	CL	Mg	NO3	K	Na	SO4	TDS mg/l	EC µS/cm
CD3499	373.9	97.6	130.3	50.1	3.8	2.7	73.1	149.8	507.4	1066
CD3454	406.9	117.4	137.7	48.8	2.2	2.4	93.6	117.1	519.2	1184
CD1150	467.3	134.7	170.4	50.0	<0.20	2.0	111.1	121.4	589.5	1362
CD3462	334.9	84.0	184.3	46.0	1.6	2.0	104.4	69.1	491.3	1266
CD1160	283.7	74.4	185.3	42.2	0.5	3.1	105.8	80.2	491.4	1200
CD3456	388.0	109.0	172.5	47.7	0.4	2.7	107.4	126.7	566.5	1311
CD3479	379.4	103.2	145.6	46.5	5.9	2.4	77.5	82.1	463.1	1181

chemical analysis results for groundwater samples taped from deep sandstone aquifer (Kurnub/Ram) (B2/A7) (mg/l)

well ID	HCO3	Ca	CL	Mg	NO3	K	Na	SO4	TDS mg/l	EC
CD3412	208.6	62.73	80.94	7.3	3.39	5.47	63.02	54.24	277.1	1256
CD3415	395.89	91.78	106.2	41	0.48	1.56	66.24	63.36	371.0	782
CD3416	188.49	49.1	150.9	20	<.2	6.26	112.7	83.52	422.9	946
CD3418	222.04	48.5	83.78	20	<.2	5.87	68.31	51.84	278.2	695
CD3464	361.12	100.4	175.7	49	0.31	2.35	94.76	110.9	533.2	892
CD3417	214.11	45.09	80.94	18	<0.20	5.08	69.69	48	266.6	699
CD3459	389.79	103.6	116.8	39	2.21	2.74	68.31	95.52	428.0	1112
CD3453	201.3	46.09	83.78	18	<0.20	4.69	68.54	53.28	274.9	701
CD3452	215.33	46.89	138.5	18	<0.20	5.87	105.1	66.24	380.6	892
CD3414	193.98	45.49	103.7	19	<0.20	4.69	75.9	60	308.6	770